

UNIVERSITÀ DEGLI STUDI DI FIRENZE
DIPARTIMENTO DI SISTEMI E INFORMATICA

Dottorato di Ricerca in
Ingegneria Informatica e dell'Automazione
XIX Ciclo
ING-INF/04

STABILITY AND PERFORMANCE IN
ADAPTIVE SWITCHING
SUPERVISORY CONTROL

CLAUDIA MANUELLI

Ph.D. Coordinator
Prof. Edoardo Mosca

Advisor
Prof. Edoardo Mosca

ANNO ACCADEMICO 2005-2006

Contents

Acronyms	iii
Introduction	1
Switching supervisory control	4
Main tasks of the supervisor	7
1 Multi-model SSC	9
1.1 Introduction	9
1.1.1 A controller falsification statistical test	11
1.1.2 Discrepancy measure between feedback loops	12
1.2 The virtual reference use	14
1.2.1 The virtual reference concept	15
1.2.2 A cost function for joint falsification and inference	16
1.2.3 Stability issues	19
1.2.4 Performance analysis	25
1.3 The non-minimum phase controller case	28
1.3.1 A cost function for joint falsification and inference	30
1.3.2 Stability issues	32
1.3.3 Performance analysis	37
1.4 Conclusions	39
2 Unfalsified adaptive control	40
2.1 Introduction	40
2.2 Minimum-phase controllers	42
2.2.1 Stability issues	43
2.2.2 Performance analysis	46
2.3 Non-minimum phase controllers	47

2.3.1	Stability issues	50
2.3.2	Performance analysis	52
2.4	Conclusions	54
3	Practical applications of SSC	56
3.1	Introduction	56
3.2	The neuromuscular blockade case of study	58
3.2.1	Mathematical model description	59
3.2.2	The control problem	62
3.2.3	Simulations results	64
3.3	The two carts position control	75
3.3.1	Problem formulation	75
3.3.2	Simulations results	77
3.4	Conclusions	91
	Conclusions	92
	Bibliography	94

Acronyms

CF	controller falsification
ICLB	inference of candidate loop behavior
LQG	linear quadratic gaussian
MMAC	multiple model adaptive control
MRAC	model reference adaptive control
SSC	switching supervisory control
STC	self tuning control

Introduction

In daily language "adapt" means to change behavior in order to conform to new circumstances. In control systems language the meaning is not too far from there. An adaptive control system can be defined as a system capable of changing its behavior in response to changes either in the dynamics of the process under control or in the disturbances [Ast87].

It has been worldwide accepted for many years that the human body includes several internal adaptive control systems whose task is to regulate some vital functions in response to possible changes in the body or in the environment. Indeed, sciences like biology or ecology, that specifically study living beings, define an organism as a complex adaptive system of organs that influence each other in such a way that they function as a more or less stable whole and have properties of life.

The definition of adaptive control system (in the automation field) suggests that adaptive control mainly pertains to plants described by models whose structure and parameters, constant or time varying, are not completely a priori known to the designer. Beyond these difficulties, many other different types of uncertainties can be encountered in the field of complex systems as faults in the system, sensor and actuator failures or presence of external disturbances. All these situations pertain to the study of handling uncertain plants. They are very likely met in practice, because most real processes are very often so much complicated that it is very hard to model them with a single set of fixed parameters or under a single operating condition.

Historically, research on adaptive control was first developed in the early 1950s in the field of space aircrafts. As they can operate in a wide range of speeds and altitudes, it was found that an ordinary constant feedback linear controller was not able to handle the change of operating conditions. Thus, a more sophisticated controller, capable of working in different operating conditions, was needed.

It is known that robust control and gain scheduling are different possible ways to tackle the control of uncertain systems. The first approach is a wide branch in the control theory and it guarantees some remarkable theoretical results on condition that it is known that the plant behaves approximately like a given nominal model. However, it is not of interest for this dissertation to deal with it. Gain scheduling requires the plant changes be predicted in advance or be directly measured when they occur. In fact, it uses auxiliary variables, supposed that they are available, which well correlate with process dynamics in order to change the controller parameters. Being an open loop scheme, there is no feedback which can compensate for an incorrect schedule.

Algorithms which govern adaptive control systems can broadly be divided into two categories: the first is constituted by the *model reference adaptive controllers* (MRAC) for which, as the name suggests, the specifications are stated in terms of a given reference model. It tells us how the process output should ideally respond to the command signal $r(t)$. A block diagram is shown in Fig. 0.1. The parameters of the controller are adjusted in such

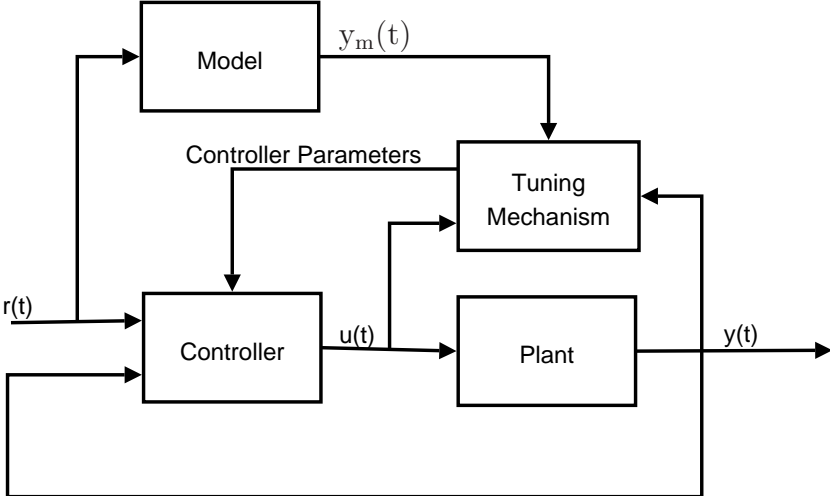


Figure 0.1. Block diagram of an MRAC system

a way that the error between the model output $y_m(t)$ and the process output $y(t)$ goes asymptotically to zero. The second category is the *self tuning controllers* (STC); in this case, specifications are stated in terms of a performance index involving, for example, a quadratic term in the tracking error: $e(t) = r(t) - y(t)$, and controller parameters are directly or indirectly adjusted on the basis of plant parameter estimates. The block diagram in Fig. 0.2 illustrates the situation. In both cases the overall control system con-

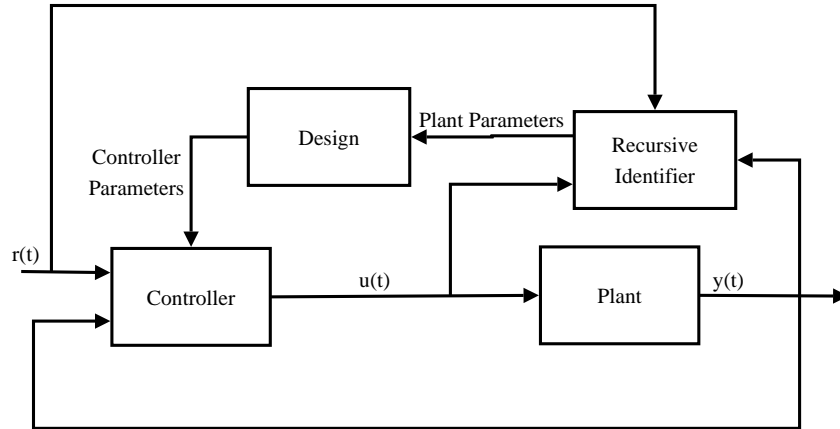


Figure 0.2. Block diagram of an STC system

sists of two loops: an outer loop which performs the tuning of the controller parameters and an inner loop constituted by the plant and the controller which guarantees some desirable behavior. The method for designing the inner loop and the techniques used for tuning the parameters in the outer loop are, however, different. According to both schemes, adaptive control has been defined as a special type of nonlinear feedback control where the state of the process can be separated into two categories, which change at different rates. The states pertaining to the ordinary feedback loop are fast time varying, whilst the estimated plant model parameters or the controller parameters can be viewed as slow time varying states [Ast87, Mos95].

However, experience shows that conventional adaptation techniques are not always capable to perform satisfactorily. The presence of large parameter variations, the poor excitation of closed loop variables or the presence of different modes of operation for the plant are all situations which can lead to slow convergence with large transient errors.

An early solution to this problem involved the use of multiple models for the identification of the plant. This methodology is commonly referred to as Multiple Model Adaptive Control (MMAC) [ACD⁺77]. A steady state Linear Quadratic Gaussian (LQG) compensator is tuned on each model whose output is the control signal that would be the optimal control signal if the plant was identical to the model. Moreover, the Kalman filter contained in each LQG compensator, on the ground of real time sensor measurements, generates a posterior conditional probability for the model to be close to the plant. The probabilities obtained by each Kalman filter weight the corresponding control signal in order to obtain the input to the plant.

A later solution to the same problem was the introduction in the adaptation mechanism of a switching process between the available controllers. One of the earlier approach in this field was proposed by Martensson [Mar86] in the mid 80s. He proposed to perform a pre-routed search among controllers until one controller is found capable of achieving the control objective. This is a very old-fashioned switching scheme where only the choice of when to switch to the next controller is performed. Since then a great deal of studies [Mor96, NB97, ST97] have been carried out on the subject in order to reach smarter and more accurate solutions.

Switching supervisory control

The basic general scheme of a Switching Supervisory Control (SSC) is illustrated in Fig. 0.3 where $\mathcal{C} = \{C_i, i = 1, \dots, N\}$ is a pre-definite set of candidate controllers that is supposed to have a finite number of elements. The supervisor is the logic which coordinates the switching process, assesses the performance of the current controller and, possibly inferring those of the candidate controllers, decides when and to which controller to switch. The main tasks of the supervisor will be extensively analyzed further.

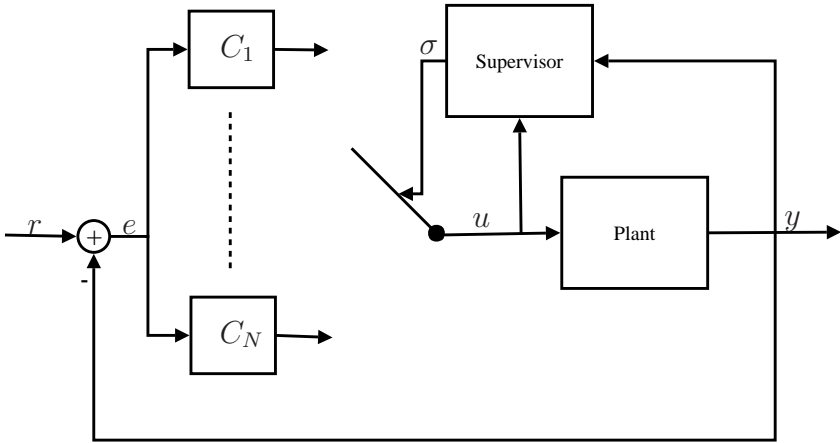


Figure 0.3. Block diagram of an SSC system

It is worth noting that a considerable difference between conventional adaptive control and switching supervisory control is that the latter exhibits a logic for the controller selection rather than a continuous tuning. Hence the supervisor, combining the continuous dynamics of the plant with the discrete logic, can be considered a hybrid system.

Using an SSC scheme rather than classic adaptive control scheme has some potential benefits. A rapid adaptation is achieved through the σ signal, in Fig 0.3, which represents the index of the controller to be placed in the feedback loop. Its ability to change in a discontinuous way allows one to face sudden modifications in process dynamics. In contrast to it, as has already been stated, a tuning algorithm of the more traditional adaptive control can fail to promptly face sudden changes in process parameters. SSC is characterized by a separation between supervision and control. By the way, nonlinearities that should occur in the supervisor do not affect the dynamics of the system, while in classical adaptive control schemes tuning mechanism always makes the overall control system non linear. Moreover, being the design of candidate controllers performed off line, it can be done accordingly to any criterion, without any concern about its computational complexity. On the contrary, in adaptive control theory, controllers have very often to be tailored on the tuning mechanism and, hence, little freedom is left to the controller designer.

Different types of supervision can be classified according to the amount of prior knowledge on the plant, particularly in relation to the availability of a set of models approximating the plant.

The so called *estimator based supervisor* relies on system identification. It continuously compares the behavior of the plant with that of several nominal models, in order to identify the model which best approximates the plant at each time. These models can be viewed as a set of open loop models, for instance representing different operating conditions. If they are available, controllers specially tuned on them can be a priori designed. Hence, during system operation, one has to identify the current behavior of the plant in order to insert the corresponding controller in the loop. The design problem is to choose the number and the structure of the models as well as their parameter vectors. The control problem is to establish suitable rules for switching between candidate controllers in such a way that the best performance is achieved, while stability is guaranteed.

In literature examples can be found of either the use of fixed parameters models or adaptive models. In the latter case the need of updating the parameters at each instant makes the whole system computationally inefficient. Moreover, if the system behavior changes after a long period of stability the tuning mechanism can fail to properly react to that situation and negative consequences on system performance may occur. Even though fixed models do not present these drawbacks, they can be used to represent only a finite number of behaviors and a large number of them can be needed to ensure stability of the switched system. By the way, a hybrid scheme, employing fixed and adaptive models together, can be found as well [NB97]. Fig. 0.4

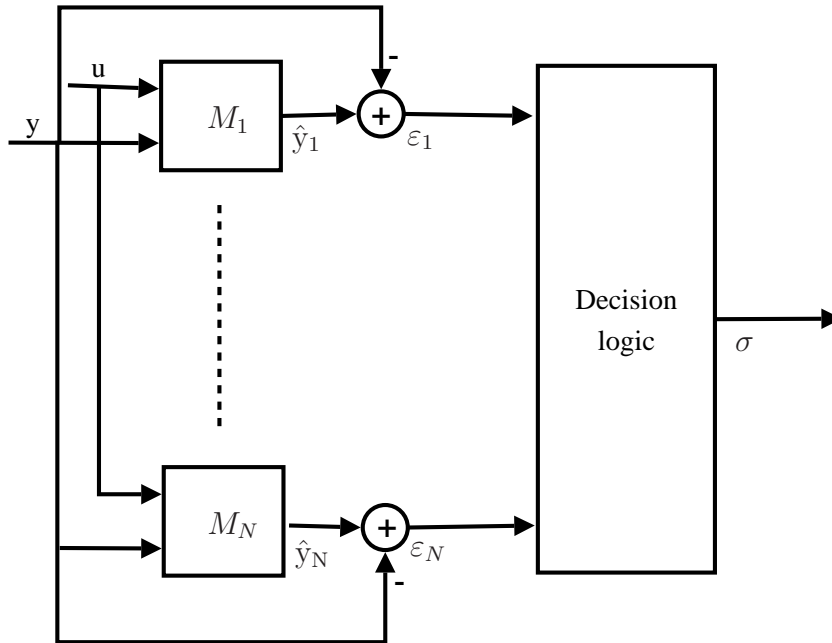


Figure 0.4. Block diagram of a generic estimator based supervisor

shows a general scheme of an estimator based supervisor. It consists of a bank of approximating models $\mathcal{M} = \{M_i, i = 1, \dots, N\}$ and a decision logic block which chooses the controller to be placed in the loop. Each reference model M_i uses the measured input u and output y of the plant to generate an estimate of y , called \hat{y}_i . The latter is calculated according to the principle that \hat{y}_i is an asymptotically correct prediction of y assuming that the plant coincides with M_i . The estimation error ε_i , viz. the difference between the output of the plant and its estimate, is used by the decision logic block which selects the controller corresponding to the model that best approximates the plant at each instant. This scheme, even if very general, is useful to explain how the mechanism works. Of course a great deal of different variants exists in the generation of the output prediction as well as in the design of the decision unit.

The so called *performance based supervisor* assesses the performance of candidate controllers by a *virtual* experiment for which only input and output data from the current loop are needed. More precisely, the performance of a candidate controller is assessed according to how good would have been the behavior of the closed loop, had that controller been in the loop. It is worth highlighting that this is achieved without physically inserting the controller in the loop, hence the name *virtual* experiment. Notice that no identification

of the unknown plant is required and the nominal models are not needed. This approach, which has been only recently introduced in the literature [ST97], is usually referred to as *unfalsified adaptive control* and, being a quite recent study, few literature is available on it. It relies on the *virtual reference* concept [ST97, MA03, CLS02] which facilitates validation of controllers from input-output data possibly acquired while another controller is in the loop. This is a key concept for this work and, hence, it will be extensively illustrated in Sec. 1.2.

Main tasks of the supervisor

The main component of a switching control system is the supervisor, a high level of appropriately designed logic which operates according to the following conceptual lines. Whenever the current controller is falsified, the candidate controller with the best inferred behavior is switched on in feedback to the plant. From this synthetic outline the two main tasks of the supervisor clearly emerge.

Controller falsification (CF) [ST97] deals with the problem of deciding whether the current controller is adequate or not to the actual operating conditions. This binary decision problem is made possible by continuously monitoring the closed loop system variables in order to detect occurrence of poor tracking performance, poor transient behaviors and loss of stabilization [MA03]. By the way, when one or more of these negative conditions occur, the supervisor should be able to establish that the current controller is not suitable to regulate the plant any longer and should falsify the operating controller, viz. switch that controller out of the loop.

Inference of candidate loop behavior (ICLB) deals with the problem of inferring the behavior of a potential loop made up by a candidate controller connected in feedback to the plant. It should be made without directly checking the behavior of all candidate controllers through their effective use in the control system. Basically, the aim of the inference of candidate loop behavior is to order the candidate controllers following some suitable criterion in order to decide to which one it is better to switch to.

Both tasks, especially the second one, are usually accomplished using a performance index or a cost function whose value should be a measure of the ability of a candidate controller to achieve good performance when placed in the loop in feedback to the plant.

This thesis aims at designing cost functions to be used in an SSC context. Different classes of cost functions are proposed in order to tackle either the case of a multi model-based supervisor or the case of a performance-based one.

Two main aspects are taken into account in the cost functions design. From one hand, stability of the adaptive system, resulting by the SSC based on such cost functions, is addressed. At the same time, it is desirable that the adaptive control system, even though stable, exhibits satisfying performance. Hence, studies are carried out with the aim of assessing performance achievable by the use of SSC systems based on the designed cost functions.

Moreover, the use of the virtual reference concept forces a further differentiation in the cost functions design, in particular between the minimum-phase controller case and the non-minimum phase one.

The thesis is organized as follows: in Ch. 1 cost functions for a multi model-based supervisor are designed. In particular, a class of cost functions is proposed for the case of minimum-phase candidate controllers and a different one is studied for cases where non-minimum phase candidate controllers act. In both cases, stability and performance issues are dealt with. Ch. 2 follows the same conceptual scheme of Ch. 1, nevertheless a performance-based supervisor is supposed to operate. Ch. 3 proposes two cases of study in order to analyze the SSC resulting from the use of cost functions proposed in previous chapters. In particular, the muscle relaxation control of patients undergoing general anesthesia is instrumental to show results for the minimum-phase controller case. Instead, the position control of a classic mechanical plant is useful to analyze the non-minimum phase case. Finally, the conclusions of the presented work are drawn and some possible future research themes on the subject are suggested.

Chapter 1

Multi-model SSC

1.1 Introduction

Throughout this chapter it is assumed that the set \mathcal{P} of all possible plants to be controlled is available to the designer. Notice that this key assumption is not illusory as one could benefit, for instance, from past studies on the subject or physical knowledge of the process under control. Then in practice, one can partition, in accordance to some suitable criterion, the set \mathcal{P} in a finite number of regions \mathcal{P}_i , $i = 1, \dots, N$ such that:

$$\mathcal{P} = \bigcup_{i=1}^N \mathcal{P}_i$$

and associate to each region \mathcal{P}_i a representative model M_i that approximates the behavior of the plants belonging to that region. By this way, the set $\mathcal{M} = \{M_i, i = 1, \dots, N\}$ of approximating models can be obtained. Different criteria for partitioning the set \mathcal{P} and finding the approximating models are possible, nevertheless it is not of interest of this work to deal with them. The aim here is at designing a supervisory unit which, exploiting the knowledge of the approximating models, selects the controller to be placed in the loop, once the operating one is discovered yielding an unsatisfactory performance. In order to appropriately accomplish this task, the supervisor should operate in accordance to theoretical principles of controller

falsification and inference of candidate loop behavior. A recently presented methodology [AM02], which tackles the outlined problem keeping the supervisory tasks well separated, is briefly revised in that it is considered the starting point for this thesis work.

Let $\mathcal{M} = \{M_i, i = 1, \dots, N\}$ denote the set of discrete time, linear deterministic and, for the sake of simplicity, SISO approximating models described by a finite-difference equation of the form:

$$M_i : \quad A_i(d)y(t) = B_i(d)\delta u(t) \quad i \in \underline{N} \quad (1.1)$$

where: $t \in \mathbb{R}_+ := \{0, 1, \dots\}$ and $\underline{N} := \{1, \dots, N\}$. The signals $y(t)$, $\delta u(t)$ denote respectively the output and the input-increment of the model, $A_i(d) = \Delta(d)a_i(d)$, $\Delta(d) = 1 - d$ and $B_i(d)$ are polynomials in the backward shift operator d and they are supposed to be coprime polynomials. The presence of the $\Delta(d)$ is due to the fact that an incremental form of the model, and, as will be shown shortly, of the controller, is used. Incremental representations are customarily adopted for control design so as to ensure constant disturbance rejection and constant reference tracking.

One or more controllers are associated to each partition \mathcal{P}_i , $i \in \underline{N}$ in such a way that they satisfactorily manage to control each plant in that partition. Without loss of generality in the present work only one controller is associated to each partition and it is tuned, according to any control design procedure, on the corresponding model M_i . Then, the set $\mathcal{C} = \{C_i, i \in \underline{N}\}$ is obtained. Linear, one degree of freedom controllers are considered in this work of the form:

$$C_i : \quad R_i(d)\delta u(t) = S_i(d)(r(t) - y(t)) \quad i \in \underline{N} \quad (1.2)$$

where $r(t)$ is the reference signal that $y(t)$ should follow. The polynomials $R(d)$ and $S(d)$ are supposed to be coprime.

For the subsequent discussion it is convenient to introduce the following notations. (P/C_i) will indicate the feedback system where the plant P is controlled by C_i . Likewise, (M_i/C_i) will denote the feedback system composed by the model M_i and the controller C_i . The I/O variables of P produced when a generic controller $C_i \in \mathcal{C}$ is acting are $d_{*/i}(t) := [\delta u_{*/i}(t) \quad y_{*/i}(t)]'$ and, likewise, $d_{i/i}(t) := [\delta u_{i/i}(t) \quad y_{i/i}(t)]'$ will be the vector containing the I/O pairs of the loop (M_i/C_i) . Moreover, the notation $(P/\hat{C}(t, d))$ will be used to refer to the adaptive feedback control system, illustrated in Fig. 1.1, composed by the plant P and the adaptive time varying controller $\hat{C} \in \mathcal{C}$ chosen by the switching supervisory mechanism at each time instant. Data d are intended to be plant I/O data collected while $\hat{C}(t, d)$ is in the loop, as Fig. 1.1 shows. When there is no confusion, the adaptive controller will be simply denoted by \hat{C} .

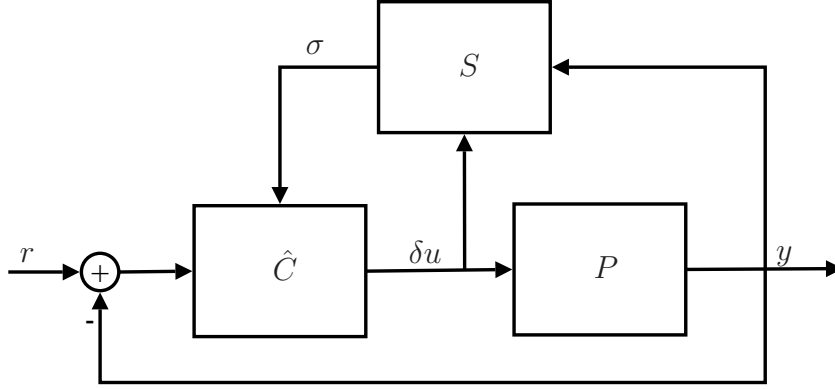


Figure 1.1. Basic scheme of the adaptive control system.

Definition 1.1.1. It is said that $x \in l_{2e}$ if:

$$\|x^t\|^2 := \sum_{\tau=0}^t |x(\tau)|^2 < \infty \quad \forall t < \infty$$

where $x^t := \{x(\tau)\}_{\tau=0}^t$ is the time truncation of $x(t)$ over the interval $[0, t]$ and $|x|$ is the Euclidean norm.

1.1.1 A controller falsification statistical test

In order to achieve a definite distinction between the supervisory tasks, a controller falsification test has been developed to assess whether the acting controller is falsified and, in the affirmative case, a cost function inferring the behavior of candidate controllers decides the next one to be switched on in the loop [AM02]. In particular, the controller falsification test is performed through a ratio, namely $g(t)$, calculated on the basis of closed loop variables, as follows:

$$g(t) := \frac{\|\varphi(t)\|}{\max |\varepsilon^t|} \quad (1.3)$$

where $\max |\varepsilon^t| := \max_{0 \leq \tau \leq t} |\varepsilon(\tau)|$ and $\varepsilon(t)$ is the output prediction error based on the plant model associated to the acting controller.

$\varphi(t) = [e(t) \cdots e(t-n) - \delta u(t-1) \cdots - \delta u(t-n)]$ is the regressor containing past samples of the tracking error $e(t) = r(t) - y(t)$ and the plant input increment. Such ratio has to be compared with a pre computed threshold T in order to detect instability or poor performance trend. The thresholds $T_i, i \in \underline{N}$ associated to each nominal loop can be a priori fixed by either computing analytic bounds or, in a sharper way, via appropriate simulation

studies. Some assumptions, extensively discussed in [MA03], guarantee that, whenever the current loop is stable $g(t)$ lies below the corresponding threshold with probability close to one, or, if the closed loop variables tend to diverge, it takes on values above the threshold with probability one.

Beyond its simplicity, another important feature of the test is the fact that, being expressed as a ratio of closed loop variables, it turns out to be insensitive to the noise intensity. This is particularly interesting because some noise has to be present in the loop in order to provide the required excitation for the test evaluation. To this end, such noise can be viewed as an intentionally injected dither whose intensity can be chosen arbitrarily small without affecting the test detection capability.

1.1.2 Discrepancy measure between feedback loops

Once the falsification test assesses that the acting controller is not suitable to control the plant any longer, the supervisor selects, among the remaining $N - 1$ candidate controllers, the “best” for the current operating conditions. This logic implicitly involves a sorting of the candidate controllers worthily reflecting their ability to achieve good performance if they were placed in feedback to the plant. To this end, usually, nevertheless not necessarily, a scalar valued cost function $V : \mathcal{C} \times \mathbb{D} \times \mathbb{R}_+ \mapsto \mathbb{R}_+$ where \mathbb{D} is the set of all possible plant data, is minimized in such a way that:

$$\sigma(t) = \arg \min_i V(C_i, d, t) \quad (1.4)$$

where $\sigma(t) \in \underline{N}$ is the index of the next controller to be placed in the loop. When no ambiguity arises $V(C_i, d, t)$ will be shorter denoted by $V_i(t)$.

In the Introduction a very seminal idea is recalled [Mor96, NB97] based on which the mean square of plant output prediction errors is used as a cost function in order to infer the behavior of the (P/C_i) candidate loop. Recall that:

$$\varepsilon_i(t) = A_i(d)y(t) - B_i(d)\delta u(t) \quad i \in \underline{N} \quad (1.5)$$

is the plant output prediction error based on model M_i , given data $y(t)$ and $\delta u(t)$ from the plant. In practice, the controller that yields the minimum of a time average of the prediction errors, viz. the controller corresponding to the model that best predicts the plant output at each instant, is inserted in the loop. This policy may involve a bad inference of candidate loop behavior in that a model, and hence the corresponding controller, which matches the plant behavior at high frequencies more than over the useful frequency band, is likely to be selected (see [MA01] for details).

In order to address the problem of inferring the behavior of a candidate loop, the preliminary question is how to quantitatively assess the performance of a generic loop (P/C_i) .

Hence, the design of a cost function suitable for measuring the performance of a closed loop is needed and the scheme in Fig. 1.2 is of great importance. Being the two loops different only for the plant block, any difference exhibited

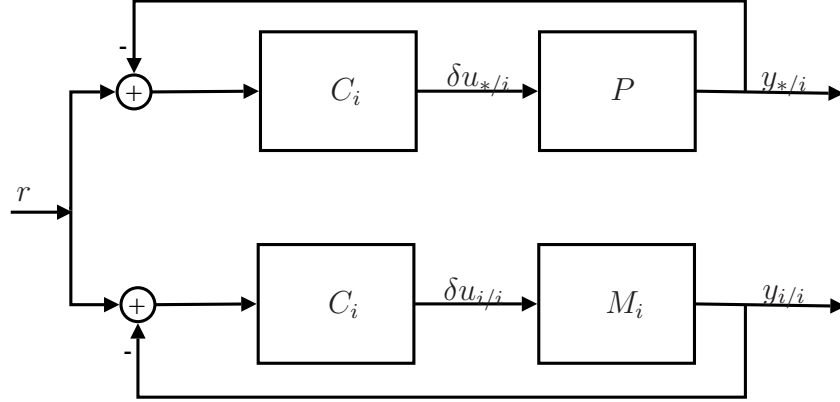


Figure 1.2. Actual loop (P/C_i) and tuned loop (M_i/C_i) for the controller C_i .

by their outputs $(y_{*/i}, y_{i/i})$ or their inputs $(\delta u_{*/i}, \delta u_{i/i})$ has to be caused by the discrepancy between P and M_i . Moreover, being intuitive that the closer (P/C_i) behaves to (M_i/C_i) the more adequate is the use of C_i for controlling P , a cost function which reflects the discrepancy between the behavior of the two loops appears suitable to be used. To this end, it seems reasonable to express the behavior of (P/C_i) over the time interval $[0, t]$ via the vector-valued variable $\zeta_{*/i}(\tau)$ [AM02]:

$$\zeta_{*/i}(\tau) := \begin{bmatrix} r(\tau) - y_{*/i}(\tau) \\ \rho_i^{1/2} \delta u_{*/i}(\tau) \end{bmatrix} \quad (1.6)$$

where $\rho_i > 0$ is an i -dependent input weight accounting for the relative importance in $\zeta_{*/i}(\tau)$ of $\delta u_{*/i}(\tau)$ with respect to $r(\tau) - y_{*/i}(\tau)$. Likewise, the behavior of (M_i/C_i) will be evaluated through $\zeta_{i/i}(\tau)$:

$$\zeta_{i/i}(\tau) := \begin{bmatrix} r(\tau) - y_{i/i}(\tau) \\ \rho_i^{1/2} \delta u_{i/i}(\tau) \end{bmatrix} \quad (1.7)$$

Hence, a possible measure of the relative discrepancy between the 2 feedback loops is:

$$V_i(t) = \frac{\|\tilde{\zeta}_{*/i}^t\|^2}{\|\zeta_{i/i}^t\|^2} \quad (1.8)$$

where $\tilde{\zeta}_{*/i}(\tau) = \zeta_{*/i}(\tau) - \zeta_{i/i}(\tau)$. For instance, the denominator in (1.8) results:

$$\|\zeta_{i/i}^t\|^2 = \sum_{\tau=0}^t |\zeta_{i/i}(\tau)|^2 = \sum_{\tau=0}^t \{[r(\tau) - y_{i/i}(\tau)]^2 + \rho_i \delta u_{i/i}^2(\tau)\} \quad (1.9)$$

Thus, the ratio (1.8) can quantify the behavior of (P/C_i) in that the smaller (1.8), the more adequate is C_i for controlling P on the basis of $[0, t]$ records. Consequently, if the quantities in (1.8) were available $\forall i \in \underline{N}$, then, accordingly to the supervisory logic (1.4), the controller which minimizes the relative discrepancy between (P/C_i) and (M_i/C_i) would be switched on in feedback to the plant.

As a matter of fact, the quantities in (1.6) are available only for the current operating loop. As a consequence, a practical use of the cost function in (1.8) would require the insertion of all candidate controllers in feedback to the plant in order to obtain the vector $\zeta_{*/i}(\tau)$ in (1.6). This procedure, commonly referred to as controllers *pre-routing*, involves an unsafe way of inferring the controllers behavior and should be consequently avoided.

1.2 The virtual reference use

The inference of candidate loop behavior should be performed without directly checking the behavior of each candidate controller via its effective use in the control system. It would be rather desirable the supervisor accomplish the task only exploiting plant data taken from the currently operating loop. As will be shown shortly, the virtual reference concept allows the supervisor to exploit a measure of the discrepancy between feedback loops via a cost function, similar to (1.8), whose calculation does not require the insertion of each candidate controller in feedback to the plant.

The virtual reference concept is not widespread in the automatic control field, possibly because it is only recently appeared in the literature [ST97, MA03, CLS02]. It is used in the SSC field, even though denoted with different names: *virtual reference signal* in [MA03], *fictitious reference signal* in [ST97] and *matching reference signal* in [Zha06]. Moreover, it is referred to as *virtual reference signal* also in [CLS02] even if there it is used for controller design purposes. Throughout the present discussion, it will be adopted the name of *virtual reference signal*.

1.2.1 The virtual reference concept

Beyond its different names and the slightly different definitions associated to it, the general idea underlying the virtual reference concept is widely accepted and it is well captured by the following definition [WPSS05]:

Definition 1.2.1. Given plant data $d := [\delta u \quad y]'$ and a candidate controller C_i , the *virtual reference signal* $\bar{r}(C_i, d)$ is the reference signal that would have produced data d had the candidate controller C_i been in feedback to the plant during the entire time period over which d were collected.

Where there is no confusion $\bar{r}(C_i, d)$ will be shorter denoted by \bar{r}_i . Fig. 1.3 shows the virtual closed loop associated to the foregoing definition.

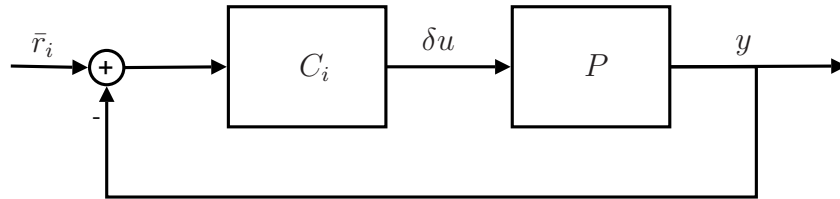


Figure 1.3. Virtual closed loop associated to the definition of \bar{r}_i .

Notice that data d are not necessarily produced by the loop in Fig. 1.3, hence the name of *virtual* loop. They can be either open or closed loop data collected during any kind of experiment. Nevertheless, if the i -th controller is actually in the loop over the entire time period over which the measured data $d = d_{*/i}$ were collected, than the i -th virtual reference signal would be the same as the actual reference signal r . Otherwise, it would be different and this is the reason it is called *virtual* for.

In accordance to Def. 1.2.1 and to Fig. 1.3, the virtual reference \bar{r}_i can be calculated as follows:

$$\bar{r}_i(t) = y(t) + C_i^{-1}\delta u(t) \quad (1.10)$$

or equivalently, in the case of linear controllers expressed in the polynomial form (1.2), \bar{r}_i is the signal which solves the following difference equation:

$$S_i(d)\bar{r}_i(t) = R_i(d)\delta u(t) + S_i(d)y(t) \quad (1.11)$$

Remark 1.2.2. In accordance to (1.10) or (1.11) it appears clear that the virtual reference calculation, involving the controller inversion, requires the controller to be stably invertible. Otherwise, the map $d \mapsto \bar{r}_i$ would turn out to be unstable, and hence numerically hard to calculate. A necessary condition for the controller to be causally stably invertible is phase-minimality and a zero I/O time-delay.

Notice that only open loop plant data or closed loop data $d = d_{*/h}$, collected for instance from a generic loop (P/C_h) , are necessary for the calculation of the virtual reference associated to a generic controller C as Fig. 1.4 shows.

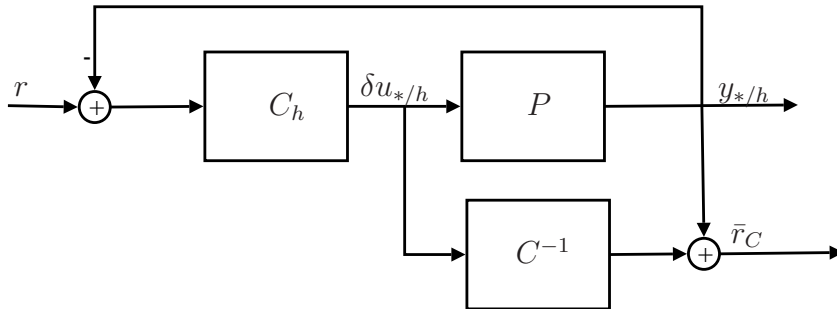


Figure 1.4. Hardware required for the virtual reference calculation in a very general case where data are taken from a closed loop system.

1.2.2 A cost function for joint falsification and inference

The virtual reference concept is important for practically exploiting the concepts illustrated in Sec. 1.1.2. To this end, Fig. 1.5 shows the same double loop of Fig. 1.2 driven by the virtual reference \bar{r}_i rather than the actual reference r . The two loops still differ only for the plant block, hence a cost

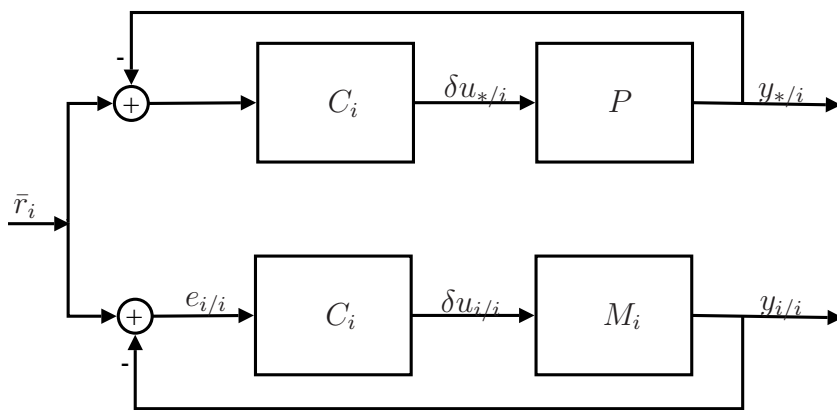


Figure 1.5. Actual loop and tuned loop for the controller C_i driven by \bar{r}_i .

function which measures the discrepancy between their I/O variables appears

a suitable way of inferring the behavior of the loop (P/C_i). Moreover, in accordance to Def. 1.2.1, being (P/C_i) driven by the virtual reference \bar{r}_i , its I/O pairs are the available I/O pairs recorded from the operating loop, let generically call them δu and y . In other words, it results: $\delta u_{*/i} = \delta u$ and $y_{*/i} = y$. Consequently, the undesirable real implementation of the upper loop in Fig. 1.5 can be avoided and only the lower nominal loop, which does not clearly present any trouble in a real implementation, actually works. By this way, the following vector-valued variables are obtained:

$$z_{*/i}(\tau) := \begin{bmatrix} \bar{r}_i(\tau) - y(\tau) \\ \rho_i^{1/2} \delta u(\tau) \end{bmatrix} \quad (1.12)$$

$$z_{i/i}(\tau) := \begin{bmatrix} \bar{r}_i(\tau) - y_{i/i}(\tau) \\ \rho_i^{1/2} \delta u_{i/i}(\tau) \end{bmatrix} \quad (1.13)$$

where \bar{r}_i is given by (1.10) and $z_{*/i}$ expresses the behavior of the candidate loop (P/C_i) and $z_{i/i}$ that of (M_i/C_i). They will replace respectively (1.6) and (1.7) and, consequently, the numerator in (1.8) will be replaced by $\|\tilde{z}_{*/i}^t\|^2$ where $\tilde{z}_{*/i}(\tau)$ is such that:

$$\tilde{z}_{*/i}(\tau) = z_{*/i}(\tau) - z_{i/i}(\tau) = \begin{bmatrix} -(y(\tau) - y_{i/i}(\tau)) \\ \rho_i^{1/2}(\delta u(\tau) - \delta u_{i/i}(\tau)) \end{bmatrix} =: \begin{bmatrix} -\eta_{y_i}(\tau) \\ \rho_i^{1/2} \eta_{u_i}(\tau) \end{bmatrix} \quad (1.14)$$

and:

$$\begin{aligned} \|\tilde{z}_{*/i}^t\|^2 &= \sum_{\tau=0}^t |\tilde{z}_{*/i}(\tau)|^2 = \\ &= \sum_{\tau=0}^t \{ [y(\tau) - y_{i/i}(\tau)]^2 + \rho_i [\delta u(\tau) - \delta u_{i/i}(\tau)]^2 \} \end{aligned} \quad (1.15)$$

Notice that (1.15), in contrast with the numerator of (1.8), turns out to be dependent on the level of the virtual reference \bar{r}_i . Such relation should be avoided in order to obtain a cost function which properly orders the candidate controllers. A controller should take advantage, with respect to another one, in consequence of an inferred better ability of achieving good performance once it was placed in feedback to the plant, and not from the particular level of the corresponding virtual reference. To this end, a normalization of (1.15) is required and a first straightforward solution is to divide it by the norm of the virtual reference, obtaining:

$$V_i(t) = \frac{\|\tilde{z}_{*/i}^t\|^2}{\|\bar{r}_i^t\|^2} \quad (1.16)$$

A slightly different cost function can be obtained dividing (1.15) by a measure

of the behavior of the i -th tuned loop, viz. the norm of the vector $z_{i/i}(\tau)$ in (1.13). Doing so, the following cost function is proposed:

$$V_i(t) = \frac{\|\tilde{z}_{*/i}^t\|^2}{\|z_{i/i}^t\|^2} = \frac{\|\eta_{y_i}^t\|^2 + \rho_i \|\eta_{u_i}^t\|^2}{\|e_{i/i}^t\|^2 + \rho_i \|\delta u_{i/i}^t\|^2} \quad (1.17)$$

This cost function does not depend on the virtual reference level and, moreover, is more similar to the one in (1.8) in that it is a measure of the relative discrepancy between the two feedback loops. Given $\delta u(t)$ and $y(t)$ from the operating loop, the scheme in Fig. 1.6 shows the supervisory logic necessary to produce all the signals involved in (1.17). A parallel implementation

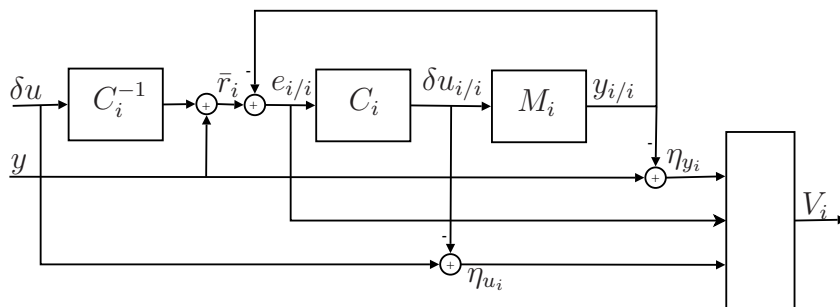


Figure 1.6. Figure shows the supervisory logic necessary to produce the cost function, V_i in (1.17), associated to the controller C_i .

of the same logic $\forall i \in \underline{N}$ permits the switching logic (1.4) to determine the next controller to be put in the loop, only providing input-output data $d = [\delta u \quad y]'$ from the operating loop.

However, it is worth noticing that cost function (1.17), requiring the virtual reference calculation, is suitable for minimum-phase controllers, as pointed out by Remark. 1.2.2. Nevertheless, different solutions that cope with this possible restrictive assumption will be analyzed in Sec. 1.3.

Although the foregoing reasonings give encouraging insights on the inference of candidate loop behavior capability of cost function (1.17), some more rigorous analysis will be carried out in Sec. 1.2.4.

In what concerns the controller falsification it should be noted that supervisory logic (1.4)-(1.17) guarantees falsification of an actively operating controller, namely C_h , that is destabilizing the plant, provided that the initial state and/or disturbances are such that unstable modes are actually excited. The cost function V_h in (1.17), related to that controller, gets actually unbounded. As a matter of fact, the numerator, containing data y and δu from the operating loop, is divergent. On the contrary, the denominator is

bounded as it contains the I/O variables of the h nominal loop driven by the true reference signal. That is because, according to Def. 1.2.1, the virtual reference signal related to the acting controller coincides to the true reference. Hence, there will be a time instant when the cost function V_h will exceed the level of at least one of the other cost functions and, consequently, the controller C_h will be switched out of the loop, viz. falsified.

On the other hand, unstable data collected while the same destabilizing controller is in the loop generally will not falsify the behavior of any other destabilizing candidate controller that is not actively operating in the loop. This is because for a C which is not operating in the feedback loop, unstable data may cause the denominator of the cost to diverge at the same exponential rate as the numerator, so that the cost function for an inactive controller will remain bounded even though that controller would be destabilizing if it were active. Thus, the ability of an inactive controller to stabilize the plant may not be falsified until after such future time as that controller is actually switched into the feedback loop.

These reasonings suggest the possibility of using an unique cost function for controller falsification and inference of candidate loop behavior purposes.

1.2.3 Stability issues

An SSC based on the minimization of cost function (1.17) does not prevent unstable candidate controllers from being switched on in the loop. Nevertheless, it guarantees that, once in operation, they are removed as soon as the instability is detected. In this case, the controller with the best inferred behavior replaces the falsified one. If the controller replacements occur too frequently, some destabilization effects may become possible. In order to cope with this situation, a first solution is the so called *dwell time* switching logic [Mor96] which imposes to wait for a dwell time after a switching instant before another switch be allowed. Although this is a very general solution, in that it is applicable to any kind of switching logic, it may be somehow criticized in that it inhibits the switching process regardless what is actually happening in the system. For instance, the performance of the currently active controller might deteriorate to an unacceptable level before the next switch is permitted or, if the unknown plant is nonlinear, the trajectories may even escape to infinity during the dwell time. These considerations motivate the study of switching algorithms that do not rely on a fixed dwell time. A possibility is the *hysteresis* switching logic described in [MMG92] where a switch occurs when the cost function related to the currently operating controller exceeds the smallest cost function by a prespecified positive number

ϵ , called *hysteresis constant*. In accordance to this principle, the switching logic in (1.4) is modified in such a way that:

$$\sigma(t) = \arg \min_i \{V_i(t) - \epsilon \delta_{i\sigma(t-1)}\} \quad (1.18)$$

where δ_{ij} is the Kronecker's δ . In this way, a greater chance is given to the currently operating controller to remain in the loop.

Hence, the hysteresis switching algorithm may limit the number of switches nevertheless, without any further assumption, it does not give any insurance whether the switching process eventually stops. In order to deal with this key point, the *Hysteresis Switching Lemma* in [MMG92] should be considered in that it represents a basic answer to the problem.

The lemma applies to a switched system of the form

$$\dot{x} = f_\sigma(x, t) \quad x(0) = x_0 \quad (1.19)$$

where $\sigma(t)$ switches among predefinite values in such a way that some cost function (called there test function) has certain desirable properties. The adopted switching algorithm is the hysteresis based one (1.18). Let $[0, T)$ be the interval of maximal length in which there is a unique pair (x, σ) , with x continuous and σ piecewise constant, which satisfy the problem constraints. The statement of the lemma goes as follows [MMG92]:

Lemma 1.2.3. *Hysteresis Switching Lemma* Under the following open loop assumptions:

1. For each switching sequence $s(t)$, each test function has a limit (which may be infinite) as $t \rightarrow T_s$, where T_s is the length of the maximal interval of existence for the solution to (1.19) corresponding to the switching sequence $s(t)$.
2. There exists at least one test function which, for each switching sequence $s(t)$, is bounded on $[0, T_s)$.

For fixed initial state (x_0, i_0) , let (x, σ) denote the unique solution to (1.19) and suppose that $[0, T)$ is the largest interval in which this solution is defined. Then, there is a time $T^* < T$ beyond which σ is constant and no more switching occurs. Moreover related test function is bounded on $[0, T)$.

In the sequel of the present section, Lemma 1.2.3 will be fitted to the discrete time case and used to prove that a hysteresis based switching logic

of the form (1.18) where:

$$V_i(t) = \max_{0 \leq \tau \leq t} \frac{\|\tilde{z}_{*/i}^\tau\|^2}{m_i + \|z_{i/i}^\tau\|^2} = \max_{0 \leq \tau \leq t} \frac{\left\| \begin{bmatrix} -\eta_{y_i}^\tau \\ \rho_i^{1/2} \eta_{u_i}^\tau \end{bmatrix} \right\|^2}{m_i + \left\| \begin{bmatrix} e_{i/i}^\tau \\ \rho_i^{1/2} \delta u_{i/i}^\tau \end{bmatrix} \right\|^2} = \max_{0 \leq \tau \leq t} J_i(\tau) \quad (1.20)$$

yields a stable control system, provided that some assumptions on \mathcal{C} and \mathcal{M} are satisfied.

Notice that the presence of the constants m_i and the maximum operator make the cost function (1.20) different from (1.17). The reason for the arbitrarily small positive constants m_i is to prevent the denominator from assuming values too close to zero. In fact, this situation may in practice occur as the denominator contains I/O variable taken from a tuned loop. On the other hand, the max operator, which obviously forces each cost function to be monotone non decreasing in time, is instrumental to the use of Lemma 1.2.3. Let \mathcal{S} denote the class of all piecewise constant functions $\sigma : \mathbb{R}_+ \mapsto \underline{N}$ and let the plant P be linear and described by a finite difference equation of the form:

$$A(d)y(t) = B(d)\delta u(t) \quad (1.21)$$

where $A(d) = \Delta(d)a(d)$ and $A(d)$, $B(d)$ are supposed to be coprime. Taking into account the following definition [WPSS05]:

Definition 1.2.4. A system G with input v and output w is said to be *stable* if for every input $v \in l_{2e}$ there exist constants β , $\alpha \geq 0$ such that:

$$\|w^t\| < \beta\|v^t\| + \alpha \quad \forall t > 0$$

Then, the main result of this section can be stated.

Lemma 1.2.5. Under the following assumptions:

1. Problem feasibility, viz. there exists at least one controller $C \in \mathcal{C}$ such that the feedback system (P/C) is stable.
2. For every $P \in \mathcal{P}$ there exists at least one stabilizing controller C whose matched model M_C has unstable poles which are also poles of P .

Then, for any switching sequence $\sigma(t) \in \mathcal{S}$ given by (1.18) and (1.20), the resulting adaptive control system $(P/\hat{C}(t, d))$ is stable, with inputs r and outputs d , where r and $d = [\delta u(t) \quad y(t)]'$ are shown in Fig. 1.1.

Proof. For any $\sigma(\cdot) \in \mathcal{S}$ and $\forall C_i \in \mathcal{C}$, $i \in \underline{N}$, the signals $\eta_{y_i}(\tau)$ and $\eta_{u_i}(\tau)$ in (1.20) can be conveniently written in terms of a suitable filtered version of the output prediction error [MA01]:

$$\eta_{y_i}(\tau) = y(\tau) - y_{i/i}(\tau) = \frac{R_i(d)}{\chi_i(d)} \varepsilon_i(\tau) \quad (1.22)$$

$$\eta_{u_i}(\tau) = \delta u(\tau) - \delta u_{i/i}(\tau) = -\frac{S_i(d)}{\chi_i(d)} \varepsilon_i(\tau) \quad (1.23)$$

where $\chi_i(d) := A_i(d)R_i(d) + B_i(d)S_i(d)$ is the characteristic polynomial of the i -th tuned loop (M_i/C_i). Moreover, the prediction error, $\varepsilon_i(\tau)$, in (1.5) can be equivalently rewritten, as a function of the virtual reference signal, taking into account the relations stated by Fig. 1.3, as follows:

$$\begin{aligned} \varepsilon_i(\tau) &= A_i(d)y(\tau) - B_i(d)\delta u(\tau) = A_i(d)\tilde{P}_i(d)\delta u(\tau) = \\ &= A_i(d)\tilde{P}_i(d)\frac{C_i(d)}{1 + P(d)C_i(d)}\bar{r}_i(\tau) \end{aligned} \quad (1.24)$$

where $\tilde{P}_i(d) := P(d) - M_i(d) = \frac{B(d)}{A(d)} - \frac{B_i(d)}{A_i(d)}$. By this way, it results:

$$\eta_{y_i}(\tau) = \frac{\tilde{P}_i(d)C_i(d)}{1 + P(d)C_i(d)} \frac{A_i(d)R_i(d)}{\chi_i(d)} \bar{r}_i(\tau) \quad (1.25)$$

$$\eta_{u_i}(\tau) = -\frac{\tilde{P}_i(d)C_i(d)}{1 + P(d)C_i(d)} \frac{A_i(d)S_i(d)}{\chi_i(d)} \bar{r}_i(\tau) \quad (1.26)$$

Let analyze the cost function related to a controller C which makes the closed loop (P/C) stable. Assumption 1 guarantees that at least one of such controllers exists in the set \mathcal{C} . Being the present goal to prove that this cost function is bounded on $[0, \infty)$, the max operator can be momentarily neglected. As a matter of fact, if $J_C(\tau)$ in (1.20) is shown to be bounded $\forall \tau \in [0, \infty)$, then $V_C(t)$ will be bounded too. To this end, omitting for the sake of simplicity the argument for all transfer functions, consider:

$$\begin{aligned} J_C(\tau) &= \frac{\left\| \begin{bmatrix} \frac{\tilde{P}_C C}{1+PC} & \frac{A_C R_C}{\chi_C} \\ \rho_C^{1/2} \frac{\tilde{P}_C C}{1+PC} & \frac{A_C S_C}{\chi_C} \end{bmatrix} \bar{r}_C^\tau \right\|^2}{m_i + \left\| \begin{bmatrix} \frac{A_C R_C}{\chi_C} \\ \rho_C^{1/2} \frac{A_C S_C}{\chi_C} \end{bmatrix} \bar{r}_C^\tau \right\|^2} \leq \frac{\left\| \begin{bmatrix} \frac{\tilde{P}_C C}{1+PC} & 0 \\ 0 & \frac{\tilde{P}_C C}{1+PC} \end{bmatrix} \begin{bmatrix} \frac{A_C R_C}{\rho_C^{1/2} \chi_C} \\ \frac{A_C S_C}{\chi_C} \end{bmatrix} \bar{r}_C^\tau \right\|^2}{\left\| \begin{bmatrix} \frac{A_C R_C}{\rho_C^{1/2} \chi_C} \\ \frac{A_C S_C}{\chi_C} \end{bmatrix} \bar{r}_C^\tau \right\|^2} \leq \\ &\leq \max_{\omega \in [-\pi, \pi]} \{ \bar{\lambda}(H_C^* H_C) \} = \max_{\omega \in [-\pi, \pi]} \left| \frac{\tilde{P}_C C}{1+PC} \right|^2 < \infty \end{aligned} \quad (1.27)$$

where:

$$H_C = \begin{bmatrix} \frac{\tilde{P}_C C}{1+PC} & 0 \\ 0 & \frac{\tilde{P}_C C}{1+PC} \end{bmatrix} \quad (1.28)$$

and $H_C^*(e^{j\omega}) = H'_C(e^{-j\omega})$ and $\bar{\lambda}(A)$ denotes the largest eigenvalue of matrix A . Notice that (1.27) holds provided that $\frac{\tilde{P}_C C}{1+PC}$ is stable. Hence, taking into account that:

$$\frac{\tilde{P}_C C}{1+PC} = \frac{PC}{1+PC} - \frac{M_C C}{1+PC} = \frac{PC}{1+PC} - \frac{aB_C S_C}{a_C \chi_{*/C}}$$

where $\chi_{*/C} := AR_C + BS_C$ is the characteristic polynomial of the feedback loop (P/C), then stability of $\frac{\tilde{P}_C C}{1+PC}$ follows from assumptions 1 and 2. It ensures that $J_C(\tau)$ is bounded $\forall \tau \geq 0$ and consequently also $V_C(t) = \max_{0 \leq \tau \leq t} J_C(\tau)$ is bounded $\forall t > 0$.

Each cost function, being forced by the max operator to be monotone non decreasing in time, admits a limit as $t \rightarrow \infty$, which can be possibly infinite. Moreover, assumption 1 guarantees that there exists at least one stabilizing controller and the foregoing reasonings prove that the corresponding cost function is bounded $\forall t > 0$. It ensures that the two assumptions stated by the Hysteresis Switching Lemma 1.2.3 are satisfied and, hence, it is guaranteed that there is a finite time, t_f , beyond which σ is constant and the cost function, V_f , related to the final controller, C_f , is bounded. Viz., there exists a positive real M such that $V_f(t) = \max_{0 \leq \tau \leq t} J_f(\tau) \leq M$, $\forall t \geq t_f$. Last inequality is equivalent to the existence of $0 < M_1, M_2 < \infty$ such that:

$$\frac{\|\eta_{y_f}\|^2}{m_f + \|e_{f/f}\|^2 + \rho_f \|\delta u_{f/f}\|^2} \leq M_1 \quad , \quad \frac{\|\eta_{u_f}\|^2}{m_f + \|e_{f/f}\|^2 + \rho_f \|\delta u_{f/f}\|^2} \leq M_2 \quad (1.29)$$

Being $\frac{A_f R_f}{\chi_f}$ and $\frac{A_f S_f}{\chi_f}$ stable transfer functions by construction, then there exist positive reals L_1 and L_2 such that:

$$\begin{aligned} \frac{\|e_{f/f}\|^2}{\|\bar{r}_f\|^2} &\leq \max_{\omega \in [-\pi, \pi]} \left| \frac{A_f R_f}{\chi_f} \right|^2 = L_1 < \infty \\ \frac{\|\delta u_{f/f}\|^2}{\|\bar{r}_f\|^2} &\leq \max_{\omega \in [-\pi, \pi]} \left| \frac{A_f S_f}{\chi_f} \right|^2 = L_2 < \infty \end{aligned}$$

Hence, considering the first inequality in (1.29), it results:

$$\frac{\|y - y_{f/f}\|^2}{m_f + (L_1 + \rho_f L_2) \|\bar{r}_f\|^2} \leq M_1 \Leftrightarrow \|y - y_{f/f}\|^2 \leq T_1 + T_2 \|\bar{r}_f\|^2$$

where $0 < T_1 = m_f M_1$ and $0 < T_2 = (L_1 + \rho_f L_2) M_1$ are positive reals. By applying the triangular inequality, it results:

$$\begin{aligned} \|y - y_{f/f}\| &\leq T_1^{1/2} + T_2^{1/2} \|\bar{r}_f\| \Rightarrow \|y\| \leq T_1^{1/2} + T_2^{1/2} \|\bar{r}_f\| + \|y_{f/f}\| \Rightarrow \\ \|y\| &\leq T_1^{1/2} + \left(T_2^{1/2} + \max_{\omega \in [-\pi, \pi]} \left| \frac{B_f S_f}{\chi_f} \right| \right) \|\bar{r}_f\| \Rightarrow \|y\| \leq \bar{T}_1 + \bar{T}_2 \|\bar{r}_f\| \end{aligned} \quad (1.30)$$

Considering the second inequality in (1.29) and following the same conceptual lines, it can be proved that:

$$\|\delta u\| \leq \bar{K}_1 + \bar{K}_2 \|\bar{r}_f\| \quad (1.31)$$

The virtual reference signal \bar{r}_f related to the final constant controller tends to the true reference signal as $t \rightarrow \infty$, viz. there exists a real α such that [WPSS05]:

$$\|\bar{r}_f^t\| \leq \|r^t\| + \alpha \quad \forall t \geq 0$$

then, inequalities (1.30) and (1.31) become:

$$\|y\| \leq (\bar{T}_1 + \alpha \bar{T}_2) + \bar{T}_2 \|r\| \quad , \quad \|\delta u\| \leq (\bar{K}_1 + \alpha \bar{K}_2) + \bar{K}_2 \|r\|$$

It concludes the proof. \square

The choice of the hysteresis constant ϵ in (1.18) is crucial in order to obtain an effective hysteresis based switching criterion. For instance, a value of ϵ lower than the order of magnitude of the cost functions will not produce any effect. Moreover, the foregoing switching criterion does not fulfill the so called *scale-independence* property which is key to prove the correctness of an adaptive switching algorithm when it operates in the presence of noise or input disturbances [Mor96]. These considerations motivated the proposal of a multiplicative hysteresis constant [Hes98], rather than an additive one as in (1.18), which results in the following *scale-independent hysteresis* or *multiplicative hysteresis* switching logic:

$$\sigma(t) = \arg \min_i \{ (1 - \epsilon \delta_{i\sigma(t-1)}) V_i(t) \} \quad (1.32)$$

The logic (1.32) operates reducing the value of the cost function related to the acting controller of $(1 - \epsilon)$ times and, in that, it is slightly different from the one originally proposed in [Hes98] which increases by h times the cost function of each non operating controller. Nevertheless, it can be easily proved that the two logics are the same for suitable choices of ϵ and h , taking into account that ϵ , based on (1.32), is constrained in the set $[0, 1)$.

In [Hes98] the same conclusions of the *Hysteresis Switching Lemma* 1.2.3 are derived in the case where a multiplicative hysteresis switching logic is used. To this end, besides the two assumptions already present in Lemma 1.2.3, a third one is stated which forces each cost function to be bounded below by a positive constant (see Th. 4.2 in [Hes98] for details). Taking it into account, the following corollary of the Lemma 1.2.5 can be easily proved:

Corollary 1.2.6. Under the following assumptions:

1. Problem feasibility, viz. there exists at least one controller $C \in \mathcal{C}$ such that the feedback system (P/C) is stable.
2. For every $P \in \mathcal{P}$ there exists at least one stabilizing controller C whose matched model M_C has unstable poles which are also poles of P .
3. There exists a positive constant ξ such that $V_i(t) \geq \xi, \forall t \geq 0, i \in \underline{N}$

then, for any switching sequence $\sigma(\tau) \in \mathcal{S}$ given by (1.32) and (1.20), the resulting adaptive control system $(P/\hat{C}(t, d))$ is stable, with inputs r and outputs d , where r and $d = [\delta u(t) \quad y(t)]'$ are shown in Fig. 1.1.

Proof. Boundedness of the cost function related to the stabilizing controller C is proved identically to the proof of Lemma 1.2.5. This result, the presence of monotone non decreasing in time cost functions and assumption 3 guarantee, based on Th. 4.2 in [Hes98], that there exists a finite time beyond which σ is constant and the cost function related to the corresponding final controller is bounded. Then, stability is derived exactly as shown in the proof of Lemma 1.2.5. \square

Remark 1.2.7. Notice that the presence of the max operator in the cost functions (1.20) is such that a single instant of time where $y(t)$ is different from $y_{i/i}(t)$ or $\delta u(t)$ is different from $\delta u_{i/i}(t)$ is enough to fulfill assumption 3 from that time onwards. Any kind of noise, always present in practical applications, will prevent the cost function (1.20) from assuming zero values $\forall t \geq 0$. Moreover, even in the ideal case only a plant exactly coinciding to one of the approximating models and starting from the same initial conditions will produce zero values in the cost function.

1.2.4 Performance analysis

Stability issues are definitely crucial for adaptive control algorithms. Nevertheless, also the capability of such algorithms of ensuring good performance to the overall controlled system, is worth to be dealt with. Very often it is

hard to establish whether the performance achieved by a system has reached a good level in that a great deal of variables may influence this decision.

In what concerns the SSC algorithms a preliminary study is to assess, based on some suitable criterion, whether the candidate controllers are correctly sorted. In other words, once the currently operating controller is falsified, one should have some guarantee that the controller selected as the one which minimizes the cost function is suitable to control the plant, possibly in a better way than the others.

Hence, a steady-state analysis of the cost function (1.17) wherein the max operator and the m_i constant are omitted, is useful in order to have some insight on the inference capability of candidate loop behavior. To this end, it is useful to write all quantities involved in (1.17) with respect to the virtual reference signal. Taking into account (1.25) and (1.26), it results:

$$\begin{aligned}\|\tilde{z}_{*/i}^t\|^2 &= \left\| \left[\begin{array}{c} \frac{\tilde{P}_i C_i}{1 + P C_i} \frac{1}{1 + M_i C_i} \\ \rho_i^{1/2} \frac{\tilde{P}_i C_i}{1 + P C_i} \frac{C_i}{1 + M_i C_i} \end{array} \right] \bar{r}_i^t \right\|^2 \\ \|\tilde{z}_{i/i}^t\|^2 &= \left\| \left[\begin{array}{c} 1 \\ \rho_i^{1/2} \frac{C_i}{1 + M_i C_i} \end{array} \right] \bar{r}_i^t \right\|^2\end{aligned}$$

Letting $t \rightarrow \infty$, supposing that all the involved signals are stationary and omitting the argument $e^{j\omega}$ for all transfer functions, it results:

$$\begin{aligned}J_i = \lim_{t \rightarrow \infty} \frac{\|\tilde{z}_{*/i}^t\|^2}{\|\tilde{z}_{i/i}^t\|^2} &= \frac{\frac{1}{2\pi} \int_{-\pi}^{\pi} \left| \frac{\tilde{P}_i C_i}{1 + P C_i} \right|^2 \frac{1 + \rho_i |C_i|^2}{|1 + M_i C_i|^2} \Phi_{\bar{r}_i}(\omega) d\omega}{\frac{1}{2\pi} \int_{-\pi}^{\pi} \frac{1 + \rho_i |C_i|^2}{|1 + M_i C_i|^2} \Phi_{\bar{r}_i}(\omega) d\omega} = \\ &= \frac{1}{2\pi} \int_{-\pi}^{\pi} \left| \frac{\tilde{P}_i C_i}{1 + P C_i} \right|^2 \frac{1 + \rho_i |C_i|^2}{|1 + M_i C_i|^2} \Phi_{\bar{r}_i}(\omega) d\omega\end{aligned}\quad (1.33)$$

where $\Phi_{\bar{r}_i}(\omega)$ is the power spectral density of \bar{r}_i and:

$$\overline{|\Sigma_i|^2 \Phi_{\bar{r}_i}(\omega)} = \frac{\frac{1 + \rho_i |C_i|^2}{|1 + M_i C_i|^2} \Phi_{\bar{r}_i}(\omega)}{\frac{1}{2\pi} \int_{-\pi}^{\pi} \frac{1 + \rho_i |C_i|^2}{|1 + M_i C_i|^2} \Phi_{\bar{r}_i}(\omega) d\omega}\quad (1.34)$$

is a quantity, normalized over the whole range of frequencies in that: $\frac{1}{2\pi} \int_{-\pi}^{\pi} |\Sigma_i|^2 \Phi_{\bar{r}_i}(\omega) d\omega = 1$. In particular, notice that:

$$\Sigma_i(d) = \begin{bmatrix} \frac{1}{1 + M_i(d)C_i(d)} \\ \rho_i^{1/2} \frac{C_i(d)}{1 + M_i(d)C_i(d)} \end{bmatrix} = \begin{bmatrix} \frac{A_i(d)R_i(d)}{\chi_i(d)} \\ \rho_i^{1/2} \frac{A_i(d)S_i(d)}{\chi_i(d)} \end{bmatrix} \quad (1.35)$$

is called the vector-valued *mixed sensitivity* of (M_i/C_i) in that its first component is the *sensitivity* and the second is the *input sensitivity* of (M_i/C_i) . Hence, $\left| \frac{\tilde{P}_i C_i}{1 + P C_i} \right|^2$, being weighted by the normalized dynamic weight $|\Sigma_i|^2 \Phi_{\bar{r}_i}(\omega)$, is more penalized at frequencies where the nominal loops have a large mixed sensitivity.

In order to further analyze (1.33), it is worth recalling a robust stability property [GGs01]. It states that, given a stable nominal loop (M_i/C_i) , a sufficient condition for stability of the loop (P/C_i) is the following:

$$\left| \frac{\tilde{P}_i(e^{j\omega})C_i(e^{j\omega})}{1 + M_i(e^{j\omega})C_i(e^{j\omega})} \right| < 1 \quad \forall \omega \quad (1.36)$$

provided that $M_i C_i$ and $P C_i$ have the same number of unstable poles. Notice that: $\left| \frac{\tilde{P}_i C_i}{1 + P C_i} \right| = \left| \frac{\tilde{P}_i C_i}{1 + \tilde{P}_i C_i + M_i C_i} \right| \simeq \left| \frac{\tilde{P}_i C_i}{1 + M_i C_i} \right|$ where the last approximation holds, provided that:

$$\left| \frac{\tilde{P}_i(e^{j\omega})C_i(e^{j\omega})}{1 + M_i(e^{j\omega})C_i(e^{j\omega})} \right| \ll 1 \quad \forall \omega \quad (1.37)$$

Then, if the model set \mathcal{M} is chosen in such a way that, for any given (expected) P , there is at least an M_i so as to satisfy (1.37), minimizing (1.33) may amount to make small the quantity on the LHS of (1.36). Thus, minimization of a cost function whose steady-state value is shown in (1.33) does not imply the robust property (1.36), but gives favorable insights on the related controller selection criterion.

Hence, the cost function in (1.20) can be reasonably used for a joint falsification and inference in an SSC context. That cost function clearly diverges when an operating controller is actually destabilizing the plant with a consequent falsification of the controller. It will be replaced by the one which minimizes a relative discrepancy, over a time interval, between the candidate loop and the corresponding nominal loop. This logic, which appears intuitively suitable, has been confirmed by some rigorous analysis. Moreover, Lemma 1.2.5 guarantees that the adaptive switching system, resulting by

the use of the hysteresis switching algorithm (either the additive one (1.18) or the multiplicative (1.32)) where the cost function is given by (1.20), is stable.

1.3 The non-minimum phase controller case

The approach presented in Sec. 1.2 is based on the virtual reference concept. This notion permits the supervisory logic to infer the behavior of a candidate controller without physically inserting it in feedback to the plant. That is because, based on Def. 1.2.1, the I/O plant data obtained by a candidate loop (P/C) when it is driven by the virtual reference associated to the controller C , are the same produced by the currently operating loop.

Even though possible non-phase minimality of the controller does not affect this concept, nevertheless, as pointed out by Remark 1.2.2, it makes the virtual reference calculation unadvisable because the map $d \mapsto \bar{r}_i, i \in \underline{N}$ turns out to be unstable. This fact motivates a revision of the approach presented in Sec. 1.2 in order to find a cost function which is computable in the case of non-minimum phase controllers, while preserves controller falsification and inference of candidate loop behavior capabilities and guarantees stability of the adaptive system.

To this end, it is worth noticing that, being the virtual reference concept not affected by the non-phase minimality of the controller, a cost function of the form (1.17) appears still reasonable to measure the relative discrepancy between the two feedback loops in Fig. 1.5. The numerator of (1.17) does not require the virtual reference calculation in that it can be obtained by filtering the output prediction errors, as shown by Eqs. (1.22) and (1.23). On the contrary, the evaluation of the denominator in (1.17) requires the virtual reference signal \bar{r}_i driving the nominal loop (M_i/C_i), $i \in \underline{N}$ in order to collect the resulting I/O pairs. A solution to this problem, already present in literature [MA01], replaces the denominator by the following approximation:

$$\bar{J}_i = \frac{1}{2\pi} \int_{-\pi}^{\pi} \left| \frac{A_i(e^{j\omega})L_i(e^{j\omega})}{\chi_i(e^{j\omega})} \right|^2 d\omega = \frac{1}{2\pi} \int_{-\pi}^{\pi} |\Sigma_i(e^{j\omega})|^2 d\omega \quad , \quad i \in \underline{N} \quad (1.38)$$

where Σ_i is given by (1.35) and L_i is a solution of the following spectral factorization problem [Mos95]:

$$L_i(d^{-1})L_i(d) = R_i(d^{-1})R_i(d) + \rho_i S_i(d^{-1})S_i(d) \quad (1.39)$$

The consequent cost function is:

$$V_i(t) = \frac{\|\tilde{z}_{*/i}^t\|^2}{\bar{J}_i} = \frac{\|\eta_{y_i}^t\|^2 + \rho_i \|\eta_{u_i}^t\|^2}{\bar{J}_i} \quad (1.40)$$

Notice that (1.38) can be computed off-line in that it is not dependent on experimental data but only on nominal loops knowledge. In order to capture the significance of the approximation (1.38), it is worth pointing out that, for the denominator of (1.8) it results:

$$\lim_{t \rightarrow \infty} \|\zeta_{i/i}^t\|^2 = \frac{1}{2\pi} \int_{-\pi}^{\pi} \left| \frac{A_i(e^{j\omega})L_i(e^{j\omega})}{\chi_i(e^{j\omega})} \right|^2 \Phi_r(\omega) d\omega$$

Then (1.38) amounts to evaluate the denominator of (1.8) for large t under the assumption that $\Phi_r(\omega)$ is constant at frequencies where $\frac{A_i(e^{j\omega})L_i(e^{j\omega})}{\chi_i(e^{j\omega})}$ is non negligible.

Inference of candidate loop behavior capability of cost function (1.40) is investigated in [MA01] and some favorable results are found out. In fact, suppose that all the involved signals are stationary and consider the steady-state value of the cost function in (1.40), omitting the argument for all transfer functions, it results:

$$\begin{aligned} \lim_{t \rightarrow \infty} V_i(t) &= \frac{\frac{1}{2\pi} \int_{-\pi}^{\pi} \left| \frac{1}{\chi_i} \right|^2 [|R_i|^2 + \rho_i |S_i|^2] \Phi_\varepsilon(\omega) d\omega}{\bar{J}_i} \\ &= \frac{1}{2\pi} \int_{-\pi}^{\pi} |\bar{L}_i|^2 \Phi_\varepsilon(\omega) d\omega = \frac{1}{2\pi} \int_{-\pi}^{\pi} |A_i \bar{L}_i|^2 |\tilde{P}_i|^2 \Phi_{\delta_u}(\omega) d\omega \end{aligned} \quad (1.41)$$

where $\bar{L}_i(d) = \frac{L_i(d)}{\chi_i(d) \bar{J}_i^{1/2}}$ and $|A_i(e^{j\omega}) \bar{L}_i(e^{j\omega})|^2 = \overline{|\Sigma_i|^2}$ is the normalized square norm of the mixed sensitivity of the loop (M_i/C_i), given by (1.35). Hence, the relevant quantity $|\tilde{P}_i(e^{j\omega})| = |P(e^{j\omega}) - M_i(e^{j\omega})|$ is weighted by the normalized weight $\overline{|\Sigma_i|^2}$ in such a way that a greater concern is posed on the model mismatch over those frequencies where the i -th tuned loop is more vulnerable to disturbances (see [MA01] for details).

In order to address the controller falsification capability, suppose that the acting controller C_h is actually destabilizing the plant. It should be noted that the cost function $V_h(t)$ in (1.40) diverges. Nevertheless, contrarily to what happens using cost function (1.17), any other $V_i, i \in \underline{N}$ is divergent as well, because of the constant in time denominator. This fact may involve an indefinite distinction between the values of the cost function related to the currently destabilizing controller and those related to the other non operating controllers. As a consequence, the controller switched out of the loop by the supervisory logic may be unpredictable. These considerations partly motivate the use of the falsification test described in Sec. 1.1.1 in order to

support a supervisory logic which performs the inference of candidate loop behavior by means of a cost function of the form (1.40) [AM02]. Moreover, it should be noticed that cost function (1.40) does not permit to exploit the conclusions of the Hysteresis Switching Lemma 1.2.3 in that assumption 2 may not be verified in this case $\forall \sigma(\cdot) \in \mathcal{S}$.

1.3.1 A cost function for joint falsification and inference

Approximation (1.38) should be avoided in order to obtain a cost function which recovers the significance of relative measure of the discrepancy between feedback loops and enables to prove a stability result similar to that stated by Lemma 1.2.5.

It has been already noticed that the evaluation of vector $\tilde{z}_{*/i}(\tau)$ in (1.14) does not present any trouble in the case of non-minimum phase controllers. Hence, the problem reduces at finding a measure of the behavior of the nominal loop in Fig. 1.5 which does not require the virtual reference calculation. To this end, it is worth noticing that the I/O variables of that nominal loop, $y_{i/i}(\tau)$ and $\delta u_{i/i}(\tau)$ can be obtained by difference from Eqs. (1.22) and (1.23):

$$y_{i/i}(\tau) = y(\tau) - \eta_{y_i}(\tau) = y(\tau) - \frac{R_i(d)}{\chi_i(d)} \varepsilon_i(\tau) \quad (1.42)$$

$$\delta u_{i/i}(\tau) = \delta u(\tau) - \eta_{u_i}(\tau) = \delta u(\tau) + \frac{S_i(d)}{\chi_i(d)} \varepsilon_i(\tau) \quad (1.43)$$

By this way, the following cost function is proposed:

$$V_i(t) = \frac{\|\tilde{z}_{*/i}^t\|^2}{\|\gamma_{i/i}^t\|^2} = \frac{\|\eta_{y_i}^t\|^2 + \rho_i \|\eta_{u_i}^t\|^2}{\|\delta y_{i/i}^t\|^2 + \rho_i \|\delta u_{i/i}^t\|^2} \quad (1.44)$$

where $\gamma_{i/i}(\tau)$ is such that:

$$\gamma_{i/i}(\tau) = \begin{bmatrix} \delta y_{i/i}(\tau) \\ \rho_i^{1/2} \delta u_{i/i}(\tau) \end{bmatrix} \quad (1.45)$$

and represents a possible measure of the nominal loop behavior to be used in the place of $z_{i/i}(\tau)$ given by (1.13). The reason for the presence of $\delta y_{i/i}(\tau) = \Delta(d)y_{i/i}(\tau)$ rather than $y_{i/i}(\tau)$ in the vector $\gamma_{i/i}(\tau)$ is to avoid a polarization of $\gamma_{i/i}(\tau)$ due to a possible non zero steady-state value of $y_{i/i}$. Given $\delta u(t)$ and $y(t)$ from the acting loop, the scheme in Fig. 1.7 shows the supervisory logic necessary to produce all the signals involved in (1.44). A parallel implementation of the same logic $\forall i \in \underline{N}$ permits the switching logic

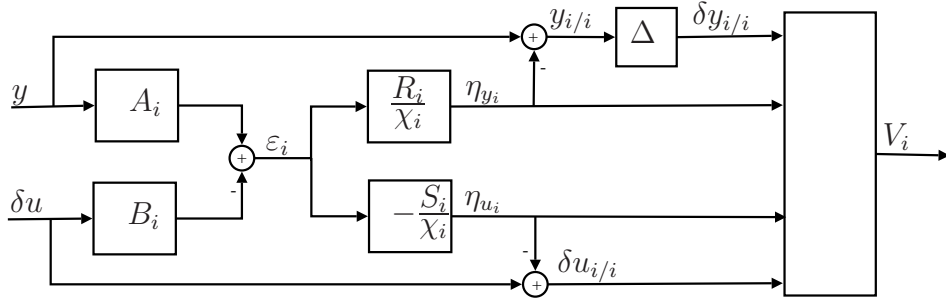


Figure 1.7. Figure shows the supervisory logic necessary to produce the cost function, V_i in (1.44) associated to the controller C_i .

(1.4) to determine the next controller to be put in the loop, only providing input-output data $[\delta u \quad y]'$ from the operating loop. Notice that any inversion of the controller is required and, hence, the procedure turns out to be suitable also for non-minimum phase controllers.

Supervisory logic (1.4)-(1.44) theoretically guarantees the falsification of a controller C_h that is actually destabilizing the plant. That is because, similarly to the reasonings already carried out to the same aim in Sec. 1.2.2, the cost function V_h in (1.44), related to that controller, gets actually unbounded. As a matter of fact, the numerator, containing data y and δu from the operating loop, is divergent. In what concerns the signals contained in the denominator, they can still be theoretically viewed as I/O variables of the h nominal loop driven by the true reference signal. That is because Def. 1.2.1 is not affected by the controller non-phase minimality. As a consequence, the virtual reference related to the acting controller coincides to the true reference and the denominator results bounded. Nevertheless, it should be noticed that being the variables $y_{i/i}(\tau)$ and $\delta u_{i/i}(\tau)$ practically calculated as a difference of diverging quantities, they may diverge as well. In order to deal with this point, the reader is referred to Ch. 3 where some simulative results will support more accurate conclusions on what actually happens in practice.

It has already been pointed out in Sec. 1.2.2 that unstable data collected with the same destabilizing controller in the loop generally will not falsify any other destabilizing controller which is not actively operating in the loop. In fact, also in this case, unstable data may cause the denominator of the cost to diverge at the same exponential rate as the numerator, so that the cost for an inactive controller will remain bounded even though that controller would be destabilizing if it were active.

1.3.2 Stability issues

Cost function (1.44) appears suitable to be used in the case of non-minimum phase controllers in that any inversion of the controllers is required for its calculation. Hence, it is worth analyzing stability results which can be achieved in an SSC driven by the minimization of such a cost function. To this end, a hysteresis based switching logic of the form (1.18) is supposed to act and the cost function is modified, in accordance to (1.20), to as:

$$V_i(t) = \max_{0 \leq \tau \leq t} \frac{\|\tilde{z}_{*/i}^\tau\|^2}{m_i + \|\gamma_{i/i}^\tau\|^2} = \max_{0 \leq \tau \leq t} \frac{\left\| \begin{bmatrix} -\eta_{y_i}^\tau \\ \rho_i^{1/2} \eta_{u_i}^\tau \end{bmatrix} \right\|^2}{m_i + \left\| \begin{bmatrix} \delta y_{i/i}^\tau \\ \rho_i^{1/2} \delta u_{i/i}^\tau \end{bmatrix} \right\|^2} = \max_{0 \leq \tau \leq t} J_i(\tau) \quad (1.46)$$

In this way, taking into account the linear plant form (1.21) and Def. 1.2.4, the main result of this section is the following:

Lemma 1.3.1. Under the following assumption:

1. Problem feasibility, viz. there exists at least one controller $C \in \mathcal{C}$ such that the feedback system (P/C) is stable.

For any switching sequence $\sigma(t) \in \mathcal{S}$ given by (1.18) and (1.46), the resulting adaptive control system $(P/\hat{C}(t, d))$ is stable, with inputs r and outputs d , where r and $d = [\delta u(t) \quad y(t)]'$ are shown in Fig. 1.1.

Proof. For any switching sequence $\sigma(t) \in \mathcal{S}$ and $\forall C_i \in \mathcal{C}$, $i \in \underline{N}$, all signals in (1.46) can be conveniently written in terms of $\bar{v}_i(\tau) := S_i(d)y(\tau) + R_i(d)\delta u(\tau) = S_i(d)\bar{r}_i(t)$. Hence, omitting the argument for all transfer func-

tions, it results:

$$\begin{aligned}\eta_{y_i}(\tau) &= \frac{R_i}{\chi_i} \varepsilon_i(\tau) = \frac{\tilde{P}_i C_i}{1 + P C_i} \frac{1}{M_i C_i} \frac{B_i}{\chi_i} (S_i y(\tau) + R_i \delta u(\tau)) = \\ &= \frac{R_i}{\chi_{*/i} \chi_i} (a_i B - a B_i) \delta \bar{v}_i(\tau)\end{aligned}\quad (1.47)$$

$$\begin{aligned}\eta_{u_i}(\tau) &= -\frac{S_i}{\chi_i} \varepsilon_i(\tau) = -\frac{\tilde{P}_i C_i}{1 + P C_i} \frac{A_i}{\chi_i} (S_i y(\tau) + R_i \delta u(\tau)) = \\ &= -\frac{S_i}{\chi_{*/i} \chi_i} (a_i B - a B_i) \delta \bar{v}_i(\tau)\end{aligned}\quad (1.48)$$

$$\begin{aligned}\delta y_{i/i}(\tau) &= \Delta(y(\tau) - \eta_{y_i}(\tau)) = \frac{\Delta B_i}{\chi_i} (S_i y(\tau) + R_i \delta u(\tau)) = \\ &= \frac{B_i}{\chi_i} \delta \bar{v}_i(\tau)\end{aligned}\quad (1.49)$$

$$\begin{aligned}\delta u_{i/i}(\tau) &= \delta u(\tau) - \eta_{u_i}(\tau) = \frac{A_i}{\chi_i} (S_i y(\tau) + R_i \delta u(\tau)) = \\ &= \frac{a_i}{\chi_i} \delta \bar{v}_i(\tau)\end{aligned}\quad (1.50)$$

where $\chi_{*/i}$, χ_i are the characteristic polynomials of respectively (P/C_i) and (M_i/C_i) and $\delta \bar{v}_i(\tau) = \Delta(d) \bar{v}_i(\tau)$ are the increment of $\bar{v}_i(\tau)$. Let analyze the cost function related to a controller C which makes the closed loop (P/C) stable. Assumption 1 guarantees that at least one of such controllers exists in the set \mathcal{C} . Being the present goal to prove that this cost function is bounded on $[0, \infty)$, the max operator can be momentarily neglected. As a matter of fact, if $J_C(\tau)$ in (1.46) is shown to be bounded $\forall \tau \in [0, \infty)$, then $V_C(t)$ will be bounded too. To this end, consider:

$$J_C(\tau) = \frac{\left\| \begin{bmatrix} -\eta_{y_C}^\tau \\ \rho_C^{1/2} \eta_{u_C}^\tau \end{bmatrix} \right\|^2}{m_C + \left\| \begin{bmatrix} \delta y_{C/C}^\tau \\ \rho_C^{1/2} \delta u_{C/C}^\tau \end{bmatrix} \right\|^2} \leq \frac{\left\| \begin{bmatrix} -\eta_{y_C}^\tau \\ \rho_C^{1/2} \eta_{u_C}^\tau \end{bmatrix} \right\|^2}{\left\| \begin{bmatrix} \delta y_{C/C}^\tau \\ \rho_C^{1/2} \delta u_{C/C}^\tau \end{bmatrix} \right\|^2}\quad (1.51)$$

In what concerns the numerator, using Eqs. (1.47) and (1.48), there exists a

positive M such that:

$$\begin{aligned}
\left\| \begin{bmatrix} -\eta_{y_C}^\tau \\ \rho_C^{1/2} \eta_{u_C}^\tau \end{bmatrix} \right\|^2 &= \left\| \begin{bmatrix} -\frac{R_C}{\chi_{*/C} \chi_C} (a_C B - a B_C) \\ -\rho_C^{1/2} \frac{S_C}{\chi_{*/C} \chi_C} (a_C B - a B_C) \end{bmatrix} \delta \bar{v}_C^\tau \right\|^2 \leq \\
&\leq \max_{\omega \in [-\pi, \pi]} \left(\frac{(|R_C|^2 + \rho_C |S_C|^2) |a_C B - a B_C|^2}{|\chi_{*/C} \chi_C|^2} \right) \|\delta \bar{v}_C^\tau\|^2 = \\
&= M^2 \|\delta \bar{v}_C^\tau\|^2
\end{aligned} \tag{1.52}$$

Taking into account that χ_C is stable by construction and $\chi_{*/C}$ is stable by hypothesis, then $M^2 < \infty$. In order to find a lower bound for the denominator of (1.51), using Eqs. (1.49) and (1.50), it results that a positive N exists such that:

$$\begin{aligned}
\left\| \begin{bmatrix} \delta y_{C/C}^\tau \\ \rho_C^{1/2} \delta u_{C/C}^\tau \end{bmatrix} \right\|^2 &= \left\| \begin{bmatrix} \frac{B_C}{\chi_C} \\ \rho_C^{1/2} \frac{a_C}{\chi_C} \end{bmatrix} \delta \bar{v}_C^\tau \right\|^2 \geq \\
&\geq \min_{\omega \in [-\pi, \pi]} \left(\frac{|B_C|^2 + \rho_C |a_C|^2}{|\chi_C|^2} \right) \|\delta \bar{v}_C^\tau\|^2 = N^2 \|\delta \bar{v}_C^\tau\|^2
\end{aligned} \tag{1.53}$$

Taking into account that a_C and B_C are coprime by construction and χ_C is stable by construction, then $N^2 > 0$. Hence, $J_C(\tau)$ is bounded $\forall \tau > 0$ in that, combining (1.52) and (1.53), it results:

$$J_C(\tau) \leq \frac{\left\| \begin{bmatrix} -\eta_{y_C}^\tau \\ \rho_C^{1/2} \eta_{u_C}^\tau \end{bmatrix} \right\|^2}{\left\| \begin{bmatrix} \delta y_{C/C}^\tau \\ \rho_C^{1/2} \delta u_{C/C}^\tau \end{bmatrix} \right\|^2} \leq \frac{M^2}{N^2} < \infty$$

As a consequence, $V_C(t) = \max_{0 \leq \tau \leq t} J_C(\tau)$ is bounded $\forall t > 0$.

Each cost function, being forced by the max operator to be monotone non decreasing in time, admits a limit as $t \rightarrow \infty$, which can be possibly infinite. Moreover, assumption 1 guarantees that there exists at least one stabilizing controller and the foregoing reasonings prove that the corresponding cost function is bounded $\forall t > 0$. It ensures that the two assumptions stated by the Hysteresis Switching Lemma 1.2.3 are satisfied. Hence, that lemma guarantees that there is a finite time, t_f , beyond which σ is constant and the cost function, V_f , related to the final controller, C_f , is bounded. Viz., there exists a positive real M such that $V_f(t) = \max_{0 \leq \tau \leq t} J_f(\tau) \leq M$, $\forall t \geq t_f$.

Last inequality is equivalent to the existence of $0 < M_1, M_2 < \infty$ such that:

$$\frac{\|\eta_{y_f}\|^2}{m_f + \|\delta y_{f/f}\|^2 + \rho_f \|\delta u_{f/f}\|^2} \leq M_1 \quad , \quad \frac{\|\eta_{u_f}\|^2}{m_f + \|\delta y_{f/f}\|^2 + \rho_f \|\delta u_{f/f}\|^2} \leq M_2 \quad (1.54)$$

Taking into account Eqs. (1.49) and (1.50) and being χ_f stable, there exist positive real L_1, L_2 such that:

$$\begin{aligned} \frac{\|\delta y_{f/f}\|^2}{\|\bar{v}_f\|^2} &\leq \max_{\omega \in [-\pi, \pi]} \left| \frac{\Delta B_f}{\chi_f} \right|^2 = L_1 < \infty \\ \frac{\|\delta u_{f/f}\|^2}{\|\bar{v}_f\|^2} &\leq \max_{\omega \in [-\pi, \pi]} \left| \frac{A_f}{\chi_f} \right|^2 = L_2 < \infty \end{aligned}$$

Hence, considering the first inequality in (1.54), it results:

$$\frac{\|y - y_{f/f}\|^2}{m_f + (L_1 + \rho_f L_2) \|\bar{v}_f\|^2} \leq M_1 \Leftrightarrow \|y - y_{f/f}\|^2 \leq T_1 + T_2 \|\bar{v}_f\|^2$$

where $0 < T_1 = m_f M_1$ and $0 < T_2 = (L_1 + \rho_f L_2) M_1$ are positive reals. By applying the triangular inequality, it results:

$$\begin{aligned} \|y - y_{f/f}\| &\leq T_1^{1/2} + T_2^{1/2} \|\bar{v}_f\| \Rightarrow \|y\| \leq T_1^{1/2} + T_2^{1/2} \|\bar{v}_f\| + \|y_{f/f}\| \Rightarrow \\ \|y\| &\leq T_1^{1/2} + \left(T_2^{1/2} + \max_{\omega \in [-\pi, \pi]} \left| \frac{B_f}{\chi_f} \right| \right) \|\bar{v}_f\| \Rightarrow \|y\| \leq \bar{T}_1 + \bar{T}_2 \|\bar{v}_f\| \end{aligned} \quad (1.55)$$

Considering the second inequality in (1.54) and following the same conceptual lines, it can be proved that:

$$\|\delta u\| \leq \bar{K}_1 + \bar{K}_2 \|\bar{v}_f\| \quad (1.56)$$

Notice that $\forall t \geq t_f$ it results:

$$R_f \delta u(t) = S_f r(t) - S_f y(t)$$

and consequently:

$$\bar{v}_f(t) = S_f y(t) + R_f \delta u(t) = S_f r(t) =: v_f(t) \quad \forall t \geq t_f \quad (1.57)$$

Hence, there exists a positive L such that:

$$\|\bar{v}_f^t\| \leq \|v_f^t\| + L \quad \forall t \geq 0 \quad (1.58)$$

Moreover, taking into account definition of v_f in (1.57), there exists a positive $K < \infty$ such that:

$$\|v_f\| \leq \max_{\omega \in [-\pi, \pi]} |S_f| \|r\| = K \|r\| \quad (1.59)$$

Using inequalities (1.58) and (1.59) in (1.55) and (1.56) it results:

$$\|y\| \leq \tilde{T}_1 + \tilde{T}_2 \|r\| \quad , \quad \|\delta u\| \leq \tilde{K}_1 + \tilde{K}_2 \|r\|$$

where $0 < \tilde{T}_1 = \bar{T}_1 + \bar{T}_2 L$, $0 < \tilde{T}_2 = \bar{T}_2 K$, $0 < \tilde{K}_1 = \bar{K}_1 + \bar{K}_2 L$ and $0 < \tilde{K}_2 = \bar{K}_2 K$. It concludes the proof. \square

The foregoing proof has been carried out in the case where an additive hysteresis based switching logic of the form (1.18) is acting. Nevertheless, some considerations in Sec. 1.2.3 highlight possible drawbacks of that logic and, consequently, a multiplicative hysteresis based switching logic of the form (1.32) is considered [Hes98]. Following the same reasonings present in Sec. 1.2.3, Th. 4.2 in [Hes98] can be exploited in order to reach the same conclusions of Lemma 1.3.1 in the case where a multiplicative hysteresis switching logic is used and the cost function is given by (1.46). Hence, the following corollary of Lemma 1.3.1 can be stated:

Corollary 1.3.2. Under the following assumptions:

1. Problem feasibility, viz. there exists at least one controller $C \in \mathcal{C}$ such that the feedback system (P/C) is stable.
2. There exists a positive constant ξ such that $V_i(t) \geq \xi$, $\forall t \geq 0$, $i \in \underline{N}$

then, for any switching sequence $\sigma(\tau) \in \mathcal{S}$ given by (1.32) and (1.46), the resulting adaptive control system is stable with inputs r and outputs d , where r and $d = [\delta u(t) \quad y(t)]'$ are shown in Fig. 1.1.

The proof is omitted in that it is analogous, *mutatis mutandis*, to the proof of Corollary 1.2.6. Moreover, the same considerations developed in Remark 1.2.7 can be used in order to suggest that assumption 2 in Corollary 1.3.2 is likely verified in practice.

Comparing the statements of Lemma 1.2.5 and 1.3.1, it should be noticed that Lemma 1.3.1 does not require assumption 2 of Lemma 1.2.5, while the same conclusions are guaranteed. Hence, even though cost function in (1.46) is originally proposed in order to replace that in (1.20) which is not computable in the presence of non-minimum phase controllers, nothing prevents the use of (1.46) also in the case of minimum-phase controllers. This consideration can

be especially useful when same restrictions may cause difficulties in satisfying assumption 2 of Lemma 1.2.5. Moreover, in the case of minimum-phase controllers, another way to calculate vector $\gamma_{i/i}(\tau)$ in (1.45) rather than the procedure described by Eqs. (1.42) and (1.43) turns out to be possible. It consists of actually implementing the nominal loop (M_i/C_i) driven by the virtual reference signal \bar{r}_i in order to collect the I/O data $d_{i/i}(\tau) = [\delta u_{i/i}(\tau) \quad y_{i/i}(\tau)]'$, $\forall i \in \underline{N}$.

1.3.3 Performance analysis

In order to have some insight on the inference capability of candidate loop behavior of cost function (1.46), a steady-state analysis of such a cost function, once the max operator and the m_i constants are omitted, is worth to be carried out. To this end, from (1.47)-(1.50), it follows:

$$\begin{aligned} \eta_{y_i}(\tau) &= \frac{\tilde{P}_i C_i}{1 + PC_i} \frac{1}{M_i C_i} y_{i/i}(\tau) = \frac{\tilde{P}_i}{1 + PC_i} \frac{1}{M_i} y_{i/i}(\tau) = \frac{\tilde{P}_i}{1 + PC_i} \delta u_{i/i}(\tau) = \\ &= \frac{\tilde{P}_i C_i}{1 + PC_i} \frac{\delta u_{i/i}(\tau)}{C_i} = \frac{\tilde{P}_i C_i}{1 + PC_i} e_{i/i}(\tau) \\ \eta_{u_i}(\tau) &= -\frac{\tilde{P}_i C_i}{1 + PC_i} \delta u_{i/i}(\tau) \end{aligned}$$

where $e_{i/i}(\tau)$ is the i -th nominal loop tracking error, shown in Fig. 1.5. Hence, cost function J_i in (1.46) can be equivalently rewritten as follows:

$$J_i(\tau) = \frac{\left\| \begin{bmatrix} \frac{\tilde{P}_i C_i}{1+PC_i} & 0 \\ 0 & \frac{\tilde{P}_i C_i}{1+PC_i} \end{bmatrix} \begin{bmatrix} e_{i/i}^\tau \\ \rho_i^{1/2} \delta u_{i/i}^\tau \end{bmatrix} \right\|^2}{\left\| \begin{bmatrix} \delta y_{i/i}^\tau \\ \rho_i^{1/2} \delta u_{i/i}^\tau \end{bmatrix} \right\|^2} = \frac{\|H_i z_{i/i}^\tau\|^2}{\|\gamma_{i/i}^\tau\|^2} \quad (1.60)$$

where:

$$H_i = \begin{bmatrix} \frac{\tilde{P}_i C_i}{1+PC_i} & 0 \\ 0 & \frac{\tilde{P}_i C_i}{1+PC_i} \end{bmatrix}$$

is as in (1.28) and $z_{i/i}$, $\gamma_{i/i}$ are respectively defined in (1.13) and (1.45). For the nominal loop (M_i/C_i) , $i \in \underline{N}$, it is conceivable to approximate the behavior of $\delta y_{i/i}(\tau)$ with $e_{i/i}(\tau)$. Under this condition, (1.60) becomes the

following:

$$\bar{J}_i(\tau) = \frac{\left\| \begin{bmatrix} \frac{\tilde{P}_i C_i}{1+PC_i} & 0 \\ 0 & \frac{\tilde{P}_i C_i}{1+PC_i} \end{bmatrix} \begin{bmatrix} e_{i/i}^\tau \\ \rho_i^{1/2} \delta u_{i/i}^\tau \end{bmatrix} \right\|^2}{\left\| \begin{bmatrix} e_{i/i}^\tau \\ \rho_i^{1/2} \delta u_{i/i}^\tau \end{bmatrix} \right\|^2} = \frac{\|H_i z_{i/i}^\tau\|^2}{\|z_{i/i}^\tau\|^2} = \frac{\|\tilde{z}_{*/i}^\tau\|^2}{\|z_{i/i}^\tau\|^2} \quad (1.61)$$

where $\tilde{z}_{*/i}$ is given by (1.14).

Letting $t \rightarrow \infty$, supposing that all the involved signals are stationary and omitting the argument $e^{j\omega}$ for all transfer functions, it results:

$$\begin{aligned} \bar{J}_i &= \lim_{t \rightarrow \infty} \frac{\|\tilde{z}_{*/i}^t\|^2}{\|z_{i/i}^t\|^2} = \frac{\text{Tr} \left(\frac{1}{2\pi} \int_{-\pi}^{\pi} \Phi_{\tilde{z}_{*/i}}(\omega) d\omega \right)}{\frac{1}{2\pi} \int_{-\pi}^{\pi} \left(\Phi_{e_{i/i}}(\omega) + \rho_i \Phi_{\delta u_{i/i}}(\omega) \right) d\omega} = \\ &= \frac{\text{Tr} \left(\frac{1}{2\pi} \int_{-\pi}^{\pi} H_i^* \Phi_{z_{i/i}}(\omega) H_i d\omega \right)}{\frac{1}{2\pi} \int_{-\pi}^{\pi} \left(\Phi_{e_{i/i}}(\omega) + \rho_i \Phi_{\delta u_{i/i}}(\omega) \right) d\omega} = \\ &= \frac{\frac{1}{2\pi} \int_{-\pi}^{\pi} \left| \frac{\tilde{P}_i C_i}{1+PC_i} \right|^2 \left[\Phi_{e_{i/i}}(\omega) + \rho_i \Phi_{\delta u_{i/i}}(\omega) \right] d\omega}{\frac{1}{2\pi} \int_{-\pi}^{\pi} \left(\Phi_{e_{i/i}}(\omega) + \rho_i \Phi_{\delta u_{i/i}}(\omega) \right) d\omega} = \\ &= \frac{1}{2\pi} \int_{-\pi}^{\pi} \left| \frac{\tilde{P}_i C_i}{1+PC_i} \right|^2 \frac{\overline{|\Sigma_i|^2 \Phi_{\bar{r}_i}(\omega)}}{\overline{|\Sigma_i|^2 \Phi_{\bar{r}_i}(\omega)}} d\omega \end{aligned} \quad (1.62)$$

where $\Phi_{e_{i/i}}(\omega)$, $\Phi_{\delta u_{i/i}}(\omega)$ and $\Phi_{\bar{r}_i}(\omega)$ are the power spectral densities of respectively $e_{i/i}(\tau)$, $\delta u_{i/i}(\tau)$ and $\bar{r}_i(\tau)$. Moreover, $\overline{|\Sigma_i|^2 \Phi_{\bar{r}_i}(\omega)}$ is a quantity normalized over the whole range of frequencies (see 1.34)) and $|\Sigma_i|^2$ is the square norm of the mixed sensitivity of (M_i/C_i) given by (1.35).

Notice that the inversion of controller C_i is required in order to obtain $e_{i/i}(\tau)$ and $\bar{r}_i(\tau)$. As a consequence, in the case of non-minimum phase controllers, $e_{i/i}(\tau)$ and $\bar{r}_i(\tau)$ are divergent signals. Nevertheless, this fact does not invalidate the foregoing analysis as $e_{i/i}(\tau)$, $\bar{r}_i(\tau)$ or their power spectral densities, are present in both numerator and denominator, giving rise to a bounded ratio.

In this way, being (1.62) identical to (1.33), the same reasonings, already developed in Sec. 1.2.4 and leading to favorable insights on the controller selection criterion, can be also carried out in the present case.

1.4 Conclusions

In this chapter the plant to be controlled, even though unknown, is supposed to belong to an universum of possible plants, available to the designer. A set of approximating models of the plant, to be used in an SSC system, is derived from this prior knowledge and the way it is accomplished is not of interest of the present work.

The study of cost functions, driving the switching process among candidate controllers, which exploit the approximating models knowledge, is addressed. In particular, a mean square measure of relative discrepancy between the loop made up by the feedback interconnection of the plant and a candidate controller and the “tuned” feedback loop related to that controller is considered. In this context, the virtual reference concept allows one to evaluate this measure from current plant data with no need of switching on in feedback to the plant all candidate controllers. By this way, a cost function which successfully accomplishes both the tasks of controller falsification and inference of candidate loop behavior is obtained. Moreover, such a cost function ensures stability of the adaptive control system, once certain assumptions on the set of approximating models and the set of candidate controllers are satisfied. Nevertheless, the virtual reference calculation, which turns out to be necessary for the cost function evaluation, is numerically unfeasible in the case of non-minimum phase controllers.

In order to cope with this possible restrictive condition, a different cost function is proposed which preserves the positive feature of measuring a relative distance between feedback loops. Moreover, the cost function evaluation is achieved without either requiring the explicit virtual reference calculation or physically switching the candidate controllers in feedback to the plant. Also, a study pertaining to the inference of candidate loop behavior capability of the cost function and giving rise to encouraging results is carried out. In what concerns stability issues, this cost function ensures stability of the adaptive control system under weaker assumptions with respect to those required by the use of the cost function suitable only for minimum-phase controllers. This consideration may suggest its use regardless the controllers phase-minimality.

Chapter 2

Unfalsified adaptive control

2.1 Introduction

The use of multiple models in an SSC context is by no means new in literature (see e.g. [Mor96, NB97]). Nevertheless, past [RVAS85] and more recent works [And05], show that the model-plant mismatch is a potential problem of this approach as may cause destabilization effects. Even though Ch. 1 shows possible techniques to be used in order to face the mentioned drawback, it is interesting to deal with frameworks which do not exploit plant approximating models.

A pioneering work in this direction was done by Martensson [Mar86] in the mid 80s. He showed how to achieve adaptive goals only providing problem feasibility without any plant assumption. A pre-routed switching among candidate controllers until one is found capable of achieving the control objective, was proposed. Even though this approach can be criticized because of possible poor transients, it represents a historically starting point for a *performance based supervisory logic* (see Introduction).

A recently proposed approach in this field is referred to as *unfalsified adaptive control* [ST97]. It is introduced as a framework for determining control laws whose ability to meet performance specifications is at least not invalidated by the available data. In particular, when this approach is implemented in an SSC context, a data driven cost function is used in order to directly either validate or invalidate the acting controller and the candidate ones. When-

ever the acting controller is invalidated, the one which minimizes the cost function is switched on in feedback to the plant. Under certain assumptions on the cost function and the set of candidate controllers, this procedure is shown to yield at convergence a controller which achieves specified performance goals, whenever such a controller exists in the set \mathcal{C} [WPSS05]. The virtual reference concept, referred to as *fictitious reference*, is customary in that it facilitates validation of controllers by means of experimental data possibly acquired while another controller is in the loop.

Key point in this approach is the absence of assumptions on the plant which allows the designer to avoid unadvisable inconveniences caused by a possible model-plant mismatch. Fundamental concepts of the *unfalsified adaptive control* approach are *unfalsified stability* of a system and *cost-detectability* of the pair (V, \mathcal{C}) . Even though the following definitions are already present in literature [WPSS05], they are nonetheless reported here for the reader's convenience.

Definition 2.1.1. Given an input-output pair (v, w) of a system, the stability, relatively to the I/O pair (v, w) , is said to be *unfalsified* by (v, w) if there exist bounded $\beta, \alpha \geq 0$ such that:

$$\|w^t\| < \beta\|v^t\| + \alpha \quad , \quad \forall t > 0 \quad (2.1)$$

Otherwise, stability of the system is said to be *falsified* by (v, w) .

Notice that unfalsified stability is established based on the data taken from one infinite-duration experiment for one input, while the classical stability definition requires that 2.1 holds for every possible input.

Definition 2.1.2. Let r denote the input and let $d = [\delta u \quad y]'$ denote the resulting plant data collected while \hat{C} is in the loop (see Fig. 1.1). The pair (V, \mathcal{C}) is said to be *cost-detectable* if for every $\hat{C} \in \mathcal{C}$ with finitely many switching times, the following statements are equivalent: 1) $V(C_f, d, t)$ is bounded as $t \rightarrow \infty$, 2) stability of the system (P/\hat{C}) is unfalsified by (r, d) .

Cost-detectability is a controller dependent but plant independent concept based on which cost functions can reliably detect any instability exhibited by the adaptive system (P/\hat{C}) . In [WPSS05] it is proved that, under problem feasibility, a hysteresis switching logic that minimizes a cost-detectable cost function yields a stable adaptive system in that stability is not falsified by any possible (r, d) . This conclusion is there achieved exploiting the Hysteresis Switching Lemma 1.2.3 and sufficient conditions are given in order to obtain cost-detectable cost functions in terms of candidate controllers phase-minimality, existence of the virtual reference signal generator

and cost functions properties (see [WPSS05] for details).

In the following sections the unfalsified adaptive control is considered as the underlying approach. In this connection, possible cost functions are presented and they are shown to yield a stable adaptive control system without directly exploiting cost-detectability or unfalsified stability concepts. Moreover, particular concern is posed on the analysis of the performance achievable by the controlled system characterized by such cost functions, an aspect not sufficiently addressed in the unfalsified adaptive control literature.

2.2 Minimum-phase controllers

Unfalsified adaptive control framework does not state any particular cost function form to be minimized in order to obtain stability of the adaptive feedback loop. In this sense, the cost function is only required to be cost-detectable. A reasonable form for such a cost function is the following [ST97]:

$$V_i(t) = \frac{\|\bar{e}_i^t\|^2 + \rho_i \|\delta u^t\|^2}{\|\bar{r}_i^t\|^2} \quad (2.2)$$

Taking into account Fig. 1.3, the signal $\bar{e}_i(t) = \bar{r}_i(t) - y(t)$ is the virtual tracking error, i.e., the tracking error that would have occurred had the controller C_i been in the loop and the reference equal to \bar{r}_i . The presence of the virtual reference at the denominator plays the role of a normalization in such a way that the cost function does not depend on the i -th virtual reference level. Moreover, the use of the virtual reference permits calculation of the cost function related to each candidate controller without physically inserting it in feedback to the plant. Notice that, based on (1.10), only input-output data from the currently operating loop are required for cost function calculation. On the other hand, the virtual reference calculation is necessary to evaluate each cost function and it makes (2.2) suitable only for minimum-phase controllers.

In what concerns the controller falsification task, it should be noted that supervisory logic (1.4)-(2.2) guarantees falsification of an actively operating controller, namely C_h , which is destabilizing the plant. The cost function V_h in (2.2), related to that controller, gets actually unbounded. As a matter of fact, the numerator, containing data y and δu from the operating loop, is divergent. On the contrary, the denominator is bounded in that it is the norm of the true reference signal.

On the other hand, unstable data collected while the same destabilizing controller is in the loop generally will not falsify the behavior of any other destabilizing candidate controller which is not actively operating in the loop. This

is because for a C which is not operating in the feedback loop, unstable data may cause the denominator of the cost to diverge at the same exponential rate as the numerator, so that the cost for an inactive controller will remain bounded even though that controller would be destabilizing if it were active. Inference of candidate loop behavior capability of cost function (2.2) will be analyzed in Sec. 2.2.2.

2.2.1 Stability issues

Stability of the adaptive feedback loop system of Fig. 1.1 achievable by an SSC based on cost function (2.2) is studied in literature [WPSS05, Zha06]. Nevertheless, the aim of this section is to obtain such results following similar conceptual lines to those illustrated in Sec. 1.2.3 and highlight common points and differences between this approach and those already present in literature [WPSS05, Zha06].

To this aim a hysteresis based switching logic of the form (1.18) is supposed to act in order to avoid too frequent controller replacements. Moreover, the cost function (2.2) is modified as follows:

$$V_i(t) = \max_{0 \leq \tau \leq t} \frac{\|\bar{e}_i^\tau\|^2 + \rho_i \|\delta u^\tau\|^2}{m_i + \|\bar{r}_i^\tau\|^2} = \max_{0 \leq \tau \leq t} J_i(\tau) \quad (2.3)$$

where the positive constants m_i are introduced in order to prevent the denominator from assuming values too close to zero. Notice that this situation may occur when a zero reference signal has to be followed. The maximum operator is instrumental for the use of Lemma 1.2.3.

Taking into account the linear form of the plant (1.21) and Def. 1.2.4 the following result can be stated:

Proposition 2.2.1. Under the assumption:

1. Problem feasibility, viz. there exists at least one controller $C \in \mathcal{C}$ such that the feedback system (P/C) is stable.

Then, for any switching sequence $\sigma(t) \in \mathcal{S}$ given by (1.18) and (2.3), the resulting adaptive control system $(P/\hat{C}(t, d))$ is stable, with inputs r and outputs d , where r and $d = [\delta u(t) \quad y(t)]'$ are shown in Fig. 1.1.

Proof. For any $\sigma(\cdot) \in \mathcal{S}$ and $\forall C_i \in \mathcal{C}$, $i \in \underline{N}$, taking into account the virtual loop showed in Fig. 1.3, it results:

$$\bar{e}_i(\tau) = \frac{1}{1 + PC_i} \bar{r}_i(\tau) = \frac{AR_i}{\chi_{*/i}} \bar{r}_i(\tau) \quad (2.4)$$

$$\delta u(\tau) = \frac{C_i}{1 + PC_i} \bar{r}_i(\tau) = \frac{AS_i}{\chi_{*/i}} \bar{r}_i(\tau) \quad (2.5)$$

where $\chi_{*/i}$ is the characteristic polynomial of (P/C_i) .

Let analyze the cost function related to a controller C which makes the closed loop (P/C) stable. Assumption 1 guarantees that at least one of such controllers exists in the set \mathcal{C} . Being the present goal to prove that this cost function is bounded on $[0, \infty)$, the max operator can be momentarily neglected. As a matter of fact, if $J_C(\tau)$ in (2.3) is shown to be bounded $\forall \tau \in [0, \infty)$, then $V_C(t)$ will be bounded too. To this end, omitting for the sake of simplicity the argument for all transfer functions, consider:

$$J_C(\tau) = \frac{\left\| \begin{bmatrix} \frac{AR_C}{\chi_{*/C}} \\ \rho_C^{1/2} \frac{AS_C}{\chi_{*/C}} \end{bmatrix} \bar{r}_C^\tau \right\|^2}{m_C + \|\bar{r}_C^\tau\|^2} \leq \frac{\left\| \begin{bmatrix} \frac{AR_C}{\chi_{*/C}} \\ \rho_C^{1/2} \frac{AS_C}{\chi_{*/C}} \end{bmatrix} \bar{r}_C^\tau \right\|^2}{\|\bar{r}_C^\tau\|^2} \leq \quad (2.6)$$

$$\leq \max_{\omega \in [-\pi, \pi]} \left(\left| \frac{A}{\chi_{*/C}} \right|^2 [|R_C|^2 + \rho_C |S_C|^2] \right) < \infty$$

where the last inequality follows in that $\chi_{*/C}$ is stable by hypothesis. It ensures that $J_C(\tau)$ is bounded $\forall \tau \geq 0$ and consequently also

$V_C(t) = \max_{0 \leq \tau \leq t} J_C(\tau)$ is bounded $\forall t > 0$.

Each cost function, being forced by the max operator to be monotone non decreasing in time, admits a limit as $t \rightarrow \infty$, which can be possibly infinite. This consideration and (2.6) ensure that the two assumptions stated by the Hysteresis Switching Lemma 1.2.3 are satisfied and, hence, it is guaranteed that there is a finite time, t_f , beyond which σ is constant and the cost function, V_f , related to the final controller, C_f , is bounded. Viz., there exists a positive real M such that $V_f(t) = \max_{0 \leq \tau \leq t} J_f(\tau) \leq M$, $\forall t \geq t_f$. Last inequality is equivalent to the existence of $0 < M_1, M_2 < \infty$ such that:

$$\frac{\|\bar{e}_f\|^2}{m_f + \|\bar{r}_f\|^2} \leq M_1 \quad , \quad \frac{\|\delta u\|^2}{m_f + \|\bar{r}_f\|^2} \leq M_2 \quad (2.7)$$

Considering the first inequality in (2.7), it results:

$$\|\bar{r}_f - y\|^2 \leq T_1 + M_1 \|\bar{r}_f\|^2$$

where $0 < T_1 = m_f M_1$ is a positive real. By applying the triangular inequality, it results:

$$\|y - \bar{r}_f\| \leq T_1^{1/2} + M_1^{1/2} \|\bar{r}_f\| \Rightarrow \|y\| \leq T_1^{1/2} + (M_1^{1/2} + 1) \|\bar{r}_f\|$$

Moreover, for the virtual reference associated to the final controller, it can be proved [WPSS05] that there exists a positive α such that:

$$\|\bar{r}_f^t\| \leq \|r^t\| + \alpha \quad \forall t \geq 0$$

Hence, combining the last two inequalities, it results:

$$\|y\| \leq L_1 + L_2\|r\|$$

where: $0 < L_1 = T_1^{1/2} + \alpha(M_1^{1/2} + 1)$ and $0 < L_2 = M_1^{1/2} + 1$ are positive reals. Following the same conceptual lines, it can be proved that there exist positive reals K_1, K_2 such that:

$$\|\delta u\| \leq K_1 + K_2\|r\|$$

This concludes the proof. □

It is worth remarking that the same conclusion of Prop. 2.2.1 in the case of possible non linear plants and controllers is achieved in [WPSS05], nevertheless under the assumption of cost-detectability of the cost function. On the other hand, the same stability result is proved in [Zha06] for the more general case of nonlinear plants and nonlinear controllers, nevertheless in the presence of a slightly different cost function from (2.3). A remarkable difference is that (2.3) allows the use of an incremental form of the plant which is advisable in control applications.

As already stated by Corollaries 1.2.6 and 1.3.2 for the cost functions in the case of approximating models availability, the same stability conclusion of Prop. 2.2.1 is derived in the presence of a scale independent switching logic of the form (1.32). To this aim, Th. 4.2 in [Hes98] is exploited and consequently each cost function is required not to assume zero values. Hence, the following proposition follows:

Proposition 2.2.2. Under the following assumptions:

1. Problem feasibility, viz. there exists at least one controller, namely $C \in \mathcal{C}$, such that the closed loop system (P/C) is stable.
2. There exists a positive constant ξ such that $V_i(t) \geq \xi, \forall t \geq 0, i \in \underline{N}$

then, for any switching sequence $\sigma(\tau) \in \mathcal{S}$ given by (1.32) and (2.3), the resulting adaptive control system is stable.

The proof is omitted in that it is analogous, *mutatis mutandis*, to the proof of Corollary 1.2.6.

2.2.2 Performance analysis

Besides stability guarantees which are obviously important in any control system, also an analysis of the performance achievable by the control system is definitely valuable. In an SSC system, it is intuitive to understand that the achievable performance partially depends on the ability of the switching criterion which, selecting the cost function minimizing controller, chooses the controller which turns out to control the plant in a better way than the others. Then, a preliminary performance study should analyze the steady-state values of cost functions related to candidate controllers.

To this aim, suppose that all involved signals be stationary, and $C_h \in \mathcal{C}$ be the current stabilizing controller switched on in the loop since the remote past. Let \mathcal{T}_h and \mathcal{T}_i be the complementary sensitivity functions of respectively the (constant) operating loop (P/C_h) and the generic candidate loop (P/C_i), $\Phi_r(\omega)$ be the power spectral density of the reference signal $r(t)$, then, omitting the argument in all transfer functions, the following results can be easily obtained:

$$\begin{aligned}\bar{r}_i(\tau) &= \frac{C_h}{C_i} \frac{1 + PC_i}{1 + PC_h} r(\tau) = \frac{\mathcal{T}_h}{\mathcal{T}_i} r(\tau) \\ \bar{e}_i(\tau) &= -\frac{\mathcal{T}_h}{\mathcal{T}_i} (\mathcal{T}_i - 1) r(\tau)\end{aligned}$$

$$\begin{aligned}J_i|_{\rho_i=0} &= \lim_{t \rightarrow \infty} \frac{\|\bar{e}_i^t\|^2}{\|\bar{r}_i^t\|^2} = \lim_{t \rightarrow \infty} \frac{\left\| \frac{\mathcal{T}_h}{\mathcal{T}_i} (\mathcal{T}_i - 1) r^t \right\|^2}{\left\| \frac{\mathcal{T}_h}{\mathcal{T}_i} r^t \right\|^2} = \\ &= \frac{\frac{1}{2\pi} \int_{-\pi}^{\pi} \left| \frac{\mathcal{T}_h}{\mathcal{T}_i} (\mathcal{T}_i - 1) \right|^2 \Phi_r(\omega) d\omega}{\frac{1}{2\pi} \int_{-\pi}^{\pi} \left| \frac{\mathcal{T}_h}{\mathcal{T}_i} \right|^2 \Phi_r(\omega) d\omega} = \frac{1}{2\pi} \int_{-\pi}^{\pi} |\mathcal{T}_i - 1|^2 \overline{\left| \frac{\mathcal{T}_h}{\mathcal{T}_i} \right|^2} \Phi_r(\omega) d\omega\end{aligned}\quad (2.8)$$

where:

$$\overline{\left| \frac{\mathcal{T}_h}{\mathcal{T}_i} \right|^2} \Phi_r(\omega) = \frac{\left| \frac{\mathcal{T}_h}{\mathcal{T}_i} \right|^2 \Phi_r(\omega)}{\frac{1}{2\pi} \int_{-\pi}^{\pi} \left| \frac{\mathcal{T}_h}{\mathcal{T}_i} \right|^2 \Phi_r(\omega) d\omega}\quad (2.9)$$

is a normalized weight in that: $\frac{1}{2\pi} \int_{-\pi}^{\pi} \overline{\left| \frac{\mathcal{T}_h}{\mathcal{T}_i} \right|^2} \Phi_r(\omega) d\omega = 1$. For the sake of simplicity the analysis is carried out for $\rho_i = 0$ and in the absence of the max

operator and the m_i positive constants in the cost function (2.3). Nevertheless, similar conclusions can be obtained for $\rho_i > 0$.

Eq. (2.8) involves some positive inference feature as it depends on the square of the difference between \mathcal{T}_i and 1, its desired value, weighted by the normalized dynamic weight $\left|\frac{\mathcal{T}_h}{\mathcal{T}_i}\right|^2 \Phi_r(\omega)$. However, it should be observed that, being the weight small at those frequencies where $|\mathcal{T}_i| \gg 1$, unsuitable candidate controllers having large complementary sensitivity, have a greater chance to be selected.

As a consequence, the use of cost function (2.3) can have limitations from the performance standpoint.

2.3 Non-minimum phase controllers

The evaluation of cost function (2.3) can not be carried out in the case of non-minimum phase controllers because the virtual reference calculation turns out to be numerically unfeasible.

The unfalsified control theory states that a necessary condition for the pair (V, \mathcal{C}) to be cost-detectable and, hence, to ensure a stable adaptive control system under the assumption of problem feasibility, is that the candidate controllers are minimum-phase [WPSS05]. Besides the numerical problems that definitely arise, further aspect is encountered in the non-minimum phase controllers case. When a candidate controller is switched on in feedback to the plant, the corresponding virtual reference may diverge regardless the values of current I/O plant data, then precluding the detection of a possible system instability. In order to cope with this unadvisable situation, a solution presented in [Zha06] introduces the concept of *matching controller state*. Taking into account that in [Zha06] the virtual reference signal is referred to as *matching controller* signal, then the matching controller state is there defined as follows:

Definition 2.3.1. For a candidate controller $C_i \in \mathcal{C}$, its *matching controller state* is the state that C_i should process at time t if C_i had been the active controller and \bar{r}_i the reference signal.

Hence, each candidate controller should be inserted in the loop with an initial state equal to its matching controller state in order to recover the property in accordance to which the virtual reference related to the actively operating controller coincides with the true reference. Consequently, a possible exhibited instability produced by an actively operating controller will be detected.

Although this solution appears suitable for solving the mentioned problem, the matching controller state may be practically hard to compute and does not solve numerical problems related to the computation of the virtual reference for non actively operating controllers.

Hence, a different approach is proposed based on the definition of a modified virtual reference signal. To this end, the following definition is adopted:

Definition 2.3.2. The ordered pair (S_i, R_i) is a *left matrix fraction description (MFD)* of the controller C_i if S_i and R_i are stable, R_i is invertible and $C_i = R_i^{-1}S_i$.

For the sake of simplicity, consider the SISO case. In such a case the generic controller $C_i \in \mathcal{C}$ can be represented in terms of the polynomials $S_i(d)$ and $R_i(d)$ as: $C_i(d) = S_i(d)/R_i(d)$. The following reasonings could be extended to the general MIMO case in accordance to Def. 2.3.2.

Following the same conceptual lines of Def. 1.2.1, it is possible, given plant data $d = [\delta u \quad y]'$ and a candidate controller C_i , to define a modified virtual reference signal $\bar{v}_i(t)$, according to the virtual configuration of Fig. 2.1, to as:

$$\bar{v}_i(t) = \frac{S_i(d)y(t) + R_i(d)\delta u(t)}{S_i(1)} \quad (2.10)$$

where $S_i(1) = S_i(d)|_{d=1}$, $i \in \underline{N}$. Note that because an incremental form of

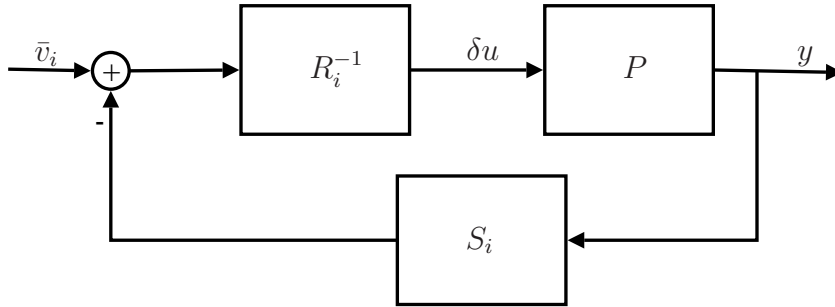


Figure 2.1. Virtual closed loop associated to the definition of $\bar{v}_i(t)$.

the system is adopted, $S_i(1) \neq 0$, $\forall i \in \underline{N}$. Whenever the virtual reference $\bar{r}_i(t)$ exists, it results:

$$\bar{v}_i(t) = \frac{S_i(d)}{S_i(1)} \bar{r}_i(t) \quad (2.11)$$

The rationale for introducing the factor $S_i(1)$ is to obtain a steady-state non polarized response of \bar{v}_i to a step input.

It is worth pointing out that the configuration of Fig. 2.1, where the factor

$R_i(d)$ is placed in the forward path and the factor $S_i(d)$ of the controller is in the backward path of the feedback loop, in order to deal with non-minimum phase controllers, is not new in the literature, see [Zha06, DAL06, MCMS07]. In order to exploit the concept of the modified virtual reference \bar{v}_i , it is necessary to reconfigure the adaptive feedback system of Fig. 1.1 to that illustrated in Fig. 2.2. In this figure $\hat{R}(t, d)$ and $\hat{S}(t, d)$ denote the factors of the

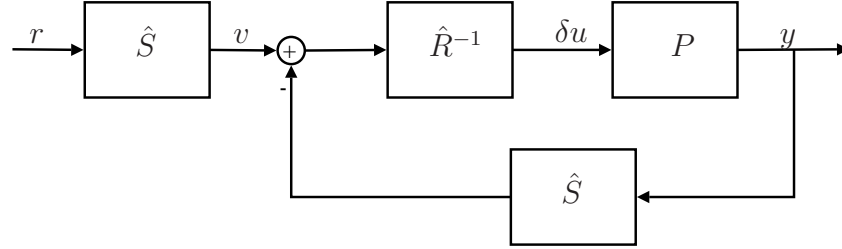


Figure 2.2. Reconfiguration of the adaptive closed loop in order to have the adaptive controller numerator in the backward path and the denominator in the forward path of the closed loop.

time varying controller, adaptively chosen by the switching logic. It is worth highlighting that configuration of Fig. 1.1 and that of Fig. 2.2 are equivalent as one can easily verify that the transfer functions from r to δu and from r to y are the same in both schemes.

In this scenario, the following cost function is proposed in order to be minimized by the switching logic:

$$V_i(t) = \frac{\|\bar{w}_i^t\|^2 + \rho_i \|\delta u^t\|^2}{\|\bar{v}_i^t\|^2} \quad (2.12)$$

where $\bar{w}_i(t) = \bar{v}_i(t) - y(t)$ and $\bar{v}_i(t)$ is given by (2.10).

Notice that the cost function evaluation does not present any trouble also in the case of non-minimum phase controllers in that no controller inversion is required and only input output data collected from the acting loop are requested.

Falsification property of a switching logic based on (1.4)-(2.12) is analogous to that described in the minimum-phase controller case in Sec. 2.2. In fact, falsification of an actively operating controller, namely C_h , which is destabilizing the plant is guaranteed. That is because the cost function V_h in (2.12), related to that controller, gets actually unbounded. As a matter of fact, the numerator, containing data y and δu from the operating loop, is divergent. On the contrary, the denominator is bounded in that it is the norm of the signal $\bar{v}_h(t)$ which turns out to be a stable filtering, through the

filter $\frac{S_h(d)}{S_h(1)}$, of the true reference signal $r(t)$. As already remarked for cost functions described in previous sections, the behavior of any other destabilizing candidate controller which is not actively operating in the loop will not be falsified by data collected while C_h is in the loop. That is because these unstable data may cause the numerator of the cost function to diverge at the same exponential rate of the denominator, thus yielding a bounded cost function level. Hence, the ability of an inactive controller to stabilize the plant may not be falsified until after such future time as that controller is actually switched into the feedback loop.

2.3.1 Stability issues

In this section stability results achievable by the use of a hysteresis based switching logic of the form (1.18) are investigated. The cost function $V_i(t)$ is the modified version of (2.12) in the following way:

$$V_i(t) = \max_{0 \leq \tau \leq t} \frac{\|\bar{w}_i^\tau\|^2 + \rho_i \|\delta u^\tau\|^2}{m_i + \|\bar{v}_i^\tau\|^2} = \max_{0 \leq \tau \leq t} J_i(\tau) \quad (2.13)$$

Hence, suppose that the plant is represented by a linear equation of the form (1.21), then the main result of the section can be stated:

Proposition 2.3.3. Under the following assumptions:

1. Problem feasibility, viz. there exists at least one controller, namely $C \in \mathcal{C}$, such that the closed loop system (P/C) is stable.

Then, for any switching sequence $\sigma(t) \in \mathcal{S}$ given by (1.18) and (2.13), the resulting adaptive control system $(P/\hat{C}(t, d))$ is stable, with inputs r and outputs d , where r and $d = [\delta u(t) \quad y(t)]'$ are shown in Fig. 2.2.

Proof. For any $\sigma(\cdot) \in \mathcal{S}$ and $\forall C_i \in \mathcal{C}$, $i \in \underline{N}$, taking into account the virtual loop showed in Fig. 2.1 and omitting the argument for all transfer functions, it results:

$$\begin{aligned} \bar{w}_i(\tau) &= \bar{v}_i(\tau) - y(\tau) = \bar{v}_i(\tau) - \frac{PR_i^{-1}}{1 + PC_i} \bar{v}_i(\tau) = \frac{R_i(1 + PC_i) - P}{R_i(1 + PC_i)} \bar{v}_i(\tau) = \\ &= \frac{1}{A} \frac{(\chi_{*/i} - B)}{\chi_{*/i}} \bar{v}_i(\tau) = \frac{\chi_{*/i} - B}{\chi_{*/i}} \bar{v}_i(\tau) \end{aligned} \quad (2.14)$$

where $\chi_{*/i}$ is the characteristic polynomial of (P/C_i) . Moreover:

$$\delta u(\tau) = \frac{R_i^{-1}}{1 + PC_i} \bar{v}_i(\tau) = \frac{A}{\chi_{*/i}} \bar{v}_i(\tau) \quad (2.15)$$

Let analyze the cost function related to a controller C which makes the closed loop (P/C) stable. Assumption 1 guarantees that at least one of such controllers exists in the set \mathcal{C} . Being the present goal to prove that this cost function is bounded on $[0, \infty)$, the max operator can be momentarily neglected. As a matter of fact, if $J_C(\tau)$ in (2.13) is shown to be bounded $\forall \tau \in [0, \infty)$, then $V_C(t)$ will be bounded too. To this end, taking into account (2.14) and (2.15), consider:

$$\begin{aligned}
J_C(\tau) &= \frac{\left\| \begin{bmatrix} \frac{\chi_{*/C} - B}{\chi_{*/C}} \\ \rho_C^{1/2} \frac{A}{\chi_{*/C}} \end{bmatrix} \bar{v}_C^\tau \right\|^2}{m_C + \|\bar{v}_C^\tau\|^2} \leq \frac{\left\| \begin{bmatrix} \frac{\chi_{*/C} - B}{\chi_{*/C}} \\ \rho_C^{1/2} \frac{A}{\chi_{*/C}} \end{bmatrix} \bar{v}_C^\tau \right\|^2}{\|\bar{v}_C^\tau\|^2} \leq \\
&\leq \max_{\omega \in [-\pi, \pi]} \left(\left| \frac{\chi_{*/C} - B}{\chi_{*/C}} \right|^2 + \rho_C \left| \frac{A}{\chi_{*/C}} \right|^2 \right) = \\
&= \max_{\omega \in [-\pi, \pi]} \left(\left| \frac{1}{\chi_{*/C}} \right|^2 [|\chi_{*/C} - B|^2 + \rho_C |A|^2] \right) < \infty
\end{aligned} \tag{2.16}$$

in that $\chi_{*/C}$ is stable by hypothesis. It ensures that $J_C(\tau)$ is bounded $\forall \tau \geq 0$ and consequently also $V_C(t) = \max_{0 \leq \tau \leq t} J_C(\tau)$ is bounded $\forall t > 0$.

Each cost function, being forced by the max operator to be monotone non decreasing in time, admits a limit as $t \rightarrow \infty$, which can be possibly infinite. This consideration and (2.16) ensure that the two assumptions stated by the Hysteresis Switching Lemma 1.2.3 are satisfied and, hence, it is guaranteed that there is a finite time, t_f , beyond which σ is constant and the cost function, V_f , related to the final controller, C_f , is bounded. Viz., there exists a positive real M such that $V_f(t) = \max_{0 \leq \tau \leq t} J_f(\tau) \leq M$, $\forall t \geq t_f$. Let the time $t \rightarrow \infty$, the last inequality is equivalent to the existence of $0 < M_1, M_2 < \infty$ such that:

$$\frac{\|\bar{w}_f\|^2}{m_f + \|\bar{v}_f\|^2} \leq M_1 \quad , \quad \frac{\|\delta u\|^2}{m_f + \|\bar{v}_f\|^2} \leq M_2 \tag{2.17}$$

Following the same conceptual lines of the proof of Prop. 2.2.1, starting from (2.17), it is easy to derive that:

$$\|y\| \leq T_1 + T_2 \|\bar{v}_f\| \quad , \quad \|\delta u\| \leq K_1 + K_2 \|\bar{v}_f\| \tag{2.18}$$

where T_1, T_2, K_1 and K_2 are positive reals. Notice that $\forall t \geq t_f$ it results:

$$\bar{v}_f(t) = \frac{S_f(d)y(t) + R_f(d)\delta u(t)}{S_f(1)} = \frac{S_f(d)}{S_f(1)} r(t) =: v_f(t) \tag{2.19}$$

Hence, inequalities (1.58) and (1.59) turn out to be valid also in this case. Using (1.58) and (1.59) in (2.18) it results:

$$\|y\| \leq \tilde{T}_1 + \tilde{T}_2 \|r\| \quad , \quad \|\delta u\| \leq \tilde{K}_1 + \tilde{K}_2 \|r\|$$

where $0 < \tilde{T}_1 = T_1 + T_2 L$, $0 < \tilde{T}_2 = T_2 K$, $0 < \tilde{K}_1 = K_1 + K_2 L$ and $0 < \tilde{K}_2 = K_2 K$.

This concludes the proof. \square

As already done in previous sections, a similar result can be stated, exploiting Th. 4.2 in [Hes98], in the case where a scale independent switching logic of the form (1.32) is used rather than the additive one (1.18).

Proposition 2.3.4. Under the following assumptions:

1. Problem feasibility, viz. there exists at least one controller, namely $C \in \mathcal{C}$, such that the closed loop system (P/C) is stable.
2. There exists a positive constant ξ such that $V_i(t) \geq \xi$, $\forall t \geq 0$, $i \in \underline{N}$

then, for any switching sequence $\sigma(\tau) \in \mathcal{S}$ given by (1.32) and (2.13), the resulting adaptive control system of Fig. 2.2 is stable.

The proof is omitted in that it is analogous, *mutatis mutandis*, to the proof of Corollary 1.2.6. Moreover, similar considerations of those stated by Remark 1.2.7 can be exploited in this case in order to highlight that assumption 2 in Prop. 2.3.4 is likely verified in practice.

2.3.2 Performance analysis

The use of the modified virtual reference $\bar{v}_i(t)$ opens the way to a new class of cost functions of the form (2.12).

The positive feature is that candidate controllers have not to be inverted in order to calculate the cost function level and, hence, possible phase non-minimality of the controllers does not represent a limitation to this approach. Moreover, stability of the controlled system, in terms of existence of a finite gain between input r and corresponding output $[\delta u \quad y]$, has been proved, under certain assumptions extensively illustrated in Sec. 2.3.1.

Nevertheless, it is also important to analyze performance achievable by the use of cost function (2.12). First of all, it is worth highlighting that the presence of $\bar{w}_i(t) = \bar{v}_i(t) - y(t)$ in the cost function numerator plays the role of making the control system goal tracking $v_i(t) = \frac{S_i(d)}{S_i(1)} r(t)$ rather than $r(t)$, for some $i \in \underline{N}$. Even though, for the final controller, the relation between

$\bar{v}_f(t)$ and $r(t)$ is given by (2.19), the transient response can be different and a performance degradation may consequently occur.

In order to further analyze the system performance, let $C_h \in \mathcal{C}$ be the current stabilizing controller switched on in the loop since the remote past, a steady-state analysis of cost function corresponding to the candidate controllers is worth to be carried out. For the sake of simplicity the analysis is carried out for $\rho_i = 0$ and in the absence of the max operator and the m_i positive constants in the cost function. Nevertheless, similar conclusions can be obtained for $\rho_i > 0$. To this aim, omitting the argument for all transfer function, the following results can be easily obtained:

$$\begin{aligned}\bar{v}_i(\tau) &= \frac{S_i y(\tau) + R_i \delta u(\tau)}{S_i(1)} = \frac{1 + PC_i}{1 + PC_h} \frac{R_i}{S_i(1)} v(\tau) = \\ &= \frac{1 + PC_i}{1 + PC_h} C_h \frac{R_i}{S_i(1)} r(\tau) = (1 + PC_i) \frac{R_i}{S_i(1)} \delta u(\tau)\end{aligned}\quad (2.20)$$

$$\begin{aligned}\bar{w}_i(\tau) &= \bar{v}_i(\tau) - y(\tau) = \frac{\frac{R_i}{S_i(1)}(1 + PC_i) - P}{1 + PC_h} C_h r(\tau) = \\ &= \left[\frac{R_i}{S_i(1)}(1 + PC_i) - P \right] \delta u(\tau)\end{aligned}\quad (2.21)$$

Suppose that all the involved signals are stationary and let $\Phi_r(\omega)$ be the power spectral density of the reference signal $r(t)$, then it results:

$$\begin{aligned}J_i|_{\rho_i=0} &= \lim_{t \rightarrow \infty} \frac{\|\bar{w}_i^t\|^2}{\|\bar{v}_i^t\|^2} = \frac{\frac{1}{2\pi} \int_{-\pi}^{\pi} \left| \frac{R_i}{S_i(1)} \frac{1 + PC_i}{1 + PC_h} C_h - \frac{PC_h}{1 + PC_h} \right|^2 \Phi_r(\omega) d\omega}{\frac{1}{2\pi} \int_{-\pi}^{\pi} \left| \frac{R_i}{S_i(1)} \frac{1 + PC_i}{1 + PC_h} C_h \right|^2 \Phi_r(\omega) d\omega} = \\ &= \frac{\frac{1}{2\pi} \int_{-\pi}^{\pi} \left| \frac{R_i}{S_i(1)} \frac{1 + PC_i}{1 + PC_h} C_h \right|^2 \left| 1 - \frac{PS_i(1)}{R_i(1 + PC_i)} \right|^2 \Phi_r(\omega) d\omega}{\frac{1}{2\pi} \int_{-\pi}^{\pi} \left| \frac{R_i}{S_i(1)} \frac{1 + PC_i}{1 + PC_h} C_h \right|^2 \Phi_r(\omega) d\omega} = \\ &= \frac{1}{2\pi} \int_{-\pi}^{\pi} \left| 1 - \frac{PS_i(1)}{R_i(1 + PC_i)} \right|^2 \left| \frac{R_i}{S_i(1)} \frac{1 + PC_i}{1 + PC_h} C_h \right|^2 \Phi_r(\omega) d\omega = \\ &= \frac{1}{2\pi} \int_{-\pi}^{\pi} \left| 1 - \frac{S_i(1)}{S_i} \mathcal{T}_i \right|^2 Z_i d\omega\end{aligned}\quad (2.22)$$

where:

$$Z_i := \frac{\left| \frac{R_i}{S_i(1)} \frac{1 + PC_i}{1 + PC_h} C_h \right|^2 \Phi_r(\omega)}{\frac{1}{2\pi} \int_{-\pi}^{\pi} \left| \frac{R_i}{S_i(1)} \frac{1 + PC_i}{1 + PC_h} C_h \right|^2 \Phi_r(\omega) d\omega}$$

is a quantity, normalized over the whole range of frequencies in that:

$\frac{1}{2\pi} \int_{-\pi}^{\pi} Z_i d\omega = 1$. Notice that:

$$\left| \frac{R_i}{S_i(1)} \frac{1 + PC_i}{1 + PC_h} C_h \right|^2 = \left| \frac{R_i}{S_i(1)} C_i \frac{\mathcal{T}_h}{\mathcal{T}_i} \right|^2 = \left| \frac{S_i}{S_i(1)} \frac{\mathcal{T}_h}{\mathcal{T}_i} \right|^2$$

where \mathcal{T}_h and \mathcal{T}_i are the complementary sensitivity functions of respectively the (constant) operating loop (P/C_h) and the generic candidate loop (P/C_i). Hence, the normalized dynamic weight turns out to be a stable filtering, through the filter $\frac{S_i}{S_i(1)}$, of that obtained in the case of minimum-phase controllers (2.9). In this way, being the weight small at those frequencies where where $|\mathcal{T}_i| \gg 1$, unsuitable candidate controllers having large complementary sensitivity, have a greater chance to be selected. As a consequence, the use of cost function (2.12) can have limitations from the performance standpoint.

2.4 Conclusions

In this chapter any a priori knowledge on the plant is admitted which is supposed to be completely unknown to the designer. Even though approximating models actually play a key role in determining what the candidate controller set should be, a different way in order to obtain the set \mathcal{C} is supposed to be used. Nevertheless, it is not of interest of this work to deal with this aspect. Besides the actual possibility in the real practice of the lack of reference models availability, another reason for studying techniques which tackle this situation is to avoid stability problems that can arise in the case of model-plant mismatch.

In this direction, the *unfalsified adaptive control* approach is based on the cost-detectability property that a cost function should have in order to obtain a stable adaptive control system, once a hysteresis based switching process among candidate controllers is determined by the minimization of such cost function and the control problem is feasible. Cost-detectable cost functions are completely I/O plant data driven and have the ability of detecting any instability exhibited by the adaptive system. The virtual reference concept is

crucial in this approach in that it permits to infer the behavior of a controller by means of data possibly collected while another controller is acting.

In this scenario, a cost function based on a square measure of the virtual behavior of each candidate loop normalized on the virtual reference level, is considered. This is actually a cost-detectable cost function, nevertheless it is shown yielding a stable adaptive system, under problem feasibility, without directly exploiting cost-detectability property. At the same time, a study concerning the performance achievable by the resulting SSC, highlights that unsuitable candidate controllers, viz. controllers with an average larger complementary sensitivity function, may have a greater chance to be selected by the switching logic in order to replace a falsified controller.

The presence of the virtual reference in this cost function makes its computation unsuitable in the case of non-minimum phase controllers. In order to solve this drawback, a modified virtual reference is proposed. It corresponds to a configuration where the controllers are synthesized via MFD stable factors. The related cost function, which does not require controller inversion for its calculation, is therefore proposed. The adaptive system deriving from a hysteresis based switching logic minimizing this cost function is showed to be stable under the common problem feasibility assumption. Nevertheless, a performance study highlights that possible performance degradation may occur in that the control target turns out to be a filtered version, even though stable, of the true reference signal $r(t)$. In Sec. 3.3.2 an attempt to improve performance will be made by using a filtered version of the modified virtual reference, so that the control target will become a suitably shaped version of $r(t)$. Nevertheless, unsuitable candidate controllers with an average large complementary sensitivity function are likely to be chosen by the supervisor and it still may corrupt system performance.

Chapter 3

Practical applications of SSC

3.1 Introduction

The supervisor represents the main component in an SSC architecture in that it completely orchestrates the switching process among candidate controllers. Previous chapters illustrate how this task can be accomplished either exploiting approximating models knowledge or different techniques are proposed when this knowledge is unavailable. Under certain assumptions, theoretical results, concerning stability of the adaptive system, are guaranteed.

Nevertheless, it is worth discussing that some conditions, which turn out to be necessary in order to guarantee such results, may be not suitable operating conditions. In order to deal with this point, let analyze the presence of the maximum operator in the cost functions (see e.g. (1.20) or (1.46)), viz.:

$$V_i(t) = \max_{0 \leq \tau \leq t} J_i(\tau)$$

The maximum operator is instrumental to ensure that each cost function admits a limit as $t \rightarrow \infty$, a necessary condition for exploiting results of Lemma 1.2.3. Nevertheless, from a practical point of view, the max operator may involve to permanently associate a candidate controller to a high cost function level, due to a single instant of time when this level had been reached in the past for any reason. As a consequence, that controller may actually turn

out to be penalized in that it may have to wait for all remaining controllers to perform at least as badly before having a chance of being switched on in feedback to the plant. A partial solution to this problem is to introduce a finite time-window and calculate the maximum of the cost function on this window rather than on the entire time interval [AM04], as follows:

$$V_i(t) = \max_{t-L \leq \tau \leq t} J_i(\tau) \quad (3.1)$$

where L denotes the window length.

The above described modification does not comply with the theoretical requirement of having non decreasing in time cost functions. As a performance degradation is likely to occur in the absence of such modification, a compromise between desired performance achievement and stability guarantees might be handled by the designer.

Another aspect to be addressed before dealing with the practical use of the theory illustrated in previous sections, is related to the signals norm computation. For a generic signal $x(t)$, it results:

$$s(t) := \|x^t\|^2 = \sum_{\tau=0}^t |x(\tau)|^2 \quad (3.2)$$

Hence, it may happen that this norm results too much influenced by past signal values. This outcome is usually avoided by introducing the so called *forgetting factor* in the norms computation. The goal of using a forgetting factor is to de-emphasize past signal samples in such a way that more emphasis is posed on current values of the signal [AM02]. Different forgetting factor policies are suggested in literature [AM04, AM02, CS06] and the one adopted in this work uses a forgetting factor $0 \leq \lambda < 1$ in the calculation of each norm present in the cost functions. By this way, for a generic signal $x(\cdot)$, the norm $s(t)$ in (3.2) is replaced by [AM02]:

$$s_\lambda(t) := \|x^t\|_\lambda^2 := \lambda s_\lambda(t-1) + (1-\lambda)|x(t)|^2 \quad (3.3)$$

$$s_\lambda(0) = 0 \quad (3.4)$$

Notice that $\lambda = 0$ corresponds to the strongest forgetting factor in that only the most recent sample of the signal is taken into account in the summation (3.2). Intermediate values of λ give the possibility to the designer of differently weighting the terms in the summation.

The use of a forgetting factor policy as well as the presence of a time window on the max operator turn out to be especially important whenever the plant is time varying.

In the sequel, two automatic control applications are analyzed and tackled by means of an SSC and the obtained simulation results are presented. The first case of study concerns the control of the neuromuscular level during a general anesthesia. The second pertains to the position control of a system composed by two carts with uncertain elastic coupling.

Remark 3.1.1. Before presenting the two control applications and showing the related simulation results, it is worth pointing out that such results are obtained in the absence of any exogenous noise in the loop. That is because theory illustrated in Ch. 1 and 2 does not take into account the presence of noise in the loop, the supervisor is rather supposed to manage the actual input/output data of the plant. Different situations and the related theoretic results are still under investigation and will be addressed in future research.

3.2 The neuromuscular blockade case of study

Anesthesia can be defined as a drug-induced reversible pharmacological state where three main requirements on the patient are met [GFG⁺01].

Hypnosis is associated with unconsciousness and absence of postoperative recall of events that occurred during surgery. The electroencephalogram (EEG), being one of the only non-invasive measures of the central nervous system while the patient is unconscious, is nowadays considered as the major source of information in order to assess the level of hypnosis.

Analgesia is associated with pain relief but, at present, no reliable measures are available in order to quantify it. This aspect is made more complicated by the fact that clinical signs such as tearing, eye movement or grimacing are partially modified by muscle relaxants or vasoactive drugs.

Muscle relaxation is induced to facilitate access to internal organs and to depress movement responses to surgical stimulations. It is commonly measured by stimulating a peripheral nerve, usually the ulnar nerve, and evaluating the muscle response either by visual or tactile observation or by a sensor measurement.

In order to achieve an adequate anesthesia, anesthesiologists regularly adjust the infusion rate level of several drugs as well as the parameters of the breathing system on the basis of some patient-specific target, physiological measures and personal experience. In some sense, anesthesiologists act as a manual feedback controller and, hence, it seems possible to support their work by the use of automatic drug delivery systems.

In this direction, around the 80s investigators developed computer-controlled

pump systems which continually adjust the drug infusion rate in order to achieve and maintain the drug concentration level, desired by the clinician. This is an open loop control in that pharmacokinetic models, derived from past studies, are used to calculate the drug infusion necessary to achieve the target concentration, nevertheless no measurement of actual concentration are made. Despite the fact that these systems ignore interpatient pharmacokinetic variability, studies have demonstrated that drug concentrations are better maintained to the target level by open loop control rather than by standard clinical practice [AS05, BH05].

Nevertheless, the significant interpatient pharmacokinetic and pharmacodynamic variability observed for most drugs suggest the use of a closed loop control whenever reliable measures of the controlled variable are available. Several benefits may be achieved by the use of a closed loop automatic drug delivery system. First of all the routine tasks are taken over by automatic controllers so that anesthesiologists may concentrate on more critical issues. Moreover, an accurate and efficient drug profile can be administered avoiding undesirable situations such as underdosing and overdosing that may involve an unsafe condition for the patient and larger costs for the medical structures.

3.2.1 Mathematical model description

From the engineering control point of view, the whole anesthesia setting can be viewed as a MIMO system [GFG⁺01], illustrated in Fig. 3.1 where the higher set of inputs are the manipulated variables, the lower set represents possible disturbances, the higher set of outputs are the three anesthesia requirements and the lower set contains the measurable outputs.

In particular, the muscle relaxation aspect pertains to the study of the SISO system obtained from the scheme of Fig. 3.1 considering the muscle relaxant drugs as input and the muscle relaxation level as output.

The description of the drug action from the injection to the effect is made accurate by the use of *pharmacokinetic* and *pharmacodynamic* modeling. Pharmacokinetics is the study of the concentration of drugs in tissue as a function of time and dose schedule. Pharmacodynamics is the study of the relationship between drug concentration and drug effect. By relating the dose to the resultant drug concentration and the concentration to the effect, a model for drug dosing can be obtained. To this end, *compartmental models*, that is dynamical models based on conservation laws which capture the exchange of material between coupled compartments, are widely used to model metabolic processes. It is typically assumed that the human body is comprised of more than one compartment. Within each compartment, the drug concentration

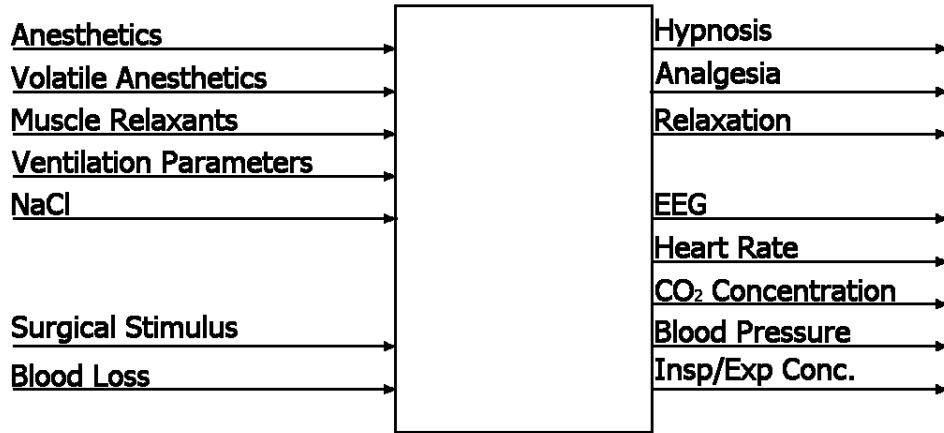


Figure 3.1. The MIMO system describing the most relevant variables involved in the anesthesia setting.

is assumed to be uniform due the instantaneous mixing. Transportation to other compartments and elimination from the body are usually assumed to occur with rates proportional to drug concentration [BH05].

In particular, the pharmacokinetic model for the muscular relaxant *atracurium* was studied in literature [WWN83, ML98] and the resulting two compartments linear model has the form:

$$\begin{aligned} \dot{x}_i(t) &= -\lambda_i x_i(t) + a_i u(t) \quad i = 1, 2 \\ c_p(t) &= \sum_{i=1}^2 x_i(t) \end{aligned}$$

where $x_i(t)$ are the state variables of the two compartments, $u(t)$ is the atracurium infusion rate [$\mu g K g^{-1} min^{-1}$], $c_p(t)$ [$\mu g ml^{-1}$] is the plasma concentration, a_i [$K g ml^{-1}$] and λ_i [min^{-1}] are patient dependent parameters. A linear second order model, described by the cascade of two first order systems of the form:

$$\begin{aligned} \dot{c}(t) &= -\lambda c(t) + \lambda c_p(t) \\ \dot{c}_e(t) &= -\frac{1}{\tau} c_e(t) + \frac{1}{\tau} c(t) \end{aligned}$$

is assumed to relate $c_p(t)$ to the effect compartment concentration $c_e(t)$ [$\mu g ml^{-1}$]. Here $c(t)$ is an intermediate variable and λ [min^{-1}] and τ [min] are patient dependent parameters. On the other hand, the pharmacodynamic effect for the atracurium is modeled by the following nonlinear memoryless

Hill equation:

$$y(t) = \frac{100C_{50}^S}{C_{50}^S + c_e(t)^S} \quad (3.5)$$

where the parameters C_{50} [μgml^{-1}] and S are also patient-dependent. The variable $y(t)$ normalized between 0 and 100 measures the neuromuscular blockade level, 0 corresponds to full paralysis and 100 to full muscular activity.

For the sake of compactness, the neuromuscular blockade response can be summarized by the cascade connection of a linear system whose transfer function is:

$$t(s) = \frac{\frac{1}{\tau}}{s + \frac{1}{\tau}} \frac{\lambda}{s + \lambda} \left(\frac{a_1}{s + \lambda_1} + \frac{a_2}{s + \lambda_2} \right) \quad (3.6)$$

followed by the Hill equation (3.5), as shown in Fig. 3.2.

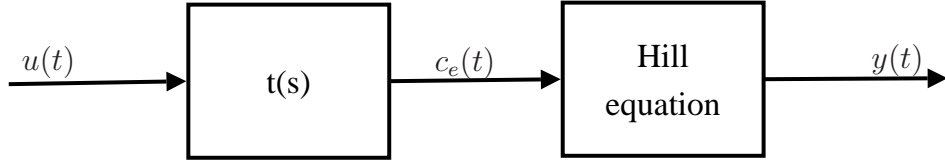


Figure 3.2. Block diagram of the neuromuscular blockade mathematical model.

The developed mathematical model depends on an uncertain parameter vector composed by 8 components as follows:

$$\vartheta = [a_1 \ a_2 \ \lambda_1 \ \lambda_2 \ \lambda \ C_{50} \ S \ \tau] \quad (3.7)$$

Previous literature on the subject [LMG98] studied an universum \mathcal{P} of possible patients (100 different subjects undergoing clinical surgery) and derived the corresponding models of the form (3.6) and (3.5). In what concerns the neuromuscular blockade response, this universum is assumed to be representative of an exhaustive range of clinical situations, except for some pathological cases corresponding to values of ϑ out of the common range. A set of 5 non linear models in the form of a cascade connection of (3.5) and (3.6)

which approximate the plants in the universum is obtained in [MM03] and it will be here referred to as:

$$\mathcal{M} = \{M_i = M(\vartheta_i), \quad i \in \underline{5}\} \quad (3.8)$$

The practical implementation of the methods described throughout this thesis requires the use of discrete time models. Hence, the models in (3.8) are obtained applying a zero-order hold input device and a sampling time T_s equal to 20 sec. to the continuous transfer function (3.6).

3.2.2 The control problem

As already remarked, a general requirement in anesthesia is to ensure a suitable level of muscle relaxation in the patient. From an engineering control point of view such a requirement can be viewed as a regulation problem. Hence, a feedback control system is designed which, based on the neuromuscular blockade level measurement and the related desired target, calculates the necessary infusion rate to be administered to the patient in such a way that the neuromuscular level tracks the desired value.

To this end, a set of 5 robust PID controllers tuned on the corresponding models of the set (3.8) were designed [MM03] of the following form:

$$u(t) = g_c \left(1 + \frac{T_s}{c_i} \frac{z}{z-1} + \frac{c_d}{T_s} \frac{z-1}{z} \right) e(t) \quad (3.9)$$

where $e(t) = r(t) - y(t)$ is the difference between the desired level, set by the anaesthetist, and respectively the induced level of neuromuscular blockade. T_s is the sampling time and g_c , c_i , c_d are the controller parameters calculated as follows:

$$g_c = \frac{1.2}{RL} \frac{1}{rd(r_0)} \quad (3.10)$$

$$c_i = 2L \quad (3.11)$$

$$c_d = L/2 \quad (3.12)$$

where L and R are obtained in accordance to the Ziegler-Nicols step response method, applied to the linear part of the model and $rd(r_0)$ is the partial derivative of $y(t)$ evaluated at the target value, which is supposed to be constant in time: $r(t) = r_0$ [ML98]. In this way the following set of controllers is obtained:

$$\mathcal{C} = \{C_i, \quad i \in \underline{5}\} \quad (3.13)$$

Muscle relaxant are in the real practice usually administered by successive bolus or through an initial bolus followed by a continuous infusion with constant or piecewise constant rate. The initial bolus drug is instrumental in order to induce total muscular relaxation in a short period of time (usually shorter than 5 minutes). This second methodology is supposed to act and the bolus dose is mathematically modeled through a Dirac δ function occurring at time $t = 0$ which is equivalent to have a non zero initial condition for the plant. Fig. 3.3 shows the simulated induced neuromuscular blockade responses to a bolus of $500\mu gKg^{-1}$ for the models corresponding to the universum of patients. During the first minutes the muscle relaxation level

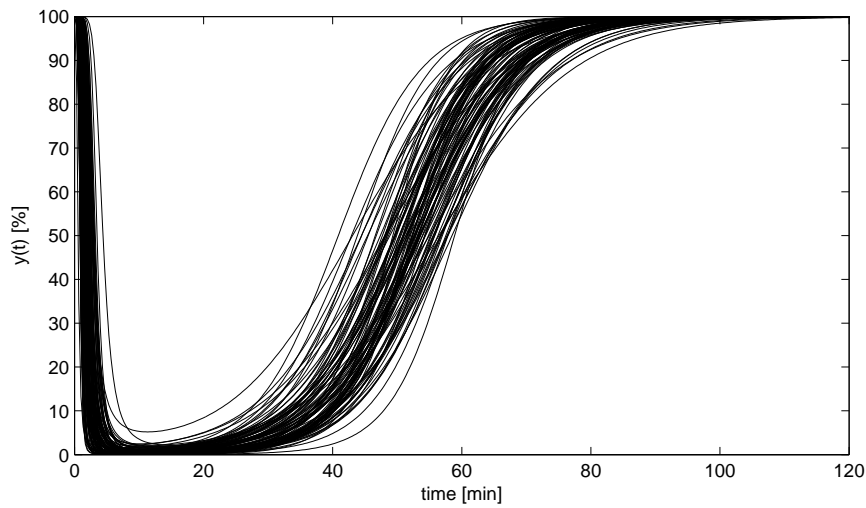


Figure 3.3. Simulated response to an input bolus for the 100 patients belonging to the universum \mathcal{P} .

drops very quickly and this is the reason for the control action to start 10 minutes after the bolus administration. The control system is consequently open during the first 10 minutes.

The problem of regulating a patient's neuromuscular blockade level through the infusion of muscle relaxants is a complicated one mainly because of the wide variability of the input-output map of the plant which depends on the physiological characteristics of the patient. In fact, a large variability of the patients' response to the same drug administration profile has been observed, as shown in Fig. 3.3.

Remark 3.2.1. For the sake of language fluidity, whenever, in the muscle relaxation context, a controller C is said stabilizing a nonlinear system described by (3.6) and (3.5), it is actually intended that the feedback system

composed by the linear part (3.6) followed by the linearized output equation (3.5) around the target value and the controller C is stable.

Experimental evidence suggested that, even though at least one controller in the set \mathcal{C} is able to stabilize each plant in the universum \mathcal{P} , none of the previous controllers could perform satisfactorily over a broad range of patients. Therefore it seems appropriate to implement a switching supervisory algorithm, which adaptively selects the controller in the loop. The control strategy uses the above mentioned sets \mathcal{C} and \mathcal{M} as respectively the set of candidate controllers and the set of approximating models. Before proceeding in this direction, the following remark is necessary.

Remark 3.2.2. The neuromuscular relaxation system exhibits some peculiar aspects that it is important to highlight. First of all, the system is non-linear, due to Eq. (3.5). Moreover, this non-linearity involves the output normalization between 0 and 100 preventing, in this way, the output from assuming divergent values. Furthermore, the saturation on the plant input for $u < 0$ is necessary as only positive drug infusion rate are allowed.

It is clear that these peculiar aspects do not comply with the theory illustrated Chs. 1 and 2. Nevertheless, next section presents simulation results obtained by means of theoretical instruments illustrated in those chapters in order to regulate neuromuscular relaxation level in patients undergoing surgery. An effort will be made to the end of highlighting those aspects which involve a critical violation of the theoretical requirements and other aspects for which this violation does not represent a critical point.

3.2.3 Simulations results

The control task is to let the output, viz. the muscle relaxation level, track the reference signal $r(t)$. The latter is fixed to a constant value, $r(t) = r_0 = 10\%$, which corresponds to a high level of neuromuscular relaxation, hence the name of *neuromuscular blockade*, typically required in many surgical activities.

The PID controllers of the form (3.9) are minimum-phase, hence approaches illustrated in Secs. 1.2 and 2.2, where the explicit computation of the virtual reference signal is required, are appropriate to be used in order to deal with the neuromuscular blockade control.

Following simulation results are related to a patient (plant) which is known to belong to the universum \mathcal{P} , nevertheless its physiological parameters are not obviously known, only I/O data, viz. atracurium infusion rate and neuromuscular relaxation level, are available to the designer.

This patient, that will be referred to as P_{16} in that 16 was its original number in the pool, is chosen as the representative plant for showing simulation results throughout this section. Even though following experiments have been carried out for all the plants in the pool, they can not be reported here for space reasons. The choice of P_{16} in order to comment the results obtained by the designed SSC schemes, is based on the fact that, in accordance to personal experience, it may exhibit a more critical behavior than the other plants. In fact, only controllers C_4 and C_5 in the set \mathcal{C} stabilize ¹ P_{16} , even though only C_5 actually achieves satisfying performance in regulating P_{16} .

In the first part of this section, the set \mathcal{M} containing the 5 approximating models is supposed to be available to the designer. Hence, the cost function studied in Sec. 1.2 can be exploited:

$$V_i(t) = \max_{10 \leq \tau \leq t} \frac{\left\| \begin{bmatrix} -\eta_{y_i}^\tau \\ \rho_i^{1/2} \eta_{u_i}^\tau \end{bmatrix} \right\|_\lambda^2}{m_i + \left\| \begin{bmatrix} e_{i/i}^\tau \\ \rho_i^{1/2} \delta u_{i/i}^\tau \end{bmatrix} \right\|_\lambda^2} = \max_{10 \leq \tau \leq t} J_i(\tau) \quad (3.14)$$

where $\eta_{y_i}(\tau) = y(\tau) - y_{i/i}(\tau)$, $\eta_{u_i}(\tau) = \Delta(u(\tau) - u_{i/i}(\tau))$, $e_{i/i}(\tau) = \bar{r}_i(\tau) - y_{i/i}(\tau)$, $\delta u_{i/i}(\tau) = \Delta u_{i/i}(\tau)$ and $y(\tau)$, $u(\tau)$ are plant I/O data taken from the adaptive loop and $y_{i/i}(\tau)$, $u_{i/i}(\tau)$ are plant I/O data taken from the loop composed by the i -th approximating non linear model and the corresponding tuned controller with $\bar{r}_i(\tau)$ as reference signal, as shown in Fig. 1.5.

Even though neither the plant nor the approximating models are incremental in this case of study, nevertheless input increments are present in the cost function in order to avoid a possible polarization in the denominator. Notice that a forgetting factor λ is introduced in the norms computation according to (3.3) and the max operator is performed on the time interval $[10, t]$ rather than $[0, t]$. Due to clinical reasons, already discussed, during the first 10 minutes the plant and the approximating models are open loop, nevertheless their outputs are non zero, according to (3.5). Hence, cost functions are reasonably calculated starting from $t = 0$, even so, being the switching process disabled until $t = 10$ min., it appears unreasonable to perform the max on the entire time interval $[0, t]$.

Experiment 1

First of all, an experiment is carried out in order to practically highlight

¹see Remark 3.2.1

the controller falsification property of such a cost function. In other words, the present goal is to show that a controller which is actually destabilizing the plant yields a cost function level higher than the others and hence it will be switched out of the loop by the switching logic. To this end, the linearized unstable feedback loop (P_{16}/C_1) is implemented and the corresponding I/O data are used in order to calculate cost functions (3.14). In this preliminary study also the approximating models are linearized around the target value r_0 . The profiles of the cost functions $J_i(t)$ in (3.14), where the max operator is omitted, in that not essential for the present goal, are shown in Fig. 3.4. Notice that the cost function corresponding to C_1 is diverging and it exceeds

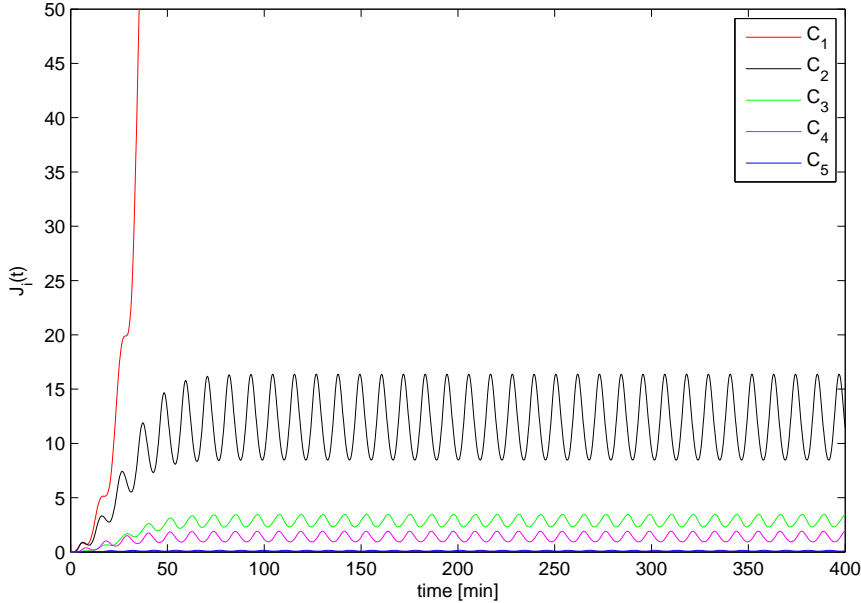


Figure 3.4. Figure shows the cost function profiles $J_i(t)$ in (3.14) related to the 5 candidate controllers with data taken from the unstable linearized feedback loop (P_{16}/C_1)

the other cost functions values at the very beginning of the simulation. As a consequence, C_1 is very quickly falsified, viz. switched out of the loop. At the same time, cost functions related to controllers C_2 and C_3 , which would destabilize P_{16} if they were put in the feedback loop, are bounded in that numerator and denominator in the cost function are diverging at the same rate. Hence, they will not be falsified until after such future time as those controllers are actually switched on in the feedback loop.

Notice that the cost function related to C_1 turns out to diverge because the plant linearization allows the output tend to infinity. In the real case, the plant output is normalized by the Hill equation (3.5) between 0 and 100 and this fact prevents the cost function related to controller C_1 from assuming divergent values. In order to better realize this point, the same experiment previously described is carried out in the case where any linearization of either the plant or the approximating models takes place and the results are shown in Fig. 3.5. Notice that during the first 10 minutes all cost functions are equal to one. The rationale for this fact is that, being the control signal permanently zero during that interval, the virtual reference signal $\bar{r}_i(t)$, $i \in \underline{5}$, equals the output $y(t)$ and it makes the cost function numerator identical to the denominator.

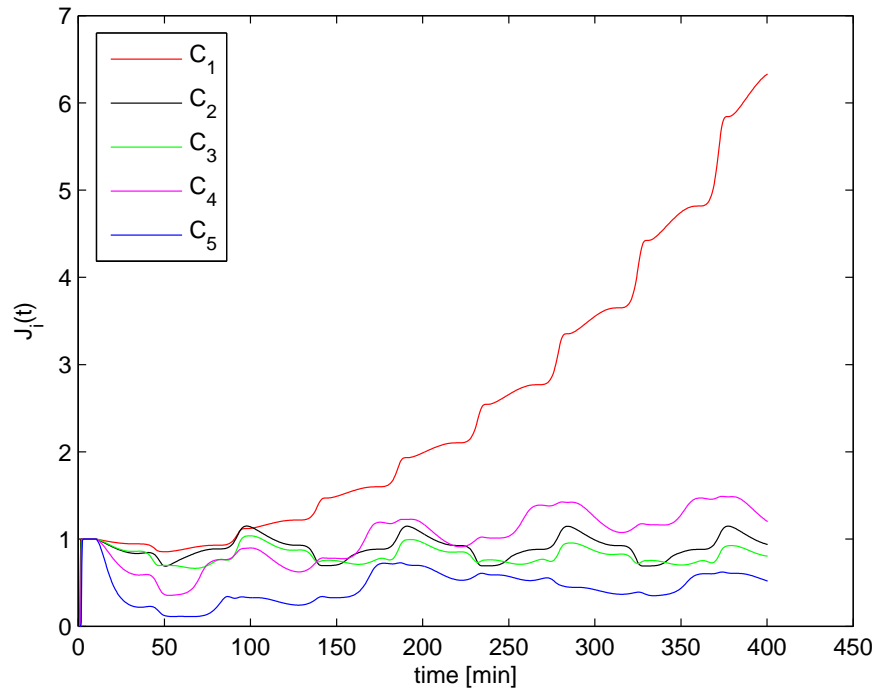


Figure 3.5. Figure shows the cost function profiles related to the 5 candidate controllers with data taken from the unstable feedback loop (P_{16}/C_1) when no linearization takes place.

It can be noticed that, even though, as already explained, any divergence occurs, the cost function related to the controller C_1 exhibits the largest average value and that related to controller C_5 the smallest. Taking into account that

controller C_5 is the only one capable of achieving satisfying performance in regulating P_{16} , the cost function profiles of Fig. 3.5 give favorable insights on the switching logic performance.

Experiment 2

After the previous preliminary study assessing the controller falsification capability of cost function (3.14), it is worth analyzing the performance of the SSC based on the following scale independent hysteresis switching logic:

$$\sigma(t) = \arg \min_i \{(1 - \epsilon \delta_{i\sigma(t-1)}) V_i(t)\} \quad (3.15)$$

where $V_i(t)$ are given by (3.14). The multiplicative hysteresis criterion is preferred with respect to the additive one (1.18) in that, besides other reasons already discussed in Sec. 1.2.3, an effective value for the ϵ hysteresis constant is easier to be chosen.

Before showing simulative results it is important to highlight that the three assumptions required by Corollary 1.2.6 are satisfied by the muscle relaxation system only around the target value $r(t) = r_0$. In fact, as already stated, each linearized plant in the universum \mathcal{P} is stabilized by at least one controller in the set \mathcal{C} . Moreover, open loop stability of each linearized plant and of all linearized approximating models guarantees assumption 2 be satisfied. Finally, the cost functions profiles in Fig. 3.5 ensure that also assumption 3 holds.

The hardware necessary to produce all signals involved in (3.14) is showed in Fig. 1.6. Notice that, in order to preserve the virtual reference properties, the plant input before the saturation block acts is used for either the virtual reference signal or the cost functions computation.

The following parameters are used in the simulative experiment: the forgetting factor is set to $\lambda = 0.998$, the hysteresis constant to $\epsilon = 0.05$, the input weights to $\rho_i = 1$, $i \in \underline{5}$ and the m_i constants in the cost function denominators are equal to 10^{-4} , $i \in \underline{5}$. The choice of $\rho_i = 1$, $i \in \underline{5}$ amounts at identically weighting the contribution of the inputs with respect to the outputs in the cost function. Even so, different choices for ρ_i are possible and similar results are obtained.

The corresponding results are illustrated in Fig. 3.6. Notice that the controlled system exhibits good performance in that any switching occurs because the switching logic chooses the best controller for the plant P_{16} from the beginning (t=10 min.) of the simulation. In fact the cost function corresponding to controller C_5 presents the lowest value. It should be noticed that the cost functions profiles are constant in time and the rationale for this

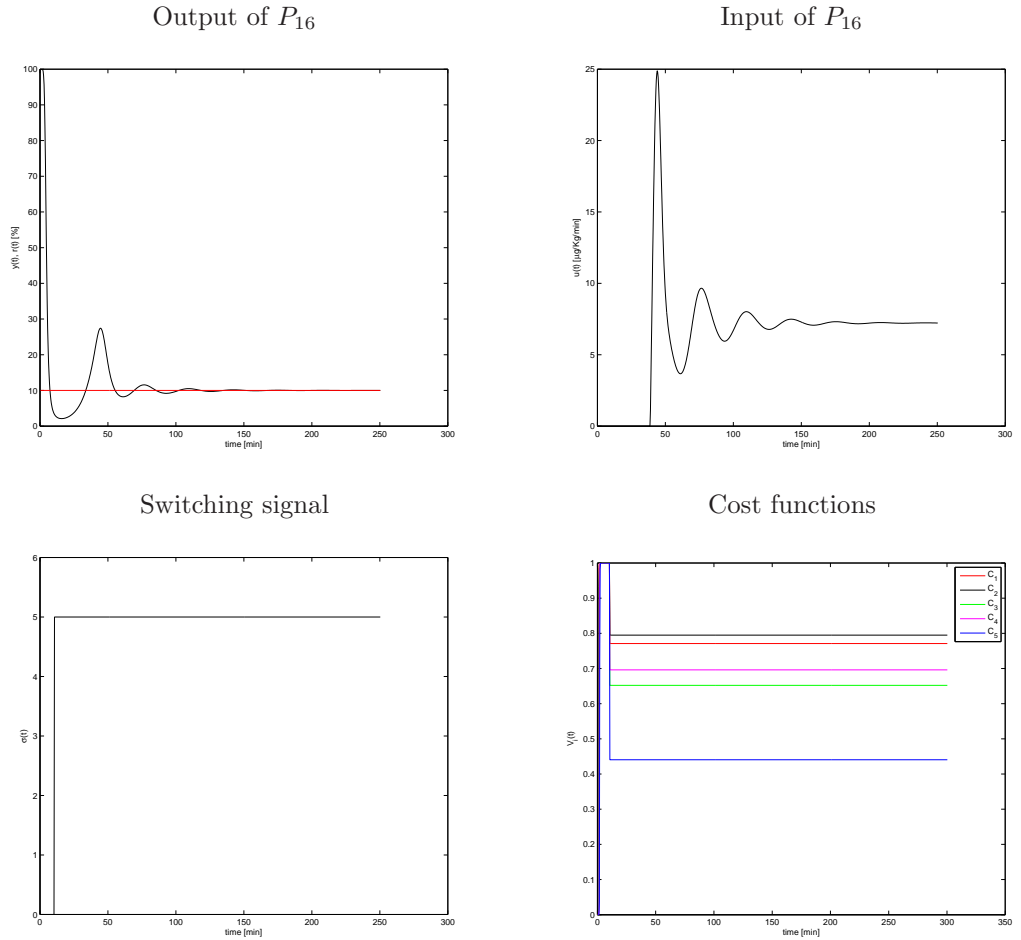


Figure 3.6. Figure shows the results of the SSC for plant P_{16} .

fact is that they assume their maximum value at $t=10$ min.. As already noticed in Sec. 3.1, this behavior might be dangerous in that performance may deteriorate in the case where a different controller is selected, for any reason, at $t=10$ min.. Nevertheless, Fig. 3.7 shows that the same switching policy would take place, if the same parameters were used in the simulation, where the max operator is omitted in the cost functions (3.14). This fact suggests that the choice of controller C_5 in the case of Fig. 3.6 is not due to a lower value of $V_5(t)$ assumed at $t=10$ min. by chance. It has been also verified that the use of a time window over which the max operator is calculated produces the same results.

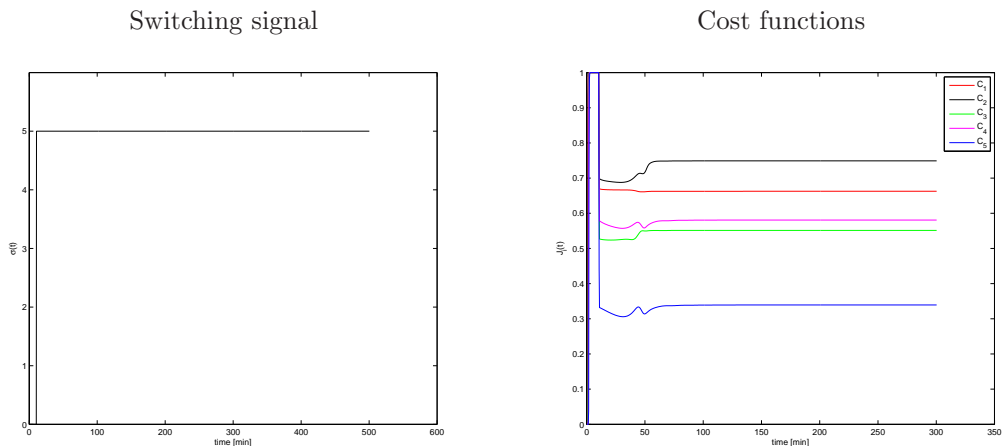


Figure 3.7. Figure shows the switching signal and the cost functions profiles whenever the switching process is based on $J_i(t)$ rather than $V_i(t)$ in (3.14).

The set \mathcal{M} of approximating models is not supposed to be available to the designer in the second part of this section.

Hence, the multiplicative hysteresis based supervisory logic (3.15) is used, nevertheless the cost function $V_i(t)$ are those analyzed in Sec. 2.2 whose form is recalled:

$$V_i(t) = \max_{10 \leq \tau \leq t} \frac{\|\bar{e}_i^\tau\|_\lambda^2 + \rho_i \|u^\tau\|_\lambda^2}{m_i + \|\bar{r}_i^\tau\|_\lambda^2} = \max_{10 \leq \tau \leq t} J_i(\tau) \quad (3.16)$$

where $\bar{e}_i(\tau) = \bar{r}_i(\tau) - y(\tau)$, $y(\tau)$ and $u(\tau)$ are I/O plant data taken from the adaptive feedback loop. As done before in (3.14), a forgetting factor λ is introduced in the norms computation and the max operator is performed on the time interval $[10, t]$.

Experiment 3

Similarly to Experiment 1, the present goal is to assess the controller falsification capability of the cost function (3.16). To this end, I/O data are taken from the unstable closed loop (P_{16}/C_1) and the cost functions related to the candidate controllers are calculated. It is easy to understand that if the plant P_{16} was linearized around r_0 , cost function related to C_1 would diverge having a divergent numerator and a bounded denominator, viz. the norm of the true reference signal. In order to address more real operating conditions, Fig. 3.8 shows the profiles of cost functions obtained without

linearizing the feedback loop (P_{16}/C_1), once the max operator is omitted in that not essential for the present goal. Notice that, as expected, $J_1(t)$ is not

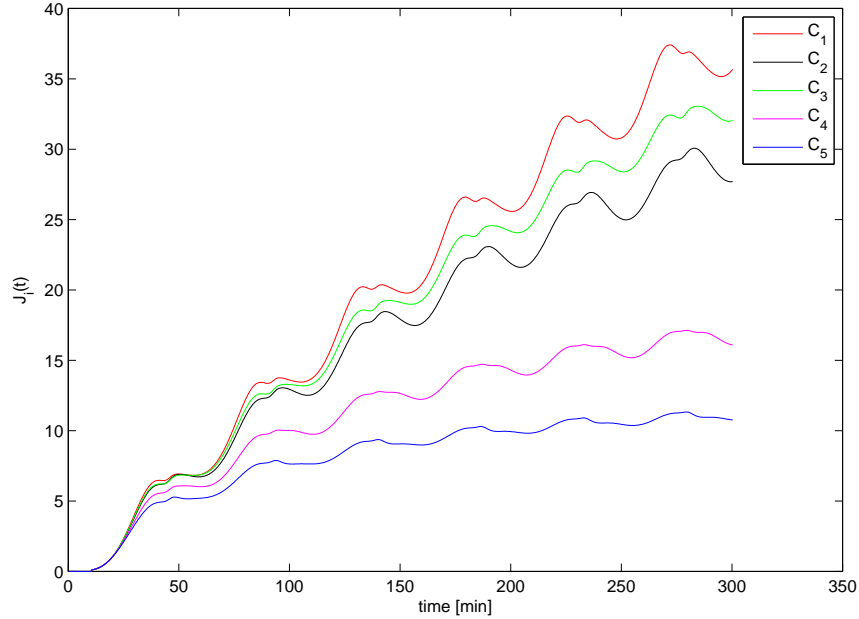


Figure 3.8. Figure shows the cost function profiles $J_i(t)$ in (3.16), related to the 5 candidate controllers with data taken from the unstable feedback loop (P_{16}/C_1) when no linearization takes place.

diverging, nevertheless its highest average value involves the falsification of controller C_1 . Moreover, the lower value of cost function $J_5(t)$ with respect to the others, seems to reflect the actual better ability of controller C_5 in regulating P_{16} .

Experiment 4

The encouraging results of the previous experiment need to be verified once an SSC scheme is implemented.

Before showing simulative results it is important to highlight that the two assumptions required by Prop. 2.2.2 are satisfied by the muscle relaxation system only around the target value $r(t) = r_0$. In fact, the problem is feasible in that, as already stated, each linearized plant in the universum \mathcal{P} is stabilized by at least one controller in the set \mathcal{C} . Moreover, the cost functions profiles in Fig. 3.8 ensure that also assumption 2 is guaranteed, once the

first 10 minutes of the plot are not considered in that the switching process is disabled during that interval.

Notice that, in order to preserve the virtual reference properties, the plant input before the saturation block acts is used for either the virtual reference signal or the cost functions computation.

The following parameters are used in the simulative experiment: the forgetting factor is set to $\lambda = 0.998$, the hysteresis constant to $\epsilon = 0.1$, the input weights to $\rho_i = 1, i \in \underline{5}$ and the m_i constants in the cost function denominators are equal to $10^{-4}, i \in \underline{5}$. Fig. 3.9 shows the corresponding results.

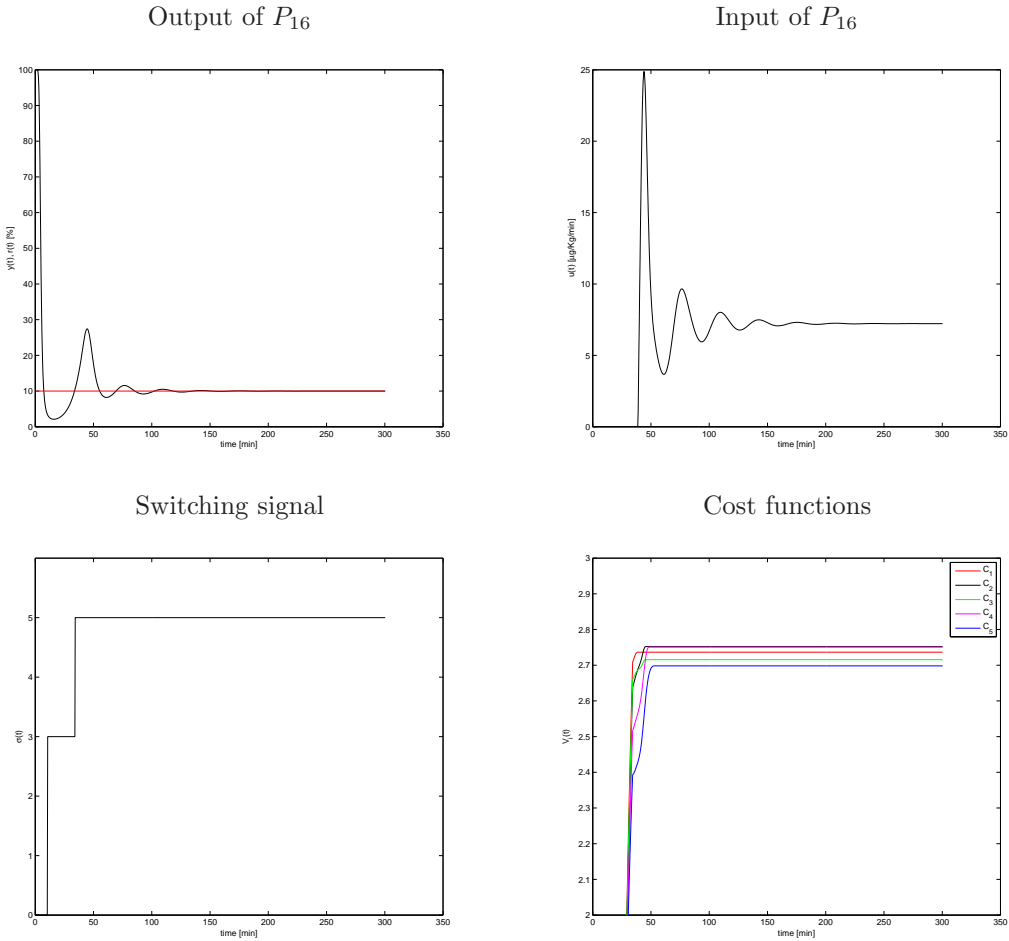


Figure 3.9. Figure shows the results of the SSC for plant P_{16} . A zoom of the cost functions profile is plotted.

The switching logic is able to discard the unsuitable controller C_3 and to

rapidly select the controller C_5 which is maintained along the entire simulation. As a consequence, the controlled system exhibits a good performance, not remarkably different from that achieved in the presence of approximating models, shown in Fig. 3.6. Moreover, the same switching policy is obtained in the case where the max operator is omitted in the cost functions as shown in Fig. 3.10. Notice that the presence of the hysteresis constant involves

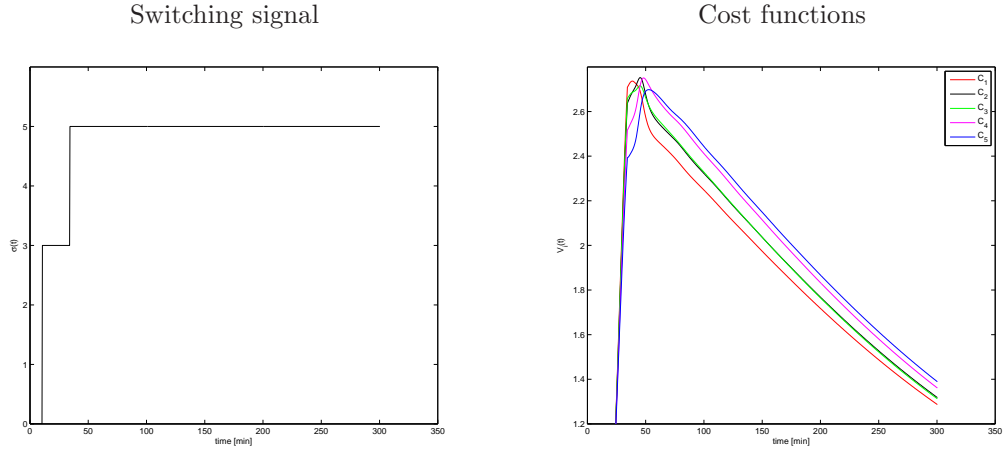


Figure 3.10. Figure shows the switching signal and the cost functions profiles whenever the switching process is based on $J_i(t)$ rather than $V_i(t)$ in (3.16).

the fact that controller C_5 remains in the loop even though its cost function gets actually slightly higher than the others. The use of a smaller ϵ would obviously switch C_5 temporarily out of the loop, with a consequent loss of performance.

It is worth making a comparison between cost functions profiles in the case of approximating models availability (Fig. 3.6 and Fig. 3.7) and those obtained in the case where the models knowledge is not exploited (Fig. 3.9 and Fig. 3.10). In the first situation cost functions reach different steady-state values, for $i \in \underline{5}$. In fact, they exhibit separated profiles and, in particular, a consistent gap is present between V_5 and the others. On the contrary, in the second situation cost functions reach a steady-state value which is almost the same for any controller. An analysis of (3.16) once the forgetting factor and the max operator are omitted shows that the steady-state value, V_{ss} , is exactly the same $\forall i \in \underline{5}$ if $\rho_i = \rho$, and $m_i = m \forall i \in \underline{5}$ and it equals: $V_{ss} = \rho u_{ss}^2 / (m + r_0^2)$ where u_{ss} denotes the steady-state value of the plant input. The foregoing reasoning highlights that the capability of cost function (3.16) of ordering the candidate controllers is more effective in the transient

than in the steady-state. A reason for that can be found taking into account that cost function (3.16) can only exploit I/O plant data. As a consequence, whenever the steady-state regimen is reached, those data carry less information and this fact may prevent the cost function from sorting the controllers. It should be remarked that a wider analysis of simulation results obtained using cost function (3.16) with different plant in the universum \mathcal{P} shows a general worse capability of ordering candidate controllers with respect to the use of cost function (3.14). In particular, performance is noticed to be strongly dependent on values of parameters such as α , ϵ and λ . For instance, the suitable controller for the plant P_{16} is chosen by the supervisory logic only if $\alpha \geq 0.9$.

The absence of approximating models in a context, as the neuromuscular relaxation system, which exhibits peculiarities such as output normalization or input saturation, may be the cause for the assessed possible loss of performance.

3.3 The two carts position control

3.3.1 Problem formulation

The second case of study is represented by a system, illustrated in Fig. 3.11, composed by two carts mechanically coupled by a link having an uncertain stiffness parameter γ . The plant space-state description is as follows:

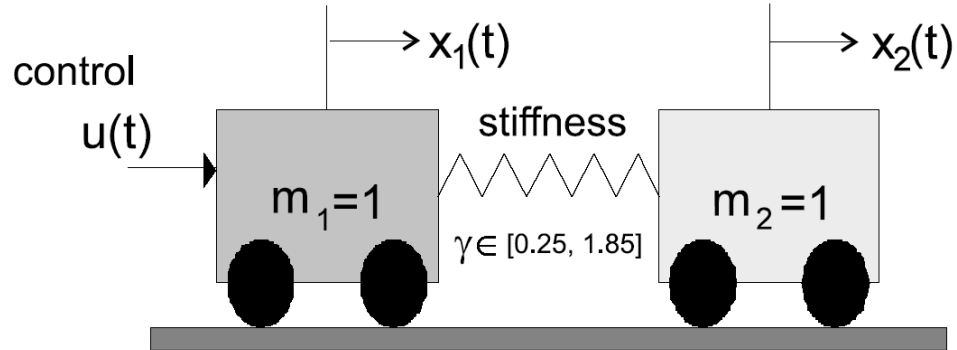


Figure 3.11. Two carts mechanically coupled system.

$$\begin{bmatrix} \dot{x}_1 \\ \ddot{x}_1 \\ \dot{x}_2 \\ \ddot{x}_2 \end{bmatrix} = \begin{bmatrix} 0 & 1 & 0 & 0 \\ -\frac{\gamma}{m_1} & 0 & \frac{\gamma}{m_1} & 0 \\ 0 & 0 & 0 & 1 \\ \frac{\gamma}{m_2} & 0 & -\frac{\gamma}{m_2} & 0 \end{bmatrix} \begin{bmatrix} x_1 \\ \dot{x}_1 \\ x_2 \\ \dot{x}_2 \end{bmatrix} + \begin{bmatrix} 0 \\ \frac{1}{m_1} \\ 0 \\ 0 \end{bmatrix} u \quad (3.17)$$

$$y = \begin{bmatrix} 0 & 0 & 1 & 0 \end{bmatrix} \begin{bmatrix} x_1 \\ \dot{x}_1 \\ x_2 \\ \dot{x}_2 \end{bmatrix} \quad (3.18)$$

where x_1 and x_2 respectively denote positions of the two carts whose mass are m_1 and m_2 . Let $P_\gamma(s)$ be the transfer function from u to x_2 of the plant (3.17) with stiffness γ . Hereafter all numerical values are given in MKS units. The control problem is to position cart No. 2 by applying a manipulable force $u(t)$ to cart No. 1.

This example was earlier proposed in [WLB92] as a benchmark problem for robust control. In [GNL95] it is shown that a single robust controller can be designed so as to yield closed loop stability and fulfill performance requirements for all values of γ in the set $[0.64, 1.8]$.

The present goal is to deal with a larger uncertainty range, viz. $\Gamma = [0.25, 1.8]$, over which no single controller is found capable of achieving closed loop stability and performance requirements. That is because the control problem under consideration becomes harder as γ decreases. To this end, the idea is to design a finite family of controllers $\mathcal{C} = \{C_i, \quad i \in \underline{N}\}$ in such a way that, whatever value γ takes on in Γ , there is at least one controller in the set \mathcal{C} which is able to stabilize the plant. In order to cover the γ uncertainty range three continuous time unity-feedback controllers are designed relatively to the nominal plant models corresponding to the following three values of γ : $\gamma_1 = 0.3$, $\gamma_2 = 0.5$ and $\gamma_3 = 1$. Each tuned controller is selected among all the stabilizing controllers according to the weighted H_∞ mixed-sensitivity synthesis method, see [Kwa91, MA01].

A zero-order hold input device and a sampling time $T_s = 0.1$ are used in order to obtain the discrete time nominal models set and the corresponding controllers set, respectively denoted by:

$$\mathcal{M} = \{M_i = M_{\gamma_i}, \quad i \in \underline{3}\} \quad (3.19)$$

$$\mathcal{C} = \{C_i = C_{\gamma_i}, \quad i \in \underline{3}\} \quad (3.20)$$

Table 3.1 reports, for each value of γ_i , $i \in \underline{3}$, the interval over which the feedback system (P_γ/C_i) , $i \in \underline{3}$, is stable.

$\gamma_1 = 0.3$	$\gamma_2 = 0.5$	$\gamma_3 = 1$
[0.25, 0.576)	(0.372, 0.914)	(0.648, 1.85]

Table 3.1. γ_i -intervals over which (P_γ/C_i) , $i \in \underline{3}$, is stable.

The control goal is to let the position of cart No. 2 track a reference signal $r(t)$, robustly with respect to values assumed by the uncertain parameter γ in the widen set Γ .

3.3.2 Simulations results

The candidate controllers in the set \mathcal{C} , obtained in accordance to the weighted H_∞ mixed-sensitivity method, turn out to be non-minimum phase. Hence, the supervisory logic should rely on cost functions which do not require an explicit computation of the virtual reference. Cost functions studied in Secs. 1.3 and 2.3, respectively for the case where the nominal models are available or not, are consequently suitable to this application.

Differently from the neuromuscular relaxation setting, here the input weights values $\rho_i, i \in \underline{3}$, in the cost functions are derived from the controllers synthesis method and are equal to:

$$\rho_1 = \rho(\gamma_1) = 10 \quad \rho_2 = \rho(\gamma_2) = 5 \quad \rho_3 = \rho(\gamma_3) = 1 \quad (3.21)$$

It is worth pointing out that the use of ρ -values which differ up to one order of magnitude is dictated by the need of providing almost uniformly well-behaved tuned loops for the three nominal values of γ . In particular, the foregoing choices for $\rho(\gamma)$ make the input dynamic range approximately the same for the three tuned loops [MA01].

In the first part of this section, the set \mathcal{M} containing the 3 nominal models is supposed to be available to the designer. Hence, the cost function studied in Sec. 1.3 can be exploited:

$$V_i(t) = \max_{0 \leq \tau \leq t} \frac{\left\| \begin{bmatrix} -\eta_{y_i}^\tau \\ \rho_i^{1/2} \eta_{u_i}^\tau \end{bmatrix} \right\|_\lambda^2}{m_i + \left\| \begin{bmatrix} \delta y_{i/i}^\tau \\ \rho_i^{1/2} \delta u_{i/i}^\tau \end{bmatrix} \right\|_\lambda^2} = \max_{0 \leq \tau \leq t} J_i(\tau) \quad (3.22)$$

where $\eta_{y_i}(\tau) = y(\tau) - y_{i/i}(\tau)$, $\eta_{u_i}(\tau) = \delta u(\tau) - \delta u_{i/i}(\tau)$ are obtained by suitably filtering the output prediction errors, $\delta y_{i/i}(\tau) = \Delta(d)y_{i/i}(\tau)$, $y_{i/i}(\tau)$ are obtained by difference, as shown in Fig. 1.7. Notice that a forgetting factor λ is introduced in the norms computation according to (3.3).

Experiment 1

First of all, an experiment is carried out in order to practically highlight the controller falsification property of such cost function. To this end, the unstable feedback loop (M_1/C_2) is implemented (see Table 3.1 to verify instability of (M_1/C_2)) with a constant in time reference signal as input and the corresponding I/O data are used in order to calculate cost functions (3.22).

The profiles of the cost functions $J_i(t)$, where the max operator is omitted, in that not essential for the present goal, are shown in Fig. 3.12. Notice that

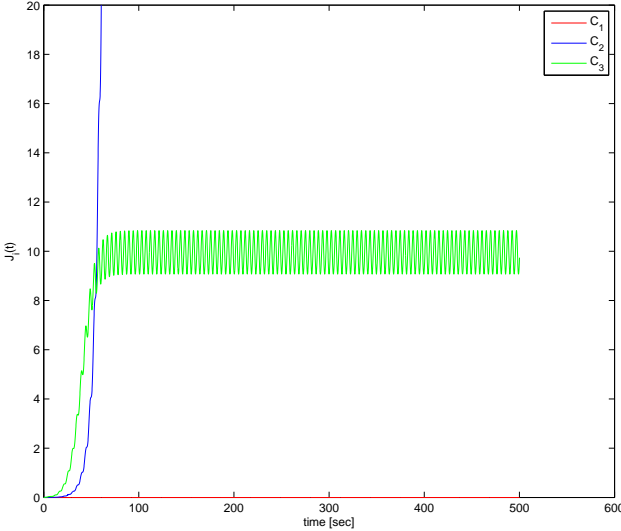


Figure 3.12. Figure shows the cost function profiles $J_i(t)$ in (3.22) related to the 3 candidate controllers with data taken from the unstable feedback loop (M_1/C_2)

the cost function corresponding to C_2 is diverging and it exceeds the cost function of C_1 at the very beginning of the simulation. As a consequence, C_2 is very quickly falsified. At the same time, cost function related to controller C_3 , which would destabilize M_1 if it was put in the feedback loop (see Table 3.1), is bounded in that numerator and denominator in the cost function are diverging at the same rate. Hence, it will not be falsified until after such future time as this controller is actually switched on in the feedback loop. Nevertheless, a positive insight on the inference of candidate loop behavior capability of the cost function is given by the lower value of $J_1(t)$ with respect to $J_3(t)$, which reflects the better ability of C_1 with respect to C_3 in regulating M_1 . This fact gives favorable expectations on the SSC performance.

Experiment 2

After the previous preliminary study assessing the controller falsification capability of cost function (3.22), it is worth analyzing the performance of the multiplicative hysteresis based supervisory logic (3.15) where $V_i(t)$ are given

by (3.22). Before showing simulation results it is worth highlighting that the control problem is feasible in that each plant corresponding to values of $\gamma \in \Gamma$, is stabilized by at least one controller in the set \mathcal{C} . Hence, assumption 1 of Corollary 1.3.2 is satisfied. Assumption 2 is also satisfied in that cost functions, even though assume very small values in the beginning of the simulation, are non zero and positive.

The following simulations are carried out in the presence of a reference $r(t)$ obtained by low-pass filtering a square-wave $\hat{r}(t)$ of amplitude ± 3 and period equal to 100 sec., as follows:

$$r(t) = \alpha r(t-1) + (1-\alpha)\hat{r}(t) \quad \alpha = 0.98 \quad (3.23)$$

Firstly, the SSC scheme is tested in the presence of a constant in time, even though unknown to the supervisory logic, value of the parameter γ . In particular, $\gamma = 0.8$ and the following parameters are used in the simulative experiment: the forgetting factor is set to $\lambda = 0.995$, the hysteresis constant to $\epsilon = 0.1$, the input weights are in accordance to (3.21), and the m_i constants in the cost function denominators are equal to 10^{-4} , $i \in \underline{3}$. The corresponding results are illustrated in Fig. 3.13. The performance of the controlled system is good in that one of the two stabilizing controllers corresponding to $\gamma = 0.8$ (see Table 3.1) is chosen by the supervisory logic. Moreover, different constant values of γ are tested and the same good performance is obtained. A different experiment is then carried out and a time-varying profile for the uncertain parameter γ is chosen as follows: over the time interval $[0, 750]$ sec. γ is linearly increased from 0.25 to 1.8 and next, over the time interval $[750, 1500]$ sec., is linearly decreased from 1.8 to 0.25, as shown in Fig. 3.14. Notice that the time-varying profile of the parameter γ does not comply with the theory developed in previous chapters which requires LTI plants. Nevertheless, for this experiment a slowly time-varying γ -profile is chosen in order to test the SSC in a more significant context than the case where γ assumes a constant value.

Hence, the switching logic, based on I/O plant data, should select at any instant of time an adequate controller to be put in feedback to the plant.

The following parameters are used in the simulative experiment: the forgetting factor is set to $\lambda = 0.995$, the hysteresis constant to $\epsilon = 0.3$, the input weights are in accordance to (3.21), and the m_i constants in the cost function denominators are equal to 10^{-4} , $i \in \underline{3}$. The corresponding results are illustrated in Fig. 3.15.

Notice that the performance of the controlled system is acceptable in that the switching signal $\sigma(t)$ is almost in accordance to the γ profile, as shown in Fig. 3.16. There, the two signals are reported in the same plot and the time intervals over which the controllers C_i , $i \in \underline{3}$, stabilize the time-varying

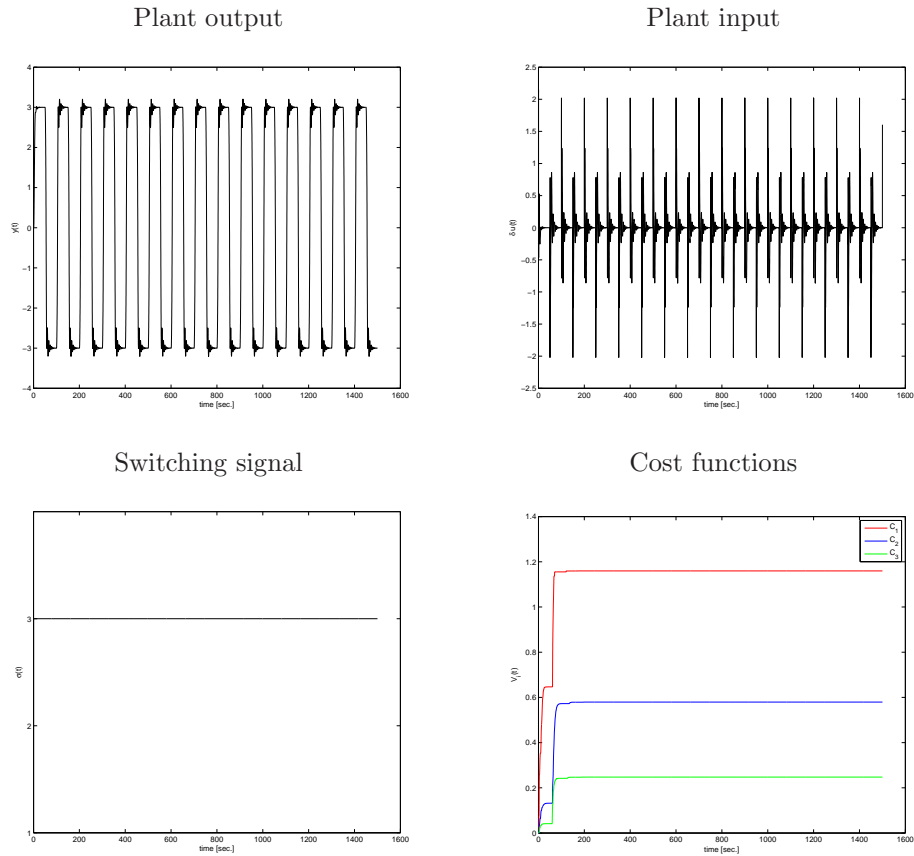


Figure 3.13. Figure shows the results of the SSC when cost functions in (3.22) are used and $\gamma = 0.8$.

plant are specified along the time axis. It should be nonetheless noticed that performance is not completely satisfying mainly in the last part of the simulation. In fact, at that time the switching logic maintains controller C_2 for a too long time before C_1 be switched on in the feedback loop. This undesired behavior is found quite insensitive to different values, even if in an acceptable range, of λ and ϵ and it is partially due to the presence of the max operator in the cost function calculation. It actually forces C_1 to wait that C_2 performs at least as badly as C_1 did in the past, before C_1 actually has the possibility of being switched on in feedback to the plant.

A possible solution to this problem is to perform the maximum of the cost function over a moving time window of fixed length of L sec., in accordance to (3.1), rather than on the entire time interval $[0, t]$, as required by (3.22). Setting the window length to $L = 100$ sec. and letting the other parameters

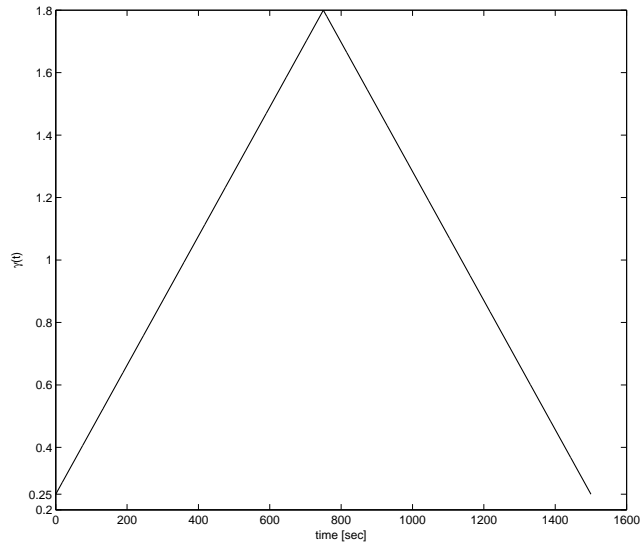


Figure 3.14. Figure shows the time-varying profile chosen for the parameter γ .

be the same as in previous simulation, the relating results are shown in Fig. 3.17. Notice that cost functions are allowed to decrease and it involves a performance improvement mainly during the final part of the simulation. In fact, an earlier falsification of controller C_2 is accomplished by the supervisory logic.

Nevertheless, a further improvement is obtained in the case where the window length equals the sampling time, $L = T_s$ sec.. It corresponds to the situation where the max operator is omitted in the cost functions. The corresponding results are shown in Fig. 3.18.

Even though the last described solution ($L = T_s$) yields the best performance of the controlled system, it is actually the farthest from the theoretical requirement of having non decreasing in time cost functions. Hence, a compromise has to be handled by the designer between desired performance achievement and stability guarantees.

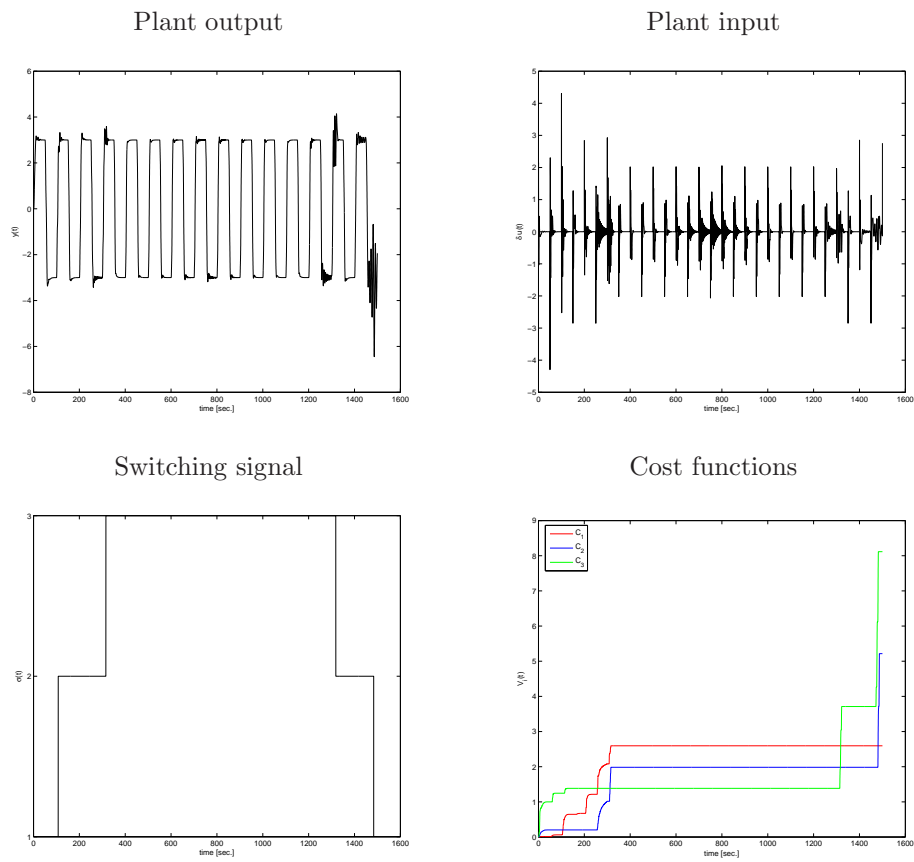


Figure 3.15. Figure shows the results of the SSC when cost functions in (3.22) are used and the γ profile is shown in Fig. 3.14.

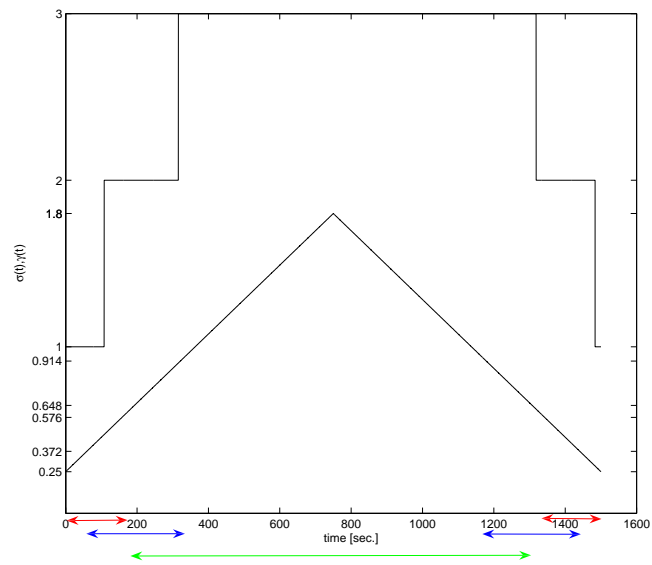


Figure 3.16. Figure shows $\sigma(t)$ and $\gamma(t)$, pointing out, along the time axis, the intervals of time over which, accordingly to Table 3.1, controller C_1 (red), C_2 (blue) and C_3 (green) stabilize the plant.

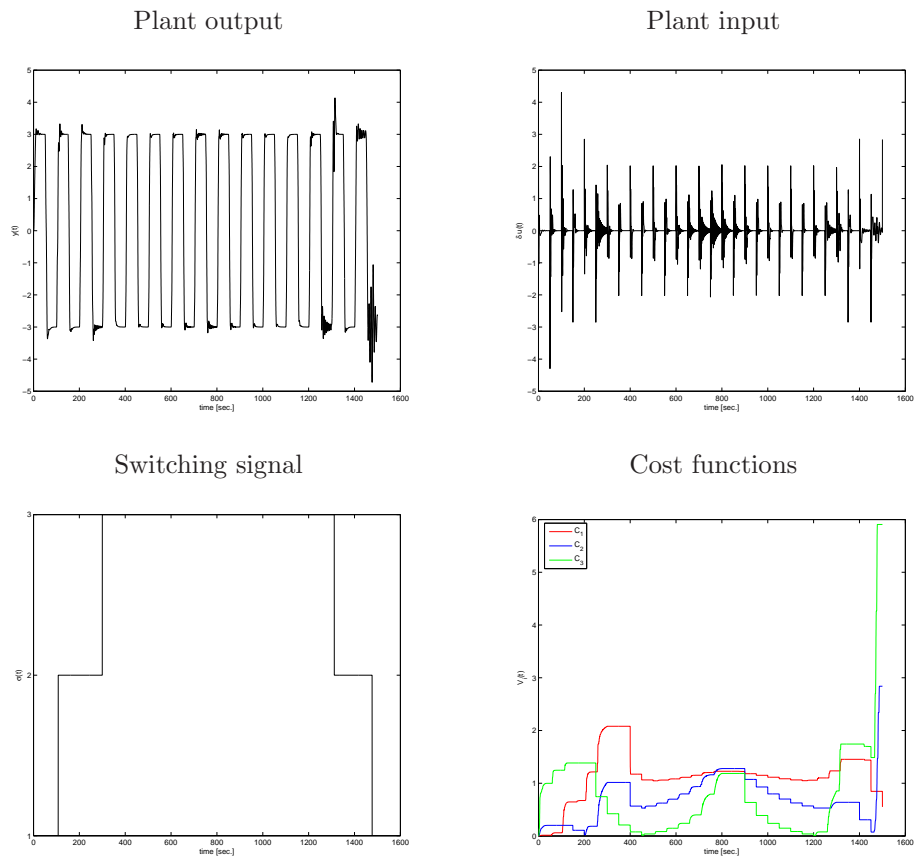


Figure 3.17. Figure shows the results of the SSC when the maximum is performed on a time window of length $L = 100$ sec..

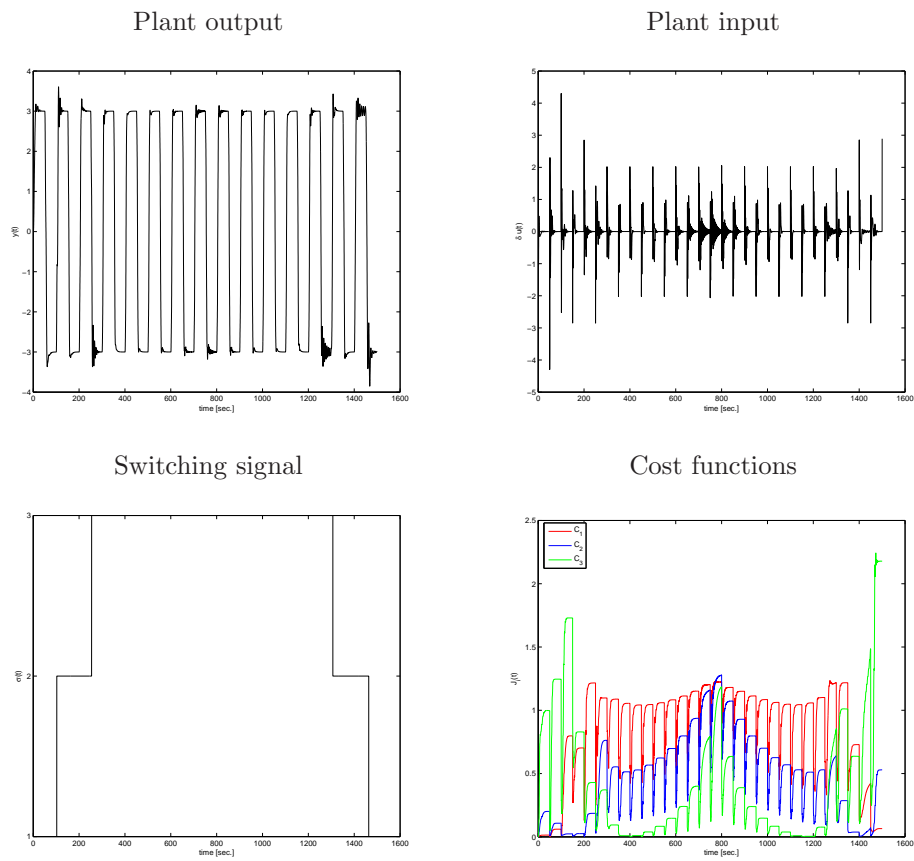


Figure 3.18. Figure shows the results of the SSC when the maximum operator is omitted in the cost function.

The set \mathcal{M} of approximating models is not supposed to be available to the designer in the second part of this section.

Hence, the multiplicative hysteresis based supervisory logic (3.15) is used, nevertheless the cost function $V_i(t)$ is that analyzed in Sec. 2.3 whose form is recalled:

$$V_i(t) = \max_{0 \leq \tau \leq t} \frac{\|\bar{w}_i^\tau\|_\lambda^2 + \rho_i \|\delta u^\tau\|_\lambda^2}{m_i + \|\bar{v}_i^\tau\|_\lambda^2} = \max_{0 \leq \tau \leq t} J_i(\tau) \quad (3.24)$$

where $\bar{w}_i(\tau) = \bar{v}_i(\tau) - y(\tau)$, $\bar{v}_i(\tau) = \frac{S_i(d)y(\tau) + R_i(d)\delta u(\tau)}{S_i(1)}$, $y(\tau)$ and $\delta u(\tau)$ are I/O plant data taken from the adaptive feedback loop. As done before, a forgetting factor λ is introduced in the norms computation.

Experiment 3

Similarly to Experiment 1, the present goal is to assess the controller falsification capability of cost function (3.24). To this end, the unstable feedback loop (M_1/C_2) is implemented in presence of a constant in time reference signal and the corresponding I/O data are used in order to calculate cost functions (3.24). The profiles of the cost functions $J_i(t)$ are shown in Fig. 3.19. Notice that $J_2(t)$ is diverging and consequently C_2 is very quickly falsified. At the same time, cost function related to controller C_3 , which would destabilize M_1 if it was put in the feedback loop, is bounded in that numerator and denominator in the cost function diverge at the same rate. Hence, it will not be falsified until after such future time as this controller is actually switched on in the feedback loop.

Differently from the analogous experiment carried out for previously analyzed cost functions, it is worth noticing that $J_3(t)$ assumes lower values than $J_1(t)$, even though C_1 would perform definitely better than C_3 if it was switched in feedback to M_1 . This fact may involve a bad inference of candidate loop behavior capability of cost function (3.24).

Experiment 4

Before implementing an SSC based on (3.24), it is worth noting that the presence of $\bar{w}_i(t) = \bar{v}_i(t) - y(t)$ in the cost function (3.24) makes the control system goal tracking $v_i(t) = \frac{S_i(d)}{S_i(1)}r(t)$ for some $i \in \underline{N}$. Hence, from a practical point of view, it seems appropriate to use a filtered version of $\bar{v}_i(t)$ in the cost function in order to shape the profile of $v_i(t)$ so that a better tracking

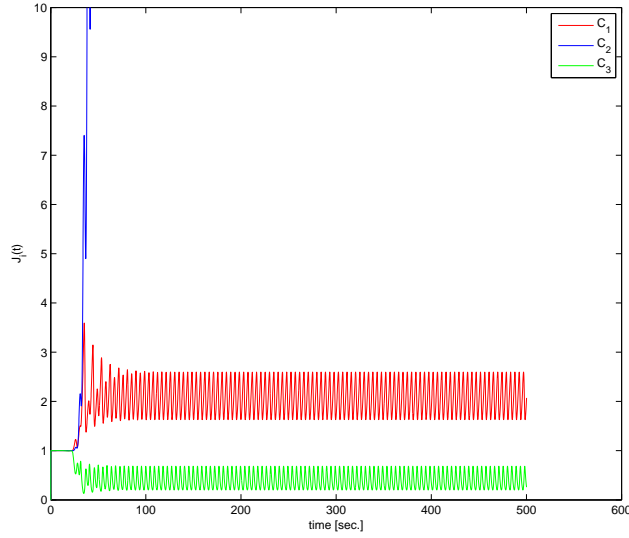


Figure 3.19. Figure shows the cost function profiles $J_i(t)$ in (3.24) related to the 3 candidate controllers with data taken from the unstable feedback loop (M_1/C_2)

performance might be achieved. To this end, different filters can be used and the one adopted in the following experiment is a filter, $F_i(d)$, which equalizes $S_i(d)$, viz:

$$|F_i(e^{j\omega})S_i(e^{j\omega})|^2 = c_i^2 \quad \forall \omega \in [-\pi, \pi]$$

where c_i , $i \in \underline{N}$ are positive reals. To this end, such filter should have the following form [Kwa91]:

$$F_i(d) = \frac{1}{c_i} \frac{1}{S_{i_s}(d)\overline{S_{i_u}^*(d)}} \quad (3.25)$$

where $S_i(d)$ is factored in terms of its stable part, $S_{i_s}(d)$, and its unstable part, $S_{i_u}(d)$ and $\overline{S_{i_u}^*(d)} = d^{\partial S_{i_u}} S_{i_u}^*(d)$, where ∂S_{i_u} denotes the degree of polynomial $S_{i_u}(d)$. Notice that the constant c_i in (3.25) is introduced to avoid a polarized response of $F_i(d)S_i(d)$ to a step input. By this way, it results:

$$\bar{v}_{i_F}(t) = S_i(1)F_i(d)\bar{v}_i(t) = F_i(d)(S_i(d)y(t) + R_i(d)\delta u(t)) \quad (3.26)$$

and

$$v_{i_F}(t) = S_i(d)F_i(d)r(t) = \frac{1}{c_i} \frac{S_{i_u}(d)}{\overline{S_{i_u}^*(d)}} r(t)$$

is such that: $|v_{i_F}(e^{j\omega})|^2 = |r(e^{j\omega})|^2, \forall \omega \in [-\pi, \pi]$.

The corresponding cost function has the following form:

$$V_i(t) = \max_{0 \leq \tau \leq t} \frac{\|\bar{v}_{i_F}^\tau - y^\tau\|_\lambda^2 + \rho_i \|\delta u^\tau\|_\lambda^2}{m_i + \|\bar{v}_{i_F}^\tau\|_\lambda^2} = \max_{0 \leq \tau \leq t} J_i(\tau) \quad (3.27)$$

where $\bar{v}_{i_F}(\tau)$ is given by (3.26).

Using such cost function, the control goal is to let $y(t)$ track $v_{i_F}(t)$ for some $i \in \underline{N}$, being $v_{i_F}(t)$ a signal with the same frequency content of $r(t)$. Moreover, it is worth highlighting that, being $F_i(d)$ a stable filter $\forall i \in \underline{N}$, results of Prop. 2.3.3 and 2.3.4 can be analogously obtained whenever cost function (3.27) is used in the place of (3.24).

Next experiment tests the SSC based on cost function (3.27) using the nominal model M_2 as the unknown plant and the filtered square wave (3.23) as reference signal. Simulation parameters are the following: the forgetting factor is set to $\lambda = 0.99$, the multiplicative hysteresis constant in the switching logic is $\epsilon = 0.1$, the input weights are in accordance to (3.21), and the m_i constants in the cost function denominators are equal to 10^{-4} , $i \in \underline{3}$. The corresponding results are illustrated in Fig. 3.20. Notice that conclusions of Prop. 2.3.4 are not violated in that a final controller is selected by the the switching logic and the adaptive system is stable. Despite that, performance is unsatisfactory because cost function $V_3(t)$ takes on lower values than the others, forcing the supervisor to spend some time to falsify controller C_3 .

An analysis of simulation results obtained in presence of different values of the unknown parameter γ shows that the lower level of $V_3(t)$ occurs irrespective to the γ -values.

In order to find an explanation for this behavior it is worth recalling the reasonings carried out in Sec. 2.3.2 and highlighting that similar reasonings are obtained in the case where $\bar{v}_i(t)$ is filtered through the equalizing filter (3.25). According to those results, candidate loops having larger magnitude of the complementary sensitivity function are supposed to undesirably take advantage in the controller selection procedure (see Sec. 2.3.2 for details). Fig. 3.21, showing the complementary sensitivity function magnitude of the three nominal loops, highlights that the one related to controller C_3 exhibits larger values than the others, for almost all frequencies. Even though in the theoretic study of Sec. 2.3.2 the complementary sensitivity function $|\mathcal{T}_i|$ of the candidate loop (P/C_i) , $i \in \underline{N}$, is present rather than that of the nominal loop (M_i/C_i) , $i \in \underline{N}$, Fig. 3.21 is nevertheless useful to give an insight on the complementary sensitivity function profiles. Notice that the larger values in Fig. 3.21 related to the third nominal loop reflect the physical condition in accordance to which the third nominal loop, corresponding to the largest

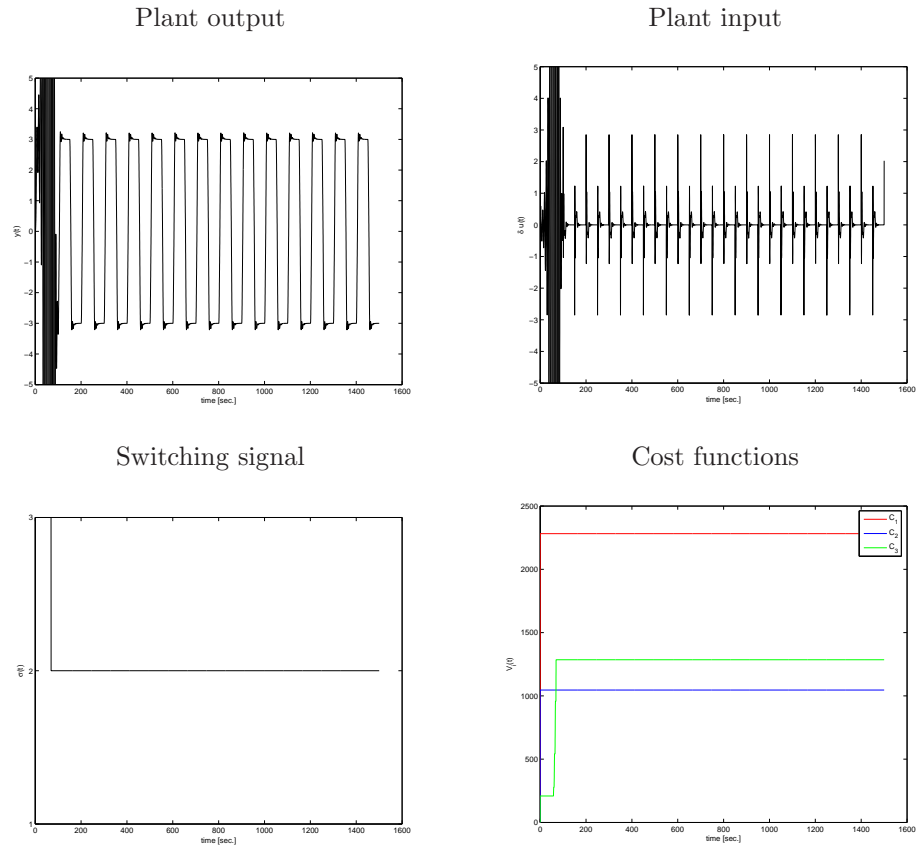


Figure 3.20. Figure shows the results of the SSC when cost functions in (3.27) are used and $\gamma = 0.5$. A zoom of the plant input and output profiles is plotted.

value of the stiffness parameter ($\gamma_3 = 1$), is the easiest to be controlled. These reasonings at least partially motivate the switching logic tendency to choose controller C_3 which is responsible for unsatisfactory performance.

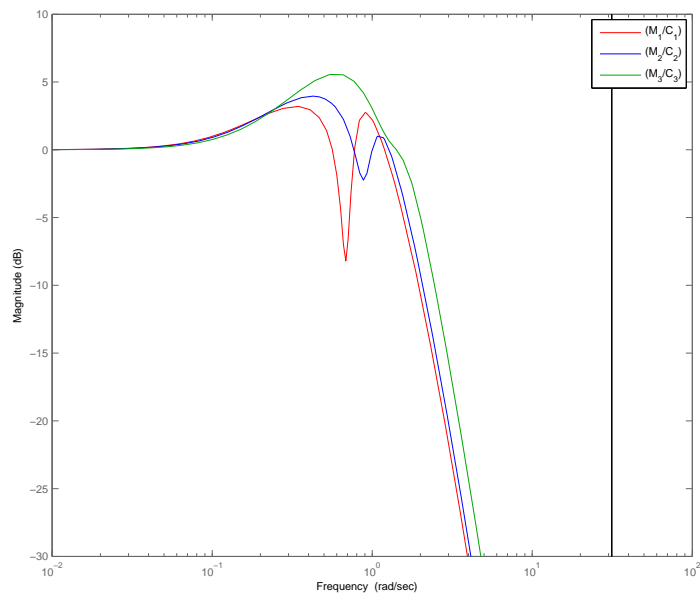


Figure 3.21. A zoom of the magnitude of the complementary sensitivity function of the 3 nominal loops is plotted.

3.4 Conclusions

In this chapter two practical applications are instrumental to test an SSC based on cost functions theoretically studied in previous chapters.

The control of the neuromuscular relaxation level of patients undergoing general anesthesia is tackled by minimum-phase PID controllers. Hence, cost functions which relies on the virtual reference calculation are tested. Controller falsification and inference of candidate loop behavior are properly accomplished in the case of approximating models availability and, consequently, good performance of the adaptive SSC system is obtained. Nevertheless, performance may deteriorate in the case where the prior plant knowledge is not exploited, partially because the inference of candidate loop behavior capability is less powerful than in the other case.

The position control of an uncertain mechanical system is tackled by non-minimum phase controllers. Hence, cost functions which do not require the virtual reference calculation are tested. Good performance of the adaptive SSC system exploiting the approximating models knowledge is illustrated. Either a correct controller falsification or a proper inference of candidate loop behavior contribute to obtain positive results. Nevertheless, also in this case, the desirable behavior deteriorates in the case where cost functions do not use the prior knowledge. A possible reason for this fact is the poor cost function inference of candidate loop behavior capability, already predicted by theoretical studies.

Conclusions

In adaptive switching control schemes, the supervisor generally accomplishes the tasks of deciding when and which candidate controller to switch, via the minimization of a cost function.

In this thesis the design of classes of such cost functions is addressed and evaluated under different prior knowledge on the unknown plant.

Whenever approximating models of the plant are available, the cost functions can be conveniently based on a measure of relative distance between the candidate loop and the corresponding reference feedback loop. This measure, which can be evaluated for the currently operating controller, is inferred for the candidate ones, through the notion of a virtual reference. This fact involves the design of a class of cost functions to be used in the case of minimum-phase candidate controllers, which enable the virtual reference calculation. Instead, non-minimum phase controllers, making the virtual reference calculation unfeasible, need a different class of cost functions which does not require this calculation. Both classes are shown, under certain assumptions, to yield stable adaptive systems. In particular, studies are carried out in order to assess the capability of the adaptive system of achieving good performance. Two simulative examples, such as the neuromuscular relaxation level control and the position control of a mechanical system, are tackled by means of a multi-model SSC. These two examples confirm the satisfactory performance, predicted by theoretical studies.

Whenever approximating models of the unknown plant are unavailable, different classes of cost functions are proposed which are based on a measure of behavior of candidate feedback loops. The virtual reference concept is essential, also in this case, in order to evaluate the behavior of candidate loops without physically inserting controllers in feedback to the plant. In order to cope with possible non-minimum phase controllers, a modified (filtered) virtual reference, which does not require the controllers inversion for its cal-

ulation, is proposed. A cost function which exploits the modified virtual reference is developed. The adaptive system resulting from an SSC based either on the cost function designed for minimum-phase controllers or that for non-minimum phase ones, is shown to be stable, under feasibility assumption. Nevertheless, the lower level of prior knowledge may involve a performance deterioration, mainly due to a poor inference capability of candidate loop behavior of the related cost functions. This fact is predicted by theoretical studies and confirmed by results obtained in simulation experiments.

Further research will involve the study on how possible noises entering the system could influence stability and performance results. Moreover, strategies for improving the system performance in the case of approximating models unavailability should be dealt with.

Bibliography

- [ACD⁺77] M. Athans, D. Castanon, K. Dunn, C. Greene, W. Lee, N. Sandell, and A. Willsky. The stochastic control of the f-8c aircraft using a multiple model adaptive control (mmac) method—part i: Equilibrium flight. *IEEE Trans. Automat. Contr.*, 22:768–780, 1977.
- [AM02] T. Agnoloni and E. Mosca. Switching supervisory control based on controller falsification and closed-loop performance inference. *Journal of Process Control*, 12:457–466, 2002.
- [AM04] D. Angeli and E. Mosca. Adaptive switching supervisory control of nonlinear systems with no prior knowledge of noise bounds. *Automatica*, 40:449–457, 2004.
- [And05] B.D.O. Anderson. Failures of adaptive control theory and their resolution. *Communications in Information and Systems*, 5:1–20, 2005.
- [AS05] A. Absalom and M. Struys. *An overview of TCI and TIVA*. 2005.
- [Ast87] K.J. Astrom. Adaptive feedback control. *Proc. of the IEEE*, 75:185–217, 1987.
- [BH05] J.M. Bailey and W.M. Haddad. Drug dosing control in clinical pharmacology. *IEEE Control System Magazine*, pages 35–51, 2005.
- [CLS02] M.C. Campi, A. Lecchini, and S.M. Savaresi. Virtual reference feedback tuning: a direct method for design of feedback controllers. *Automatica*, 38:1337–1346, 2002.

- [CS06] S.Y. Cheong and M.G. Safonov. Unfalsified control for slowly varying plants using fading memory and windowing. In *Submitted to AIAA Guidance Navigation and Control Conf.*, 2006.
- [DAL06] A. Dehghani, B.D.O. Anderson, and A. Lanzon. Unfalsified adaptive control: a new controller implementation and some remarks. In *Private communication*, 2006.
- [GFG⁺01] A. Gentilini, C.W. Frei, A.H. Glattfedler, M. Morari, T.J. Sieber, R. Wymann, T.W. Schnider, and A.M. Zbinden. Multitasked closed loop control in anesthesia. *IEEE Engineering in Medicine and Biology*, pages 39–53, 2001.
- [GGS01] G.C. Goodwin, S.F. Graebe, and M.E. Salgado. *Control system design*. 2001.
- [GNL95] P. Gahinet, A. Nemirovski, and A.J. Laub. *LMI Control Toolbox User's Guide*. 1995.
- [Hes98] J.P. Hespanha. Logic-based switching algorithms in control. In *PhD Dissertation*, Yale University, New Haven (CT), 1998.
- [Kwa91] H. Kwakernaak. *The polynomial approach to H_∞ -optimal regulation*. 1991.
- [LMG98] P. Lago, T. Mendonca, and L. Goncalves. On-line autocalibration of a pid controller of neuromuscular blockade. In *Proc. of the 1998 IEEE International Conf. on Control Applications*, pages 363–367, Trieste (I), 1998.
- [MA01] E. Mosca and T. Agnoloni. Inference of candidate loop performance and data filtering for switching supervisory control. *Automatica*, 37:527–534, 2001.
- [MA03] E. Mosca and T. Agnoloni. Closed-loop monitoring for early detection of performance losses in feedback-control systems. *Automatica*, 39:2071–2084, 2003.
- [Mar86] B. Martensson. Adaptive stabilization. In *PhD Dissertation*, Lund Institute Techol., Lund, Sweden, 1986.
- [MCMS07] C. Manuelli, S.G. Cheong, E. Mosca, and M.G. Safonov. Stability of unfalsified adaptive control with non SCLI controllers and related performance under different prior knowledge. In *Accepted for the European Control Conference*, Kos, 2007.

- [ML98] T. Mendonca and P. Lago. Pid control strategies for the automatic control of neuromuscular blockade. *Control Engineering Practice*, 6:1225–1231, 1998.
- [MM03] C. Manuelli and E. Mosca. A reduced-complexity adaptive switching supervisory control of neuromuscular blockade. In *Proc. of the 16th Int. Conf. on Sys. Eng.*, pages 463–466, Coventry, 2003.
- [MMG92] A.S. Morse, D.Q. Mayne, and G.C. Goodwin. Applications of hysteresis switching in parameter adaptive control. *IEEE Trans. Automat. Contr.*, 37:1343–1354, 1992.
- [Mor96] A. S. Morse. Supervisory control of families of linear set-point controllers- part 1: Exact matching. *IEEE Trans. on Automatic Control*, 41:1413–1431, 1996.
- [Mos95] E. Mosca. *Optimal, Predictive, and Adaptive Control*. 1995.
- [NB97] K.S. Narendra and J. Balakrishnan. Adaptive control using multiple models. *IEEE Trans. Automat. Contr.*, 42:171–187, 1997.
- [RVAS85] C.E. Rohrs, L. Valavani, M. Athans, and G. Stein. Robustness of continuous-time adaptive control algorithms in the presence of unmodeled dynamics. *IEEE Trans. on Automatic Control*, 30:881–889, 1985.
- [ST97] M. G. Safonov and T. C. Tsao. The unfalsified control concept and learning. *IEEE Trans. on Automatic Control*, 42:843–847, 1997.
- [WLB92] B. Wie, Q. Liu, and K.W. Byun. Robust h_∞ control synthesis method and its application to benchmark problems. *Journal Guidance and Control*, 15:1140–1148, 1992.
- [WPSS05] R. Wang, A. Paul, M. Stefanovic, and M.G. Safonov. Cost-detectability and stability of adaptive control systems. In *Proc. of the 44nd Conf. on Dec. Contr.*, Seville, 2005.
- [WWN83] B. Weatherley, S. Williams, and E. Neill. Pharmacokinetics, pharmacodynamics and dose-response relationships of atracurium administered. *British Journal of Anaesthesia*, 55:39–45, 1983.

- [Zha06] J. Zhang. Practical adaptive control: theory and applications. In *PhD Dissertation*, University of Southern California, Los Angeles (CA), 2006.